Development of a Carbon Dioxide Continuous Scrubber (CDOCS) System for Alkaline Fuel Cells

---

A thesis
submitted in partial fulfilment
of the requirements for the Degree of

Doctor of Philosophy in Mechanical Engineering

in the
University of Canterbury

by
J. S. Wallace, B.E. (Honours)

University of Canterbury
2005

ABSTRACT

Alkaline fuel cells (AFC's) using renewable fuels are a developing technology capable of meeting market niches in standby, standalone and distributed power generation. AFC's generate electricity, heat and water using hydrogen and oxygen as fuels. While AFC's have been known and the principles demonstrated for over sixty years, their use has been restricted primarily to space applications.

Recent technological developments have seen the cost of AFC stacks fall considerably; this together with several other advantages over competing fuel cell technology, has rekindled interest in commercial systems. The main deterrent to wide spread commercialisation of AFC systems is susceptibility to carbon dioxide (CO_2) in atmospheric air used as the oxygen supply. AFC's require a low cost, low energy, continuous scrubbing device to reduce CO_2 in air from approximately 380 parts per million (ppm) atmospheric concentration to below 50 ppm. Current technology to overcome this problem, a solid expendable absorbent called soda lime, is not viable for commercial systems.

The project scope included concept generation of a device to remove CO_2 from air, the development of a CO_2 measurement technique, investigation of chemistry and flow phenomena to determine design relations, and product design and embodiment. The scrubber system conceived specifically for AFC systems uses the temperature swing chemistry of a liquid chemical absorbent, monoethanolamine, and a packed bubble column apparatus to provide intimate gas-liquid interaction. Prototype development proved the Carbon Dioxide Continuous Scrubber (CDOCS) concept and a Patent Cooperation Treaty (PCT) patent was granted, followed by a full American patent.

A gas chromatographic measurement technique was developed to measure low ppm concentration CO_2 in air, enabling regular monitoring of scrubbed gas. Carbon dioxide was separated from a small sample of scrubbed air by chromatographic columns, and the gases analysed with a thermal conductivity detector. The GC system was capable of measuring to 10 ppm with good resolution and accuracy.

Experimental studies were carried out to characterise the flow dynamics and absorption phenomena in the packed bubble column absorber. The relationship between absorption performance and gas-liquid contact time, an important operating parameter for use with AFC's, was theoretically determined and later confirmed by experiment. The regeneration process was studied and the optimal regenerator design determined to be second, smaller packed bubble column. Experiments were conducted to establish design relations for regeneration temperature, flush gas flow rate and the effect of multiple regeneration cycles.

A prototype CDOCS system was built to enable experimental characterisation of scrubbing performance as a function of primary design and operating parameters including liquid depth, regenerator operating temperature and solution composition. This resulted in a good understanding of the system, and an optimised experimental run was performed for cost and performance comparison to existing scrubbing technology.

The CDOCS was capable of reducing CO_2 in air from 380 to 80 ppm for thirty days, providing low cost, low maintenance scrubbing compared to soda lime. The capital cost of the CDOCS is considerably more than for soda lime scrubbers, and the penalty for extended operation is parasitic power consumption by the CDOCS system totalling less than 7% of fuel cell output. It is suggested that a combination of the two technologies be used initially to provide effective, low cost scrubbing for AFC and CDOCS co-development.

Future work on the CDOCS project should include reduction of chemical vapour carry over to the fuel cell, followed by integration with an AFC system. This would allow further development, refinement and design for production to reduce capital cost.

ACKNOWLEDGEMENTS

I owe the deepest debt of gratitude to my family, Mardi, Ella and McGregor. I thank them for the sacrifices made to enable me to pursue this opportunity. Though it has not always been easy, I could always count on support from these quarters. It has been an interesting few years indeed.

I gratefully acknowledge the efforts and patience of my supervisor Dr. Susan Krumdieck. Her technical and moral support, guidance and optimism were invaluable. Thanks also to technical, workshop and academic staff at University of Canterbury, in particular Ron Tinker (Mechanical Engineering) and Trevor Berry (Chemical and Process Engineering) for continued support throughout the project. Contributions and advice from Prof. Arthur Williamson, Prof. Ken Marsh, Dr. Owen Curnow and Prof. Alan Mather are thankfully recognised.

My sincerest thanks to ASCO Carbon Dioxide Ltd, Graham Jack and Warren Holland; their continued and resolute support, especially through some unusual developments early in the project, will not be forgotten. I also appreciate support from Canterprise, Terry Fullerton and John Chang throughout the project.

Many summer and international students have contributed to this project, notably Elizabeth Jenkins, Christopher Carl, Carston Shulz and Micheala Reagan. My thanks are extended for their help and input.

This work was financially supported by The Foundation for Research, Science and Technology under a Technology for Industry Fellowship (TIF) grant. The project could not have proceeded without this support, and my appreciation is extended to this organisation.

CONTENTS

Chapter 1

Introduction 1

1.1 Motivation 1
1.2 Alkaline Fuel Cells 2
1.3 Scrubbing 5
1.4 Research Objectives 5
1.5 Conclusion 7
1.6 Thesis Overview 8

Chapter 2

Scrubber Concept 10

2.1 Prior Art 10
2.2 Method Selection 18
2.3 MEA Review 19
2.4 MEA Applications 22
2.5 Concept Generation 25
2.6 Concept Selection 30

Chapter 3

Analysis Techniques 31

3.1 Low Concentration Carbon Dioxide Detection 31
3.2 High Concentration Carbon Dioxide Detection 54
3.3 MEA Analysis 55

Chapter 4

Component Embodiment 58

4.1 Apparatus Concepts 58
4.2 Absorber 59
4.3 Regenerator 62
4.4 Chemical Solution Selection 69
4.5 Materials Selection 75
4.6 Developmental Prototype 76

Chapter 5

Experimental Characterisation 94

5.1 Absorber 94
5.2 Investigation of Soda Lime Performance 104
5.3 Investigation of Regenerator Performance 106

Chapter 6

Scrubber System Embodiment 120

6.1 Regenerated Solution Heat Exchanger 120
6.2 Provision for Regenerator Solution Flow 126
6.3 Prototype System Component Integration 128
6.4 Final Prototype CDOCS System 131

Chapter 7

CDOCS Experimental Characterisation 133

7.1 100 Degree Regeneration 134
7.2 120 Degree Regeneration 136
7.3 Solution Addition 137
7.4 Chemical Mixture 139
7.5 CDOCS Performance 143
7.6 Residence Time Maximum 144

Chapter 8

Product Concept 146

8.1 Integration 146
8.2 Chemical Production and Disposal 156
8.3 CDOCS and Soda Lime Cost Analysis 157
8.4 CDOCS Performance Comparison with Soda Lime 160
8.5 Scaling 166

Chapter 9

Future Work 169

9.1 Developmental 169
9.2 Integration with Fuel Cell System 170
9.3 Refinement of CDOCS System 170

Chapter 10

Conclusions 173

References 177

Appendix 1 Eneco 9 kW Alkaline Fuel Cell System Information Sheet 182

Appendix 2 Independent Power Technologies Regenerative Scrubber 184

Appendix 3 Chemical Properties 187

Appendix 4 Air Flow Meter Calibration Curve 189

Appendix 5 Ametek Air Blower 116639 190

Appendix 6 Buerkert Flow Solenoid Control Valve Type 6223 192

TABLES

Table 2.1 Selected properties of Monoethanolamine (MEA).....22
Table 2.2 Absorber Concept Matrix.....26
Table 2.3 Regenerator Concept Matrix. 29

Table 3.1 Thermal conductivities of selected gases at 100°C. 38
Table 3.2 Gas chromatograph and TCD analysis parameters.....45
Table 3.3 Gas chromatograph and TCD bake out parameters.....46
Table 3.4 Shimadzu Chromatopak processing parameters.....48

Table 4.1 Solubility of CO_2 in 30 wt% MEA solution.....71
Table 4.2 Monoethanolamine material compatibility. 75
Table 4.3 Contributions to supply pressure required of blower. 86

Table 5.1 Physical properties of packing materials. 104

Table 8.1 Key parameters for CDOCS unit suited to 6 kW AFC system. 147
Table 8.2 Absorber components and costing.....158
Table 8.3 Regenerator components and costing. 159
Table 8.4 Remaining system components and costing. 159
Table 8.5 31 day direct cost comparison between CDOCS and soda lime. 162

FIGURES

Figure 1.1 Single AFC cell schematic. 3
Figure 1.2 Hohsen Corporation 240 W 'LC200' AFC Stack. 4
Figure 1.3 Schematic of an AFC system. 7

Figure 2.1 (a) Packed Column and (b) Plate Column for mass transfer operations. ...16
Figure 2.2 Process diagram of basic amine based scrubber system.....19
Figure 2.3 MEA - CO_2 Chemistry. 20
Figure 2.4 Liquid phase speciation and concentration in MEA solution. 21
Figure 2.5 Schematic apparatus for CO_2 production. 23
Figure 2.6 Photograph of a natural gas treating plant. 24
Figure 2.7 Schematic apparatus for ammonia production.....25
Figure 2.8 Operating diagram for CO_2 absorption from flue gas. 27

Figure 3.1 Draeger gas sampling tubes and sample acquisition pump. 34
Figure 3.2 Schematic of the FTIR spectrometer, with Gas Cell overlaid. 35
Figure 3.3 Diagram of SIFT-MS spectrometer.....36
Figure 3.4 Simple representation of a gas chromatograph. 37
Figure 3.5 Detector temperature and current correlations for various carrier gases. ...39
Figure 3.6 Diagram of TCD circuit and gas flows during analysis. 40
Figure 3.7 Photograph of a Porapak separation column. 41
Figure 3.8 Six port rotary gas sample valve. 44
Figure 3.9 Typical chromatogram of a scrubbed air sample. 46
Figure 3.10 (a) Peak detection by analysis of slope, (b) Peak tailing with subsequent peaks on tail, (c) Unresolved (coincident) peaks and (d) Baseline drift. 48
Figure 3.11 Draeger Polytron IR CO_2 detector.....55

Figure 4.1 (a) Absorber concept and (b) Regenerator concept.....58
Figure 4.2 Packing elements for bubble column reactors. 60
Figure 4.3 Visualisation of flow regimes. 61
Figure 4.4 Liquid and emulsion levels of the packed bubble column. 63
Figure 4.5 Molar flow rates of CO_2 through absorber and regenerator. 64

Figure 4.6 Change in solution pH with amine concentration. 70
Figure 4.7 Carbon dioxide vapour pressure with MEA concentration and loading. ...70
Figure 4.8 Investigation of boiling points for various chemical solutions. 73
Figure 4.9 Developmental prototype absorber, main body sectioned. 77
Figure 4.10 Single layer of woven mesh mist eliminator. 79
Figure 4.11 Pall Corporation Seprasol Liquid/Gas Coalescer. 80
Figure 4.12 Immersed 500 W heating element. 81
Figure 4.13 Developmental prototype regenerator. 82
Figure 4.14 Blower performance graph for Ametek 116639. 87
Figure 4.15 Model for thermodynamic analysis of regenerator. 89
Figure 4.16 Problem setup and parameters for regenerator insulation calculation. 92

Figure 5.1 (a) Air bubbles rise through solution in a packed bubble column and (b) Variation in CO_2 concentration with height. 95
Figure 5.2 Effect of residence time on scrubbing performance. 98
Figure 5.3 Effect of amine concentration on scrubbing performance. 99
Figure 5.4 Absorption performance with standard solution. 101
Figure 5.5 (a) Change in MEA concentration and (b) Change in pH of solution during absorption experiment. 101
Figure 5.6 Cumulative quantity of CO_2 absorbed during absorption experiment. 102
Figure 5.7 Influence of packing media on performance. 103
Figure 5.8 Experimental soda lime apparatus. 105
Figure 5.9 Scaled soda lime apparatus performance. 105
Figure 5.10 Schematic of regenerator characterisation apparatus. 107
Figure 5.11 Typical solution temperature and CO_2 evolution profile during regenerator prototype experiments. 108
Figure 5.12 Regeneration achieved by blowing 6.8 litres/minute nitrogen across the liquid surface in a reaction vessel at various solution temperatures. 109
Figure 5.13 Regeneration achieved by injecting 7 litres/minute nitrogen into the solution, as per a bubble column, at various temperatures. 110
Figure 5.14 Effect of nitrogen flow rate on regeneration at 90°C with gas injection. 111
Figure 5.15 Regeneration achieved with air injected into the MEA solution. 112
Figure 5.16 Multiple regeneration of standard solution at 90°C, nitrogen flush gas. 113

Figure 5.17 Multiple regeneration of standard solution at 90°C, air flush gas.....114
Figure 5.18 Representation of three inseparable factors affecting regeneration. 116
Figure 5.19 Evolution of CO_2 at 90°C for various solution loadings. 118
Figure 5.20 Total regeneration of CO_2 at 90°C for various solution loadings. 118

Figure 6.1 Thermodynamic model for solution cooling helix calculations.....121
Figure 6.2 Absorber and regenerator apparatus with the solution cooling helix. 125
Figure 6.3 Integrated absorber and regenerator. 127
Figure 6.4 Detail of Pall coalescer from Figure 4.11. 128
Figure 6.5 Isometric and detail views of pressure equalising valve assembly. 130
Figure 6.6 Model of integrated experimental CDOCS prototype. 132

Figure 7.1 CDOCS prototype system, main components and functions labelled.....133
Figure 7.2 CDOCS performance at 100°C regeneration temperature. 134
Figure 7.3 CDOCS performance at 120°C regeneration temperature. 136
Figure 7.4 CDOCS performance at 120°C regeneration temperature with solution addition. 138
Figure 7.5 CDOCS performance with a 50 wt% MEA aqueous solution. 140
Figure 7.6 CDOCS performance with a water free solution. 141
Figure 7.7 CDOCS performance with increased MEA content of 60 wt%.....142
Figure 7.8 Optimum CDOCS performance. 143
Figure 7.9 CDOCS performance with increased residence time. 145

Figure 8.1 CDOCS function and form for 6kW AFC System. 147
Figure 8.2 Diagram of thermal integration between CDOCS and AFC system. 148
Figure 8.3 CDOCS blower control feedback loop. 150
Figure 8.4 Basic architecture of main AFC and CDOCS components. 155
Figure 8.5 Comparison of performance between CDOCS and soda lime systems. ..160
Figure 8.6 Direct-cost comparison of CDOCS and soda lime systems. 163
Figure 8.7 Projected power cost comparison of CDOCS and soda lime systems. 164
Figure 8.8 Projected maintenance cost comparison of CDOCS and soda lime systems. 165
Figure 8.9 Total projected cost comparison of CDOCS and soda lime systems. 166

Chapter 1

INTRODUCTION

Chapter 1 summarises the motivation for alkaline fuel cell development, and background information on alkaline fuels cells is presented. The main technical hurdle to further AFC development is introduced and resulting research objectives discussed. Chapter 1 concludes with a brief overview of the thesis.

1.1 Motivation

Population increase, industry evolution and increasing reliance on electrical devices cause existing electricity networks to endure ever-increasing pressure for stationary power supply. In many places around the world, running close to system capacity has caused reliability to fall, leading to supply shortages and blackouts.

As demand approaches supply or system capacity, electricity suppliers must endeavour to ensure reliable supply at any time. When generation or network capacity is limited, suppliers may discourage consumption at peak demand times by financial disincentive. If the distribution network is capable, load shifting (storing energy at low demand times for release at high demand times) effectively increases generation capacity. If demand exceeds generation capacity, providing extra generation when required (peak load assistance) can relieve pressure.

Some electricity consumers cannot afford power outages for economic, security and safety reasons. These users include banks, computer facilities, some manufacturing plants, emergency service centres, hospitals, telecommunication providers and military posts. To overcome the threat of power outage, where there is no alternative or the adverse consequence due to failure is costly, consumers may build expensive supplementary capacity into their own systems, creating an uninterruptible power

supply (UPS). This is traditionally achieved using diesel generators and/or batteries, and more recently with fuel cell systems.

Distributed and stand alone power systems are gaining popularity where connection to a major grid is unrealistic, uneconomic, or where the grid is fully employed. Examples of such circumstances are boats, station houses in sparsely populated regions, and isolated telecommunications outposts.

Renewable energy technology is a fast growing industry driven by the foreseeable shortage and environmental impact of fossil fuels. Fuel cells, using renewable fuels, are a popular energy conversion device being investigated as the world decreases reliance on traditional fuels. Fuel cells, first proposed by Sir William Grove in 1839, convert hydrogen and oxygen gases into electricity, heat and water without pollution.

Fuel cells are not subject to the Carnot thermodynamic efficiency limit, and therefore have inherently higher efficiencies than heat engines and are more environmentally friendly. Fuel for fuel cells can be stored as hydrogen or hydrogen containing compounds and consumed as demand requires. While there are many types of fuel cell, the alkaline fuel cell (AFC) has some key benefits that make it an appropriate choice for stationary, remote or emergency power supply.

1.2 Alkaline Fuel Cells

Alkaline fuel cells are energy generating devices first described by Reid in 1902 [1] and demonstrated by Bacon in the 1940's. A simple illustration is shown in Figure 1.1.

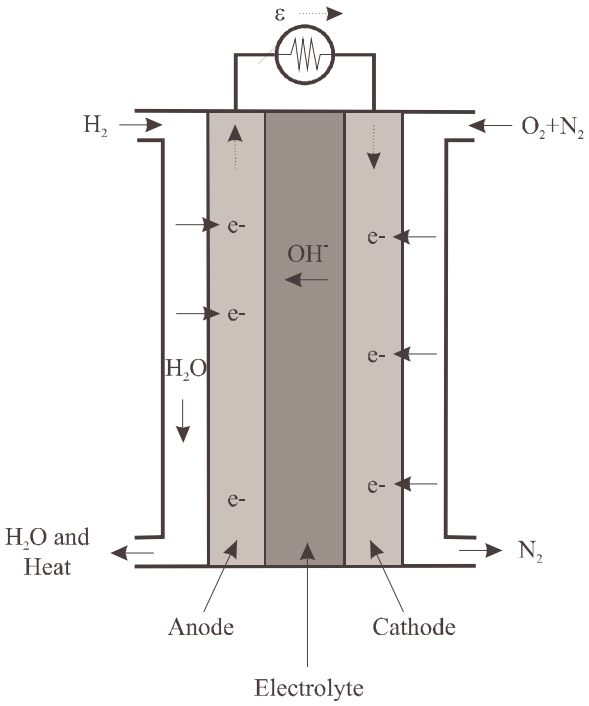

Figure 1.1 Single AFC cell schematic.
Hydrogen and oxygen generate a current, heat and water.

Hydrogen and oxygen gases are delivered to the anode and cathode respectively. The OH^- species (hydroxide ions) generated at the cathode travel through the alkaline electrolyte and recombine at the anode, forming water with the hydrogen fuel and releasing electrons. The anode half cell reaction is [1]:

$$2H_2 + 4OH^- \rightarrow 4H_2O + 4e^- \quad (1.1)$$

Electrons travel through the external circuit and react at the cathode to produce OH^- ions according to the half cell reaction:

$$O_2 + 2H_2O + 4e^- \rightarrow 4OH^- \quad (1.2)$$

The illustration in Figure 1.1 constitutes one cell. To generate useful power many cells are electrically and mechanically joined together to form a fuel cell stack, as shown in Figure 1.2.

Figure 1.2 Hohsen Corporation 240 W 'LC200' AFC Stack.
The LC200 measures 230 x 180 x 180 mm.

Alkaline fuel cells boast the highest energy conversion efficiency of any fuel cell type [2] at 80% [1]. AFC's operate at atmospheric pressure and relatively low temperature (about 70°C), and therefore have a short start up period. Unique to fuel cells, the AFC does not require expensive precious metal electrode catalyst material, significantly decreasing production costs. Like other fuel cells, AFC's are quiet due to the absence of moving parts, and are readily scalable.

AFC's are a relatively mature technology for specialist applications such as space vehicles, and powered the first demonstrated fuel cell vehicles of the 1960's and 1970's. These advantages led to the selection of AFC's to provide power to NASA space shuttle missions for several decades, including the Apollo missions sending man to the moon.

The AFC gains its name from the alkaline electrolyte within the fuel cell, which allows the migration of OH^- ions. The electrolyte is typically aqueous potassium hydroxide (KOH), an excellent conductor of hydroxide ions. For economic terrestrial application, the AFC must derive oxygen fuel from air (78% N_2, 21% O_2, 1% Ar, 0.04% CO_2), as opposed to pure oxygen from a refined source. Carbon dioxide, an acid gas, reacts readily with a strong alkaline solution such as KOH (Eq 1.3). The

other constituents of air are chemically inert, and act only as diluents in the oxygen stream.

$$2KOH\ (aq) + CO_2\ (g) \rightarrow K_2CO_3\ (s) + H_2O\ (l) \qquad (1.3)$$

Carbonation caused by absorption of CO_2 from the oxygen (and possibly hydrogen) supply remains the biggest problem faced by AFC developers, beyond research and prototype testing [3] [4] [2]. Carbon dioxide reacts to form carbonate (CO_3^{2-}) ions, reducing the concentration of OH^- ions in solution. This reduces conductivity and fuel cell efficiency over time, and eventually the precipitate potassium bicarbonate, K_2CO_3, forms. The precipitate can reduce active electrode area, dry out or electrodes, damage electrode catalyst [1] and render the fuel cell inoperative.

1.3 Scrubbing

A solution to the carbonation problem is the separation and removal of CO_2 from air, a process known industrially as scrubbing. It is generally agreed [1] [3] that a scrubbing system is required on any but the smallest commercial AFC system. An expendable absorbent material called soda lime (primarily calcium hydroxide and sodium hydroxide) is almost exclusively used to scrub air for fuel cell research and early development purposes. Due to cost and maintenance issues, soda lime is not realistic for mature, marketable systems.

1.4 Research Objectives

The aim of the CDOCS project was to develop a novel scrubbing system to remove CO_2 from air for an AFC, dubbed the Carbon Dioxide Continuous Scrubber or CDOCS. A survey of prior art in CO_2 removal from air identified a small number of specialist applications, but no suitable commercial products. The exact form, market and specifications of an AFC system, to which the CDOCS should be applied, are not yet established as AFC system development is still in its infancy; therefore there are currently no well defined product specifications available.

The development milestones for the CDOCS project were focused on establishing a fundamental understanding of underlying physics and design relations, and determining compatible materials of construction. This approach allowed development of a generic and flexible product to a stage where the concept was proven, but further development would be completely specific to an actual AFC system.

The specific system used as a basis for the CDOCS project is a 6 kilowatt (kW) AFC intended to power remote telecommunications outposts in Australia. Outposts are typically isolated, requiring extended, maintenance free operation (long term goal of 6 months).

The 6 kW AFC requires air at 40 m^3/hr, approximately 20 times the stoichiometric oxygen requirement, to ensure adequate dispersion throughout the stacks. For acceptable efficiency and life of the AFC, CO_2 must be reduced from atmospheric concentration, typically 380 ppm, to less than 10 ppm. At the current stage of development, fuel cell developers are generally content with reduction to 50 ppm. Operating conditions are close to sea level elevation and temperatures between -10 and +40°C.

Analogous to the internal combustion engine in an automobile, fuel cell stacks are just part of a much larger assembly. Balance of plant including power electronics, control, monitoring and scrubbing are necessary to provide a standalone system [2]. Figure 1.3 gives some insight to the nature of the AFC system.

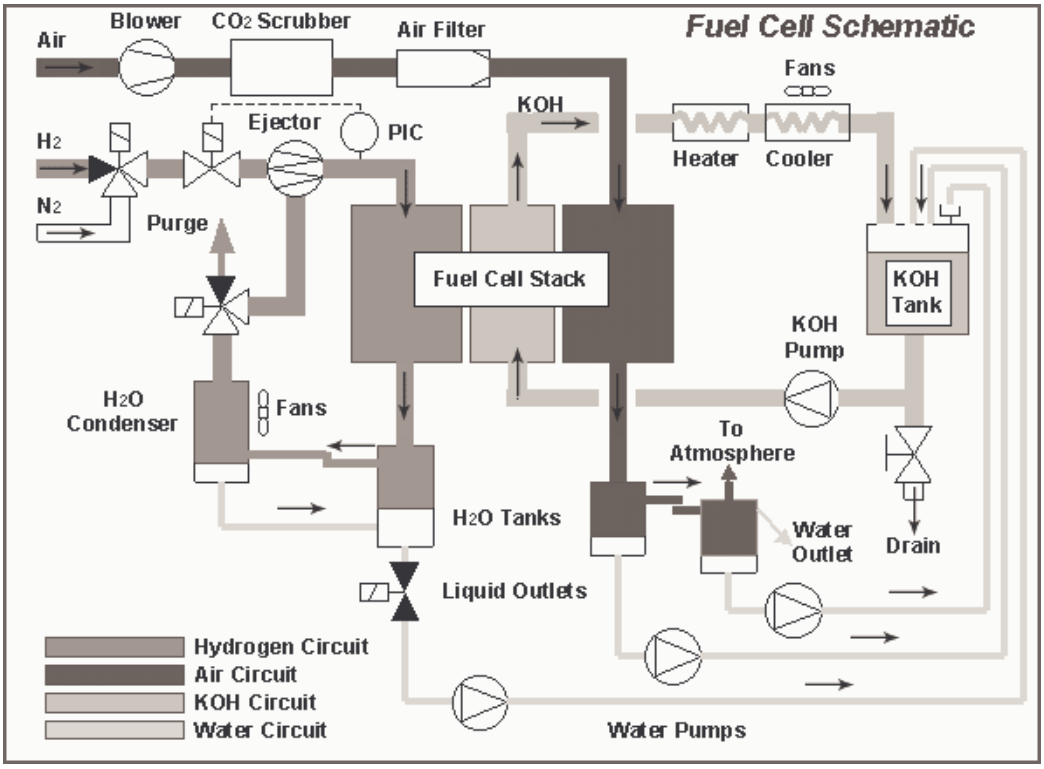

Figure 1.3 Schematic of an AFC system.

Illustration of balance of plant required for autonomous operation (Fuel Cell Control Ltd [5]).

The scrubber must not be unduly complicated or overbearing with regard to cost, maintenance or manufacturing. The size of the system, and therefore the scrubber, is restricted to enable transportation to remote locations. Parasitic power consumption, energy generated and used by the system itself, causes reduced useful generation capacity and efficiency. The 6 kW AFC is designed to produce 5 kW of useful power, and the scrubber is allocated 5% of power output, or 300 W.

1.5 Conclusion

Due to increasing consumption, reliability concerns with electricity networks and demand for remote power generation, there is a market need for small scale, reliable power generators on the order of 5 kW capacity. AFC systems are an emerging technology suited to meet these needs, offering fast start-up, no pollution and efficient energy conversion. However, one of the final hurdles to further development of AFC

systems is susceptibility to CO_2, present in air used as the oxidant. A low maintenance, low power consumption scrubber is required to make AFC systems attractive economically and practically. This work reports the research and development of a new scrubbing apparatus for use with AFC's.

1.6 Thesis Overview

This thesis introduces the alkaline fuel cell and the potential importance of AFC systems for power generation. The key challenge in AFC system development, carbon dioxide removal from air (scrubbing), is presented and research objectives stated. A literature review of prior art in Chapter 2 describes known methods of scrubbing CO_2 from air and other gases for various applications. A chemical absorption method used in industry is identified as a suitable process on which to base the carbon dioxide continuous scrubber (CDOCS) system. Concept matrices enable selection of apparatus to perform the scrubbing process continuously while meeting stringent size, power and performance targets set by AFC requirements.

Carbon dioxide measurement techniques for monitoring the performance of the scrubbing system are discussed in Chapter 3. The CO_2 analysis technique developed to measure very low concentration CO_2 in scrubbed air is described in detail. The measurement systems used to monitor high CO_2 concentration and MEA solution concentration are presented.

Chapter 4 presents a literature review of bubble columns, the apparatus chosen to perform the absorption and desorption of CO_2. Physical characteristics and empirical relations are presented, and analysis completed to determine the general form and operation of a prototype CDOCS system. The chemical solution components and composition are selected based on absorption characteristics and physical properties. A developmental prototype absorber and regenerator are described, and important parameters relevant to an AFC system quantified.

The prototype apparatus is used to gather experimental data in Chapter 5 and aid characterisation of the system. An important operational parameter for the system,

liquid depth, is theoretically determined and experimentally verified. The performance of the system in its simplest form, the absorber only, is then experimentally evaluated. The performance of current scrubbing technology, soda lime, is evaluated by a scaled experiment for comparison to the CDOCS system. The regenerator apparatus is characterised independently by experiments varying operational parameters.

Chapter 6 describes the components developed to enable integration of the absorber and regenerator apparatus for continuous operation: heat exchangers, an exhaust filter and a pressure equalising valve. The assembled components form the developmental CDOCS prototype system, the performance of which is evaluated in Chapter 7. The effect of varying operational parameters is measured by monitoring scrubbing performance over long periods. Parameters investigated include regeneration temperature and chemical solution mixture.

The form of a CDOCS unit suitable for a 6 kW AFC system is presented in Chapter 8 and resources available for integration described. Control and monitoring of the CDOCS in conjunction with an AFC system are described, and maintenance requirements noted. The manufacture and disposal of CDOCS chemical solution and current scrubbing media are evaluated for cost and sustainability. The capital and running costs of the CDOCS and soda lime scrubbing systems are compared, including maintenance and power consumption. Scaling of the CDOCS system, an important aspect for AFC applications, is discussed. Finally, recommendations are made for future work in Chapter 9 prior to concluding comments in Chapter 10.

Chapter 2

SCRUBBER CONCEPT

Existing carbon dioxide separation technology is reviewed and evaluated in chapter 2, for application to AFC systems. From the various methods discussed, the most suitable process for continuous removal of CO_2 from air for alkaline fuel cells is chosen. The chemical absorbent on which the process relies is then reviewed, and existing industry contrasted to the unique AFC application. Concept apparatus to perform the absorption and desorption are developed, resulting in selection of the apparatus able to provide conditions necessary for each process, within AFC system limitations.

2.1 Prior Art

Existing scrubbing systems and related technology were researched to determine progress made in the field and alternative technologies that may be adapted to the AFC problem. Applications for CO_2 removal from air include submarine atmospheres [6] [7], diving apparatus [8], anaesthetics [9], space vehicle atmospheres [10], and existing fuel cell scrubbers [3]. Removal from other gas streams includes petrochemical refinement, gas purification and chemical manufacture. The methods used for CO_2 removal are summarised below.

2.1.1 Sacrificial Electrolyte

Proposed solution for AFC's

The AFC electrolyte absorbs CO_2 from air, and routine electrolyte exchanges are made before any ill effect [3]. Sacrificial electrolyte has its place in AFC research, but preservation of the electrolyte by scrubbing CO_2 is a preferable solution to low maintenance and economically viable power generation.

2.1.2 Soda Lime

Anaesthetics, diving equipment, fuel cell scrubbers

Soda lime is a mixture of primarily calcium hydroxide ($Ca(OH)_2$, approximately 75%), sodium hydroxide (NaOH, approximately 4%) and water (approximately 20%), formed into solid granules. When air contacts soda lime, CO_2 reacts with water, and subsequently hydroxides, on the granule surface (Eq's 2.1 - 2.3). Over time diffusion of CO_2 into the heart of the granule occurs, replenishing the reactive surface. For maximum absorption performance, the relative humidity of soda lime granules should be maintained greater than 50% [3].

$$CO_2 + H_2O \rightarrow H_2CO_3 \quad (2.1)$$

$$2H_2CO_3 + 2NaOH \rightarrow Na_2CO_3 + 4H_2O + Heat \quad (2.2)$$

$$2Ca(OH)_2 + Na_2CO_3 \rightarrow 2CaCO_3 + 2NaOH + Heat \quad (2.3)$$

A similar function is performed by lithium hydroxide, used extensively in space applications [10], but with increased capacity and cost. Soda lime is available in a variety of granule sizes. Smaller granules provide more surface area per unit volume and shorter diffusion distances, but also increase pressure drop and risk of blockage by any water and dust slurry generated. Soda lime can contain a pH sensitive exhaustion indicator, which causes granules to change colour as CO_2 is absorbed (for example white to violet with ethyl violet indicator). The granules revert to the original colour upon continued exposure to CO_2.

Soda lime is the current scrubbing method used by fuel cell researchers and developers. The apparatus is very simple, cheap and requires no power input. However, soda lime is relatively bulky, and it is expensive because the primary uses are specialist applications including anaesthetics and diving rebreathers. Soda lime waste (primarily calcium and sodium carbonate) can be decomposed to oxides and subsequently converted to hydroxides by humidification. The resulting ash would then require reprocessing to standard sized granules. However decomposition occurs at 1100ºC, which makes it uneconomical to recycle compared to using raw materials. Effectively, therefore, soda lime is non regenerable.

Available published data for CO_2 absorption characteristics vary, making it unclear exactly how soda lime performs. Appleby [3] states that 1 kg of soda lime can reduce CO_2 from 300 to 10 ppm for 1000 m^3 of air [11], equivalent to approximately 135 kWh generation per kilogram of soda lime. This figure appears to be based on complete reaction of soda lime with CO_2. Approximating the soda lime as 80 wt% $Ca(OH)_2$ (molar mass 74.1 grams/mole) and 20 wt% water, there are 10.8 moles of $Ca(OH)_2$ per kilogram of soda lime. The volume of CO_2 removed from 1000 m^3 of air scrubbed from 300 to 10 ppm is 0.29 m^3 or, using the ideal gas equation with pressure P = 101325 Pa, the universal gas constant R = 8.314 J/moleK and temperature T = 300 K, the number of moles of CO_2 absorbed, n, is:

$$\begin{aligned} n &= \frac{PV}{RT} \\ &= 11.8 \,(\text{moles}) \end{aligned} \qquad (2.4)$$

One mole of $Ca(OH)_2$ can absorb one mole of CO_2 (Eq's 2.1 - 2.3), so to scrub 1000 m^3 air as stated implies that all of the $Ca(OH)_2$ must react (allowing for inaccuracies such as a possible 4 wt% NaOH content). This is unlikely in practice, with continuous operation, due to restricted availability of $Ca(OH)_2$ within the granules.

The Merck Index [12] refers to soda lime as a mixture of calcium oxide, CaO, and NaOH and states that the mixture can absorb 25% to 35% of its weight in CO_2. Calcium oxide absorbs CO_2 to form calcium carbonate, $CaCO_3$, or can be hydrated to form $Ca(OH)_2$, both reactions being exothermic. According to The Merck Index, one kilogram of soda lime can absorb up to 350 grams CO_2 or, again using the ideal gas equation with the same parameters as Eq 2.4, 8 moles of CO_2. For a 6 kW AFC system using 40 m^3/hr air, the flow rate of CO_2 is 0.6 moles/hr, giving 13.3 hours generation per kilogram of soda lime. This equates to 80 kWh per kilogram of soda lime.

Ahuja [13] quotes several sources stating 1 kg of soda lime corresponds to 9.6 [13], 9.4 [14] and 0.4 [15] kWh respectively. Fuel Cell Control Ltd specify soda lime consumption for a 2.5 kW AFC corresponding to 53 kWh/kg [5]. A 9 kW Eneco Ltd AFC system requires soda lime replacement every 160 hours, corresponding to an

estimated 26 kWh per kg [16] (Appendix 1). Finally, the Industrial Research Limited AFC system holds approximately 20 kg of soda lime requiring replacement every 24 hrs, or 7.2 kWh/kg.

No authoritative measure of absorption rate or capacity exists in literature. As part of this research, the performance of soda lime was studied with the same measurement system used to evaluate the CDOCS apparatus. Results of this investigation are presented in Chapter 5.

2.1.3 Membrane Permeation and Molecular Sieve (Adsorption)

Petrochemical refinement, inert gas generation, emissions filtering and raw material processing for plastics

Solid adsorbents such as zeolites, activated carbon and other molecular sieves separate gases by selective adsorption of gaseous components. Molecular size and properties of the gas relative to the adsorbent material, such as polarity and electrical charge, determine if a molecular species is adsorbed or rejected. Molecular sieves can achieve a high degree of removal but are expensive, have a large pressure drop and require high energy temperature or pressure swings to regenerate [17]. Water is preferentially adsorbed [17], reducing usefulness in a humid air stream.

Membranes separate gases by selective permeation of gas components. Selected gases dissolve into one side of the membrane (permeate stream) and are transported to the other side by a concentration gradient driving force. The concentration gradient is preserved by maintaining a high partial pressure of the dissolved gas on one side of the membrane, and low partial pressure on the other side. Membranes are generally used for bulk separation [17] and require gas at high pressure.

Oak Ridge National Laboratory, a division of the United States Department of Energy, is developing an electrically conductive carbon fibre molecular sieve for CO_2 separation from various gas streams. By the application of a low voltage, a process called electrical swing adsorption enables CO_2 evolution. Judkins [18] reports removal of CO_2 from air to less than 50 ppm, but gives no further details for this

application. The pressure required for reported adsorption, at least 35 kPa, is prohibitive for AFC use.

2.1.4 Sacrificial Cell

Proposed solution for AFC's

For a sacrificial cell the fuel cell stack design allows CO_2 absorption into the electrolyte [19]. A dedicated high current density cell continuously regenerates the electrolyte by converting carbonate ions to CO_2 at the anode. Excess hydrogen fuel sweeps away CO_2 as it evolves. The sacrificial cell still generates power, but at very inefficient conditions [3]. This design would be integral to the fuel cell stacks, but has not been adopted by any known manufacturer. It is unclear what effect the operating conditions may have on the sacrificial cell in the long term [13].

2.1.5 Cryogenics

Proposed solution for AFC's

Ahuja [13] attempted to demonstrate freezing CO_2 (freezing point -78°C) out of an air stream for AFC's. Expansion of liquid hydrogen to gas provided the cooling, so this method applies only to those systems using liquid hydrogen fuel. Liquid hydrogen is energy intensive to produce and is not a likely long-term fuel source. Ahuja states that it is possible to remove CO_2 to less than 10 ppm by cryogenic freezing, and reports experimental data for the removal of CO_2 from a 70 litres/minute gas flow to 20 ppm for 1 ½ hours, and 50 ppm for 2 ½ hours. However the separation was performed on dry, bottled air, so avoiding inevitable complications with moisture. Significant reported difficulties with the mass spectrometer measurement system, including inaccurate atmospheric CO_2 measurements, scatter and the inability to quantitatively calibrate the instrument, make the results dubious.

2.1.6 Independent Power Technologies Ltd

Regenerative AFC scrubber

During the course of the project Independent Power Technologies Ltd (IPT) [20], an AFC stack and system development firm, released promotional information on a regenerative CO_2 scrubber for AFC's (Appendix 2). The technology is commercially sensitive, but IPT claim the 'zero waste regenerative scrubber' can remove CO_2 from an atmospheric air stream to 20 ppm for 5000 - 10 000 hours with a commercially available sorbent. For a 3 kW AFC the scrubber contains 2 litres of sorbent, uses 200 W power and has a 1.6 kPa pressure drop. From patent details it appears the scrubber uses hydrated transition metal oxides, specifically zirconium oxide. Transition metal oxides are known to absorb CO_2, the resulting carbonates being unstable upon heating. IPT claim to regenerate the sorbent by flushing with hot, humid air.

2.1.7 Wet Scrubbing

Petrochemical refinement, chemical manufacture, gas separation

Used for almost a century, wet scrubbers (packed and plate columns, Figure 2.1 (a) and (b) respectively) are commonplace on a large industrial scale. Packed columns are cylinders filled with a porous material designed to enhance gas liquid contact. The liquid absorbent trickles down the column over the packing material, met by an upward gas flow from the bottom the column.

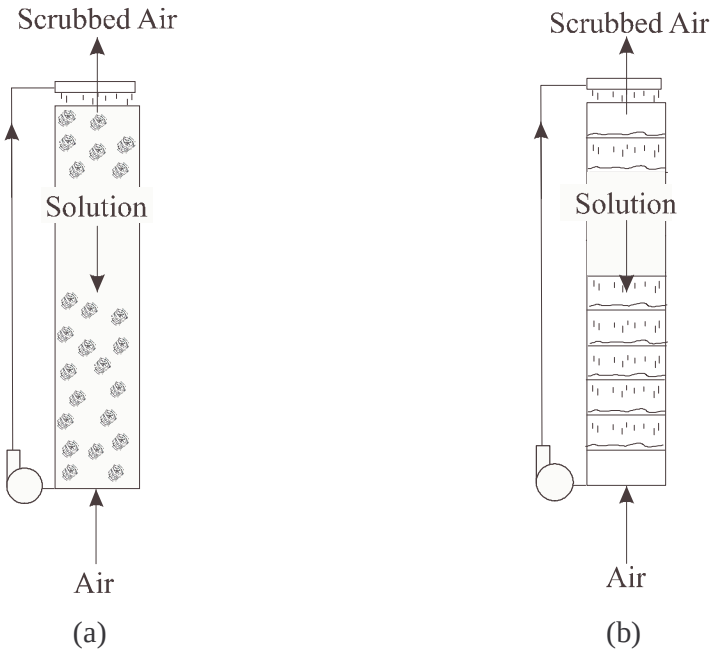

Figure 2.1 (a) Packed Column and (b) Plate Column for mass transfer operations.

By wetting the packing, a large surface area of liquid ensures maximum opportunity for absorption. Plate columns are similar in appearance and operation but have a series of sieve like plates distributed over the column length. Liquid flow down and gas flow up the column are designed to cause the liquid to pool slightly and rain down from each plate, generating gas-liquid interfacial area. The following methods of CO_2 removal employ wet scrubbers.

Hot Potassium Carbonate (Benfield) Process

Natural gas treatment, ammonia production

Hot potassium carbonate, up to 150°C [21], has a high capacity to absorb CO_2. The process design takes advantage of the high CO_2 partial pressure and temperature available in synthesis gas streams. Regeneration is achieved at lower temperature than absorption by flashing the solution to low pressure [17]. The process requires a high CO_2 concentration in the processed gas, and although conceptually no heat is required for regeneration, in practice steam is used to enhance performance [17].

Potassium or Sodium Hydroxide Scrubber

Proposed solution for AFC's

An external KOH or NaOH scrubber absorbs CO_2 prior to air contacting the fuel cell electrolyte. Electrolytic regeneration, similar to the process used by a sacrificial cell, enables continuous operation [6]. Sodium hydroxide has been used for ppm level removal for other applications, but regeneration is not practical due to the stability of sodium carbonate formed. Sodium hydroxide is usually replaced once half of the OH^- ions have reacted [21]. Sodium hydroxide is a cheaper alternative to KOH, however carbonate solubility is lower and reaction kinetics slower, therefore KOH is a better alternative for the same method.

Amine Scrubber

Petrochemical refinement, chemical manufacture, gas separation

Amines are the most widely used solvents for CO_2 removal from process gas streams, and find application in many unrelated industries [12]. Using large wet scrubbers, amines absorb and desorb CO_2 in a temperature or pressure swing process. Amine plants most frequently reduce CO_2 content from around 15% to 1%, but some installations remove CO_2 to less than 1000 ppm [22] and it is possible to attain 50 ppm [23].

2.1.8 Membrane Gas/Liquid Contactor (Pervaporation)

Gas turbine flue gas on off shore oil rigs

A CO_2 permeable membrane separates an amine solution from the flue gas. Carbon dioxide is selectively dissolved into the membrane, with increased driving force due to the amine maintaining a low CO_2 partial pressure on the liquid side. The technology is intended for bulk removal from large plants such as multiple (5 plus) gas turbine generators, making use of waste heat [24]. Initial studies and experiments show promise, with a large reduction in plant size. For the demonstration plant, the original 4.5 metre diameter, 22 metre tall absorber was replaced by a 72% smaller pervaporation unit measuring 4 x 4.5 x 5 metres and achieving 86% CO_2 removal. A

60% volume reduction was achieved for the regenerator, though the pervaporation desorber was not tested in service. No reference was made to the service life or cost of the pervaporation units.

2.1.9 Solid amine

Space vehicle and submarine atmosphere control

Amine functional groups may be adhered to a solid substrate [25] giving CO_2 absorption capacity with lower running costs than aqueous solvents, since there is no pumping or liquid pressure head to overcome. Regeneration generally involves steam and/or a vacuum. Solid amine technology is in relatively early stages, with significant interest in space applications [10] where solid amines are being developed for the removal of CO_2 to near ambient levels for vehicle atmosphere control [10]. The CO_2 requirement for this application remains intolerable for AFC's.

2.2 Method Selection

While the operating parameters of existing amine applications are very different to those dictated by a fuel cell, the review of literature indicated that the MEA - CO_2 chemical system is a process capable of continuous removal of CO_2 from air for an AFC. The process offers a good balance of affinity for CO_2, to achieve absorption to very low concentrations, with low energy regeneration enabling continuous operation. The basic function of such a system is shown in Figure 2.2.

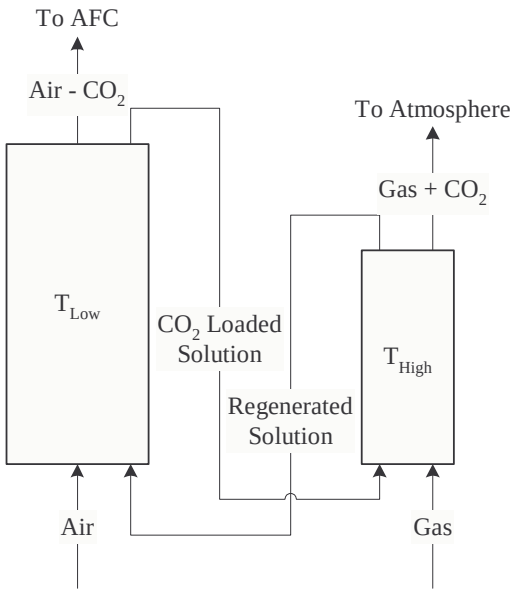

Figure 2.2 Process diagram of basic amine based scrubber system.

2.3 MEA Review

The use of alkanolamines for gas separation was first patented by RR Bottoms in 1930 [26]. Monoethanolamine (MEA) is the most widely employed solvent for CO_2 absorption, used for over seventy years in the CO_2 production and gas sweetening industries. Though new amines and amine mixes have been developed, MEA is still the preferred absorbent for low pressure and low concentration CO_2 absorption [17]. The properties and behaviour of amine solutions, while not entirely understood [22], have been empirically documented over time to provide engineers with a useful database for design [27].

> "Gas absorption with chemical reaction is widely used in the chemical and petroleum industries. Although the operation has been studied for many years, most process designs are still based on experience or 'rule of thumb'…"[28].

For very low CO_2 concentrations the rate of reaction with MEA determines the overall rate of absorption [29]. MEA is favoured for complete removal of CO_2 due to a fast reaction rate, high alkalinity [30] and relatively low molecular weight, allowing more moles per kilogram of solvent in the column. Detailed mechanisms for the

reactions involved in the MEA - CO_2 system have been proposed. Figure 2.3 is an elegant representation of the chemical system reproduced from Hook [7].

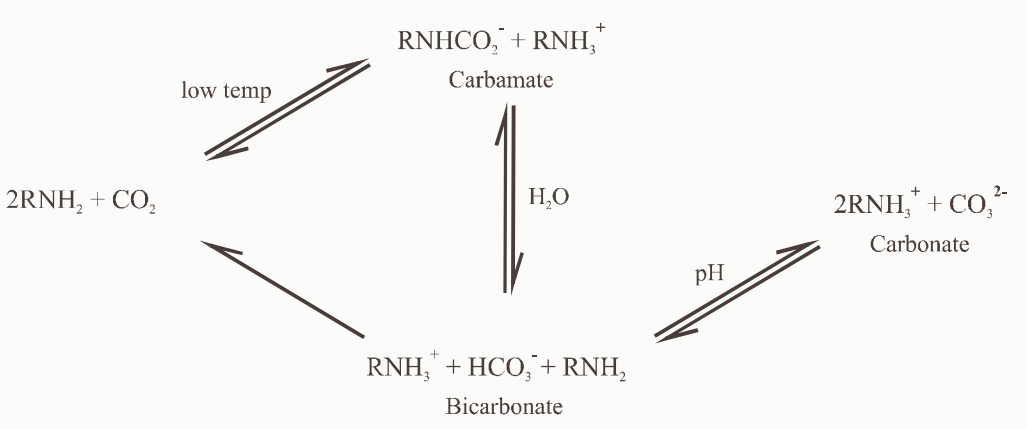

Figure 2.3 MEA - CO_2 Chemistry.
RNH_2 represents an amine, where R = CH_2CH_2OH for MEA.

Absorption occurs at temperatures up to approximately 60°C. Yeh [31] reported no significant difference in absorption ability in the range 38-50°C for a 20 weight percent (wt%) aqueous MEA solution. The MEA – CO_2 reaction is exothermic and reversible by supplying heat to the system. The temperature swing absorption/evolution process reverses at approximately 70°C.

Carbamate formation is dominant for primary amines (MEA) because it is relatively stable. This limits the capacity, or loading, of MEA to 0.5 moles CO_2 per mole MEA - lower than other amines [32] [33]. Bicarbonate formation allows a theoretical loading of 1 mole CO_2 per mole MEA, but the rate of hydrolysis is low [17], as seen by the concentration of HCO_3^- ions at low loading in Figure 2.4. The rate of hydrolysis depends on several factors including solution strength, CO_2 concentration, pH [34] and sufficient time for reaction [33].

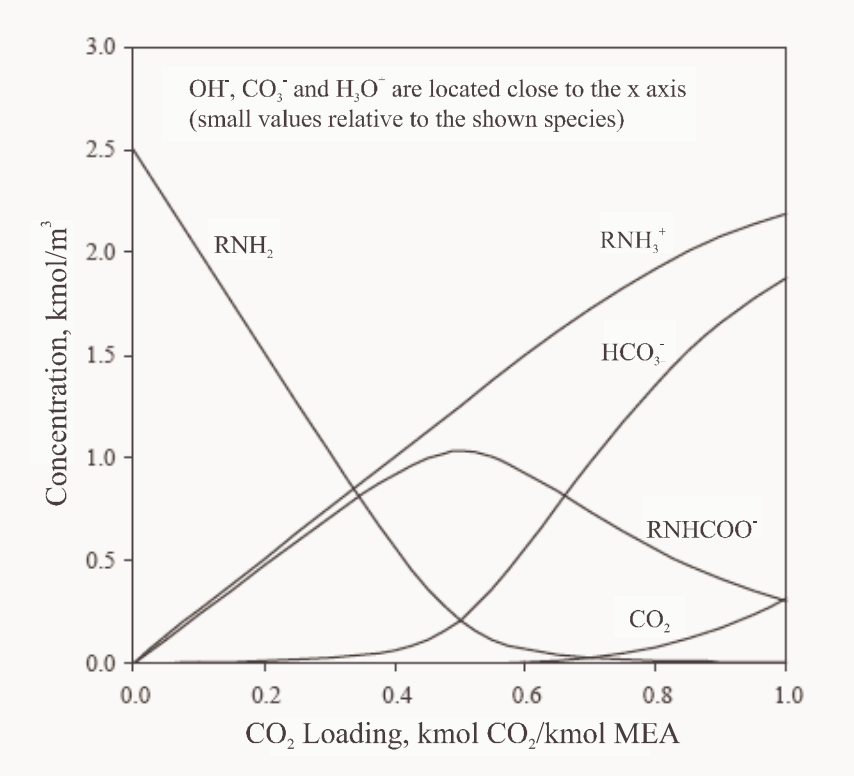

Figure 2.4 Liquid phase speciation and concentration in MEA solution.

2.5Molar (~ 15 wt%) MEA solution at 313 K. $MEACOO^-$ = carbamate, HCO_3^- = bicarbonate. Reproduced from Abdouheir [35].

Strong absorption and formation of a stable carbamate (an exothermic reaction) inherently makes MEA solutions more energy intensive to regenerate than other amines; however regeneration to very low loading is feasible [22]. Other disadvantages of MEA are relatively high vapour pressure and adverse reaction with oxygen (degradation), particularly at elevated temperature. Relevant physical properties of MEA are summarised in Table 2.1. Full data with references are included in Appendix 3.

Table 2.1 Selected properties of Monoethanolamine (MEA).

MEA		
Molecular Formula	C_2H_7NO	
Molecular Weight	61.08	g/mole
pH	12.5	
Density, ρ	1012	kg/m^3
Boiling Point (P_{atm})	171	°C
Melting Point (P_{atm})	10.5	°C
Specific Heat, c_p	3200	J/kgK (25°C)
Thermal Conductivity, k	0.299	W/mK (25°C)
Absolute Viscosity, μ	0.021	Pas (25°C)
Surface Tension, γ	0.048	N/m (25°C)
Vapour Pressure	0.05	kPa (25°C)
Vapour Pressure	0.1	kPa (35°C)
Vapour Pressure	10	kPa (110°C)

2.4 MEA Applications

Common applications for CO_2 removal from process gas streams are ammonia production, petroleum refining, hydrogen, ethylene and CO_2 production, and natural gas sweetening [22]. Usual applications absorb CO_2 at high pressure [22] and have little or no oxygen present in the treated gas streams. High temperature and the presence of oxygen exacerbate amine degradation and plant corrosion.

2.4.1 Carbon Dioxide Production

The process used for CO_2 production is represented in Figure 2.5 [36]. Fossil fuel (e.g. diesel, kerosene, gas) is burned in a strictly controlled atmosphere to generate a CO_2 rich gas stream. The CO_2 is then absorbed at near atmospheric pressure in a packed column with circulated amine solution (traditionally between 8 and 20 wt%).

Carbon dioxide is reclaimed by regeneration of the MEA solution using pressurised steam generated from heat of combustion.

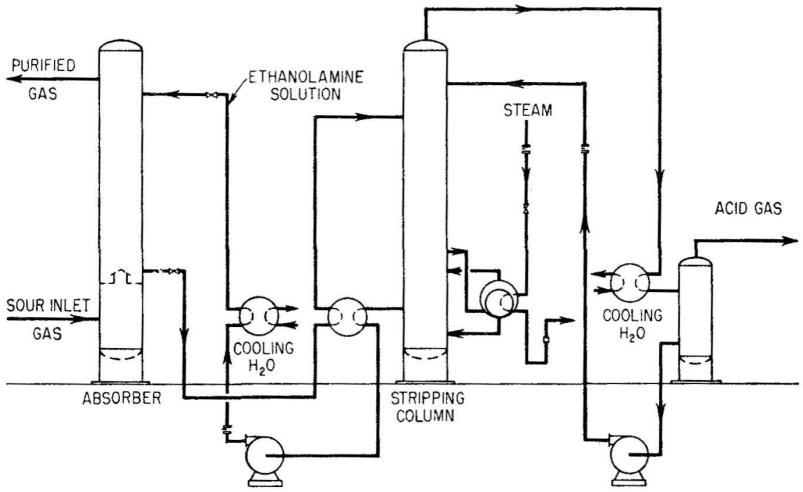

Figure 2.5 Schematic apparatus for CO_2 production.

The gas stream post combustion contains approximately 15% CO_2, and scrubbing is considered successful if the exhaust stream contains less than 1% (10 000 ppm).

2.4.2 Gas Sweetening

Natural gas supplies and liquid natural gas (LNG) may naturally contain up to 20% CO_2 [22], and must be purified to enhance calorific value or prevent malfunctions in a down stream process, such as solidification of CO_2 on cooling or protection of a catalyst [22]. The target CO_2 concentration varies for the application between 10 and 1000 ppm [22]. A packed or plate column is typically used in these applications, with plant similar to the apparatus for CO_2 production [22] [36] (Figure 2.6). Since the feed gas is naturally available at high pressure, absorption is also performed at high pressure. The reclaimed CO_2 may be collected or exhausted as by product [22].

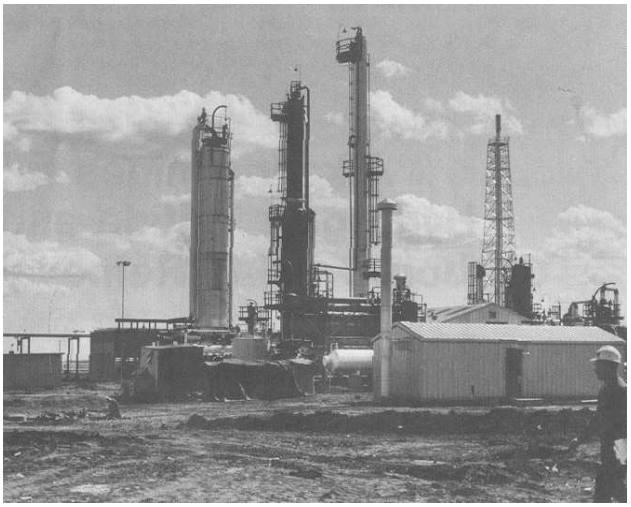

Figure 2.6 Photograph of a natural gas treating plant.
Note building in foreground for scale [36].

MEA concentration is in the same range as that used for CO_2 production. Concentration has in the past been limited to around 15 wt% [23], an empirical balance between performance and corrosion given that the corrosion rate of plain carbon steel is directly proportional to the solution MEA concentration [37].

More recently corrosion inhibitors (including copper and vanadium salts and several proprietary formulations) have allowed investigation of higher MEA concentrations, up to 30 wt% [17] and 50 wt% [38]. Corrosion inhibitors act by forming a stable, adherent oxide layer on carbon steel components, protecting them from further corrosion. The inhibitors also act as oxygen scavengers, preventing oxidative MEA degradation and the resulting corrosive chemical species such as organic acids [17].

Higher concentration solutions provide better performance, though the effect is not linear and enhancement reduces as concentration is increased. Disadvantages include increased vapour losses, solution viscosity and corrosion. Many proprietary amines (with additives) are available [17] with claims of enhanced performance, but these are extremely expensive.

2.4.3 Gas Scrubbing

Some industrial processes (ammonia and ethylene manufacture, LNG feedstock), require gas scrubbing - the removal of almost all of the contaminant - typically to 100 ppm. On an industrial scale this often requires gas sweetening and a subsequent process such as methanation [22] (Figure 2.7). Though it has been suggested amine plants can reduce CO_2 to 50 ppm [23] or even circum 10 ppm, the column height required would be considerable [21].

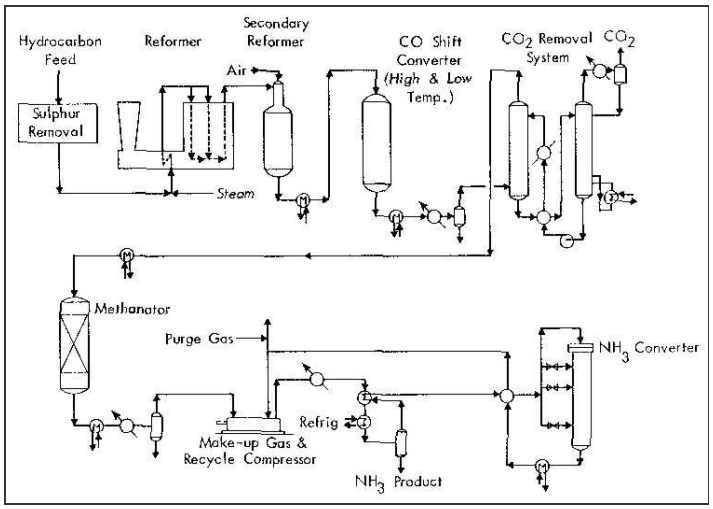

Figure 2.7 Schematic apparatus for ammonia production.

2.5 Concept Generation

2.5.1 Absorber

From the review of prior art with wet scrubbing absorption of CO_2, it was clear that the key function achieved by the absorber apparatus is gas-absorbent interaction [17]. A concept matrix (Table 2.2) enabled an empirical assessment, based on the literature review, of methods for providing interaction in a gas-liquid system. Concepts were evaluated against the criteria listed in the table. Figure (e) within Table 2.2 is an original concept considered to provide the required conditions.

Table 2.2 Absorber Concept Matrix.

	Key + Positive	 - Negative	 • Neutral
	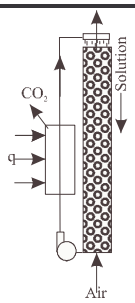 (a) Packed Column [17]	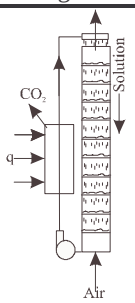 (b) Plate Column [17]	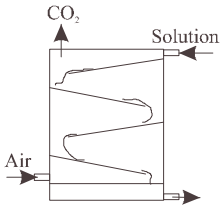 (c) Ramped Column [39]
Common Apparatus	+	+	-
Interfacial Area	+	+	-
Known at Conditions	-	-	-
Physical Size	-	-	•
Cost and Complexity	-	-	•
Operate at $P_{atmosphere}$	-	-	•
Pressure Drop	+	•	+
Stable Operation	+	+	•
Total	**0**	**-1**	**-2**
	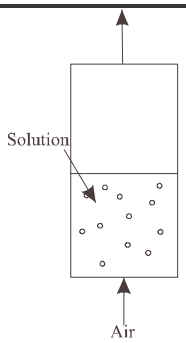 (d) Bubble Column [39]	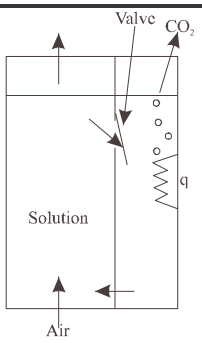 (e) Partitioned Bubble Column	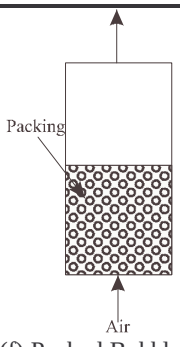 (f) Packed Bubble Column [40]
Common Apparatus	+	-	+
Interfacial Area	+	+	+
Known at Conditions	-	-	-
Physical Size	+	+	+
Cost and Complexity	+	•	+
Operate at $P_{atmosphere}$	+	+	+
Pressure Drop	-	-	-
Stable Operation	-	-	+
Total	**2**	**-1**	**4**

Packed and plate columns (concepts (a) and (b)) are the most common apparatus used in industry [41] to provide gas liquid interaction for absorption and desorption processes. Such applications are invariably designed for large plants (as described in

section 2.4) and usually operate at pressure to enhance performance relative to physical size.

Columns of this type are generally designed by a mixture of theoretical and empirical knowledge [42] established over almost a century. A common design process relies on the concept of the height equivalent of a theoretical plate (HETP). This is the height of packing required for a theoretical 'stage' (degree) of separation, and requires equilibrium data between the solvent and solute. The design can be represented graphically in an operating diagram similar to Figure 2.8 for a MEA - CO_2 absorption process.

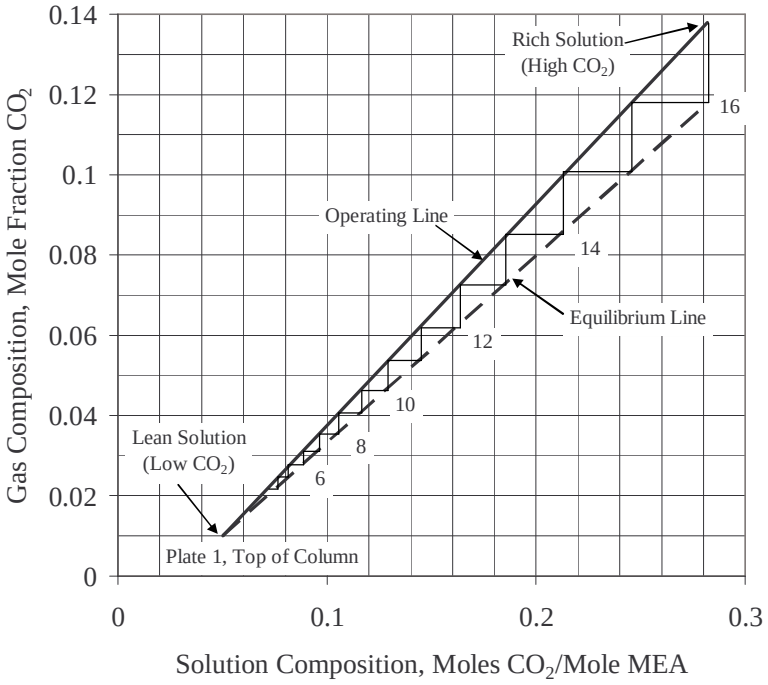

Figure 2.8 Operating diagram for CO_2 absorption from flue gas.
Absorption at atmospheric pressure with 14.5% aqueous MEA solution.
Reproduced from Kohl [17].

The number of theoretical stages is determined by stepping between the operating line, determined algebraically from inlet and outlet conditions of the column, and the equilibrium line, determined from equilibrium data. Each step represents a stage of separation, which is converted to column height by multiplying by the HETP. HETP values depend on the process, solvent and solute concentrations and the apparatus, and are typically a half to several metres in height [17]. As the stepped line

approaches the origin, the stages become smaller, approaching infinite theoretical stages (pinch point) for complete separation in this system.

For CO_2 in air, the mole fraction of CO_2 (y axis of Operating Diagram) is 0.00038 – well below the range of common applications. No chemical equilibrium data between MEA and very low concentrations of CO_2 is available, so although an experienced chemical engineer may instinctively be able to size a pilot plant, rigorous design of a separation column is not possible. Based on available information for the MEA - CO_2 system, the number of stages and therefore height of the column for absorption of CO_2 from air would be very large, and most likely well beyond the size acceptable for AFC systems. A further disadvantage of a packed column is the need for expensive, chemically resistant solution pumps to circulate MEA solution to the top of the column and through the regeneration cycle.

A simpler, cheaper bubble column (concept (d)) is known to provide intimate gas-liquid contact with a relatively small apparatus. Concept (f), a packed bubble column, is a well known advance on the standard bubble column to enhance gas-liquid interaction and process performance.

2.5.2 Regenerator

Carbon dioxide - amine chemistry is preferred because the reaction is reversible, lending itself to continuous operation. Regeneration can be achieved by pressure and/or temperature swing processes. A temperature swing is more appropriate for AFC systems due to the nature of operation and resources available within the system. The key condition for regeneration is heat transfer to the MEA solution, in order to reverse the reaction and evolve CO_2. A concept matrix enabled comparison of possible methods to achieve this (Table 2.3). Figures (a), (b) and (c) in the table are original concepts considered for the regenerator apparatus.

Table 2.3 Regenerator Concept Matrix.

	Key + Positive	 - Negative	 • Neutral
	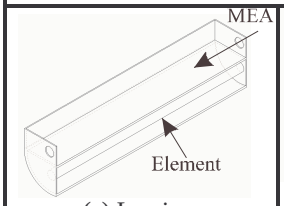 (a) Laminar Flow/Element	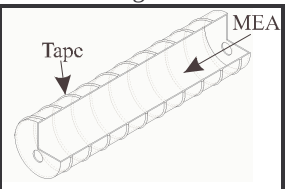 (b) Heater Tape	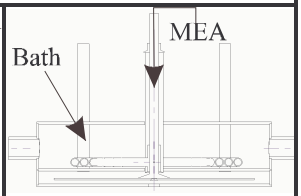 (c) Oil Bath and Cone
Common Apparatus	-	-	-
Good Heat Transfer	-	•	+
Energy Use	+	+	+
Size	•	•	-
Complexity	-	•	-
Continuous	+	+	+
Operate at $P_{atmosphere}$	+	+	+
Aid CO_2 Evolution	-	-	-
Controllable	+	+	+
Passive Heat	-	-	+
Pump Free	+	+	+
Total	**0**	**2**	**3**
	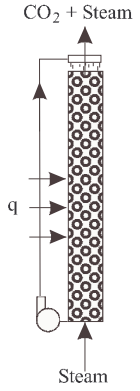 (d) Packed Column [17]	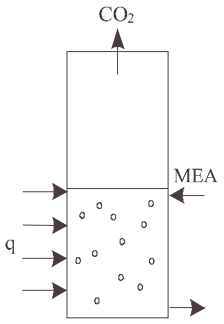 (e) Bubble Column Batch Regenerator [39]	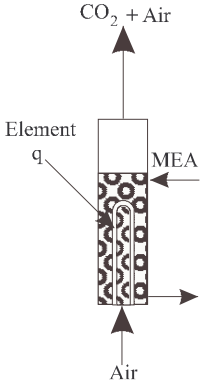 (f) Packed Bubble Column [40]
Common Apparatus	+	-	-
Good Heat Transfer	+	•	+
Energy Use	-	•	+
Size	-	•	+
Complexity	•	+	•
Continuous	+	-	+
Operate at $P_{atmosphere}$	-	+	+
Aid CO_2 Evolution	+	-	+
Controllable	+	+	-
Passive Heat	+	•	-
Pump Free	-	-	+
Total	**2**	**-1**	**4**

2.6 Concept Selection

The concepts presented in Table 2.2 and Table 2.3 were developed from the simplified physical requirements of the absorption and regeneration processes. In both instances concept (f), the packed bubble columns, are most suited to provide the very high gas-liquid interaction conducive to absorption and regeneration within the constraints of the AFC system.

The packed bubble column has not been reported in literature or industry as an apparatus for CO_2 absorption from air or other gas streams. This novel application of the packed bubble column is the basis of an international patent [43] relating to the CDOCS process. Since little information relating packed bubble columns and CO_2 absorption from air was available, experimental characterisation and performance evaluation was necessary. This work is reported in Chapter 4 and Chapter 5.

Chapter 3

ANALYSIS TECHNIQUES

Quantification of scrubber performance requires a measurement system able to accurately measure carbon dioxide in air at low ppm concentrations. In chapter 3 techniques and instruments for measuring high and low concentration CO_2 in air are described and evaluated. The measurement technique selected for ppm measurements of CO_2 is described in detail. More common apparatus for measurement of high concentration CO_2 in air and MEA strength in solution are also described.

3.1 Low Concentration Carbon Dioxide Detection

Determination of absorber performance requires a measurement technique capable of detecting low ppm CO_2 content in air. Atmospheric air contains approximately 380 ppm CO_2 (compared to 280 ppm in the early 1800's) and is currently increasing by about 1.6 ppm per annum. AFC systems require reduction to less than 50 ppm.

A dedicated apparatus capable of real time measurement is preferable, as a delayed analyses method necessitates the capture and storage of samples. Sample storage could introduce inaccuracies including absorption of CO_2 by condensed water or MEA vapour, and CO_2 absorption or generation by reaction with the storage vessel material. These effects could be significant given the extremely low concentration of CO_2 expected in the samples. Capture of the sample and reintroduction to the analytical equipment also exposes the analyses to a higher risk of pollution from air.

3.1.1 Lime Water

Bubbling gas through limewater ($Ca(OH)_2$) is a simple indicator for CO_2, which causes the normally clear solution to go cloudy as a precipitate, $CaCO_3$, forms:

$$CO_2\ (g) + H_2O\ (l) \rightarrow H_2CO_3\ (aq) \quad (3.1)$$

$$Ca(OH)_2\ (aq) + H_2CO_3\ (aq) \rightarrow CaCO_3\ (s) + 2\ H_2O\ (l) \quad (3.2)$$

However, it is extremely difficult, if not impossible, to get accurate, quantitative measurements in the low ppm range with this technique. To get quantities (for example of precipitate) large enough to measure accurately, a large amount of gas is required, creating the somewhat circular problem of designing an absorption apparatus to ensure all of the CO_2 is absorbed from the large volume of gas. This method would be more suited as a long term indicator for the presence of CO_2.

Similarly, gas can be bubbled through barium hydroxide to form a precipitate:

$$CO_2\ (g) + H_2O\ (l) \rightarrow H_2CO_3\ (aq) \quad (3.3)$$

$$BaOH\ (aq) + H_2CO_3\ (aq) \rightarrow BaCO_3\ (s) + 2H_2O\ (l) \quad (3.4)$$

The precipitate $BaCO_3$ is then filtered, dried, weighed, redissolved and titrated with hydrochloric acid. By careful measurements of weight and volume, the CO_2 concentration in the sample gas is back calculated. This method is also difficult for very low CO_2 concentrations and prone to error for such small quantities of CO_2. The process is time consuming and tedious for processing of many samples.

3.1.2 Soda Lime

Soda lime contains a pH indicator, ethyl violet, which causes the colour of the granules to change as CO_2 is absorbed. This provides a long term indicator as to the presence of CO_2, but does not yield quantitative concentration values at specific times, nor enable direct comparison of CO_2 concentrations between two subtly different experiments. Like limewater, soda lime is suitable as an indicator, but with the advantage of reduced pressure drop across the absorber.

3.1.3 Orsat Apparatus

The Orsat apparatus absorbs CO, CO_2 and O_2 from a gas sample, in the order of 100 millilitres, into strong, selective absorbents. Upon sample introduction, the system is sealed and the gas sample is forced through absorbent liquids (KOH for CO_2 absorption) several times using valves and gravity. The reduction in gas volume due to absorption is measured, corresponding to the percentage of absorbed gas originally present.

For atmospheric air, the CO concentration is negligible, and for this application the O_2 absorption step is redundant. While effective down to about ½ a percent of absorbed gas, ppm accuracy is not obtainable with a practical apparatus and gas sample size [44]. For atmospheric air analysis (380 ppm CO_2), the volume of gas absorbed from a 100 millilitre sample is:

$$100 \times 0.038\% = 0.038\,(\text{millilitres}) \tag{3.5}$$

This is too small a volume to measure with the apparatus. Again the method is tedious if performing multiple analyses.

3.1.4 Gas Sampling Tubes

Gas sampling tubes (Figure 3.1) are single use analysers available for a large range of gases and concentrations. They are small glass tubes containing a chemical reagent appropriate to the analyte gas, and an indictor which changes colour as the reagent-gas reaction occurs.

Figure 3.1 Draeger gas sampling tubes and sample acquisition pump.

The tubes are calibrated, so that for a specific volume of gas (typically 100 millilitres), the level of colour change corresponds to a percentage, printed on the tube, of target gas present in the sample. Sample tubes are very quick and easy to use, but are expensive for frequent use and are not available to measure below 100 ppm CO_2.

3.1.5 Fourier Transform Infra Red Spectroscopy

Fourier Transform Infra Red Spectroscopy (FTIR) is a well established gas analysis method. Chemical bonds have vibrational frequencies that are excited by absorption of infra red (IR) light. By choosing frequencies appropriate to the target molecule (CO_2), the amount of radiation absorbed by CO_2 bonds is measured. By caparison to the original source radiation, this is equated to the quantity of CO_2 present. The FTIR system is shown schematically in Figure 3.2.

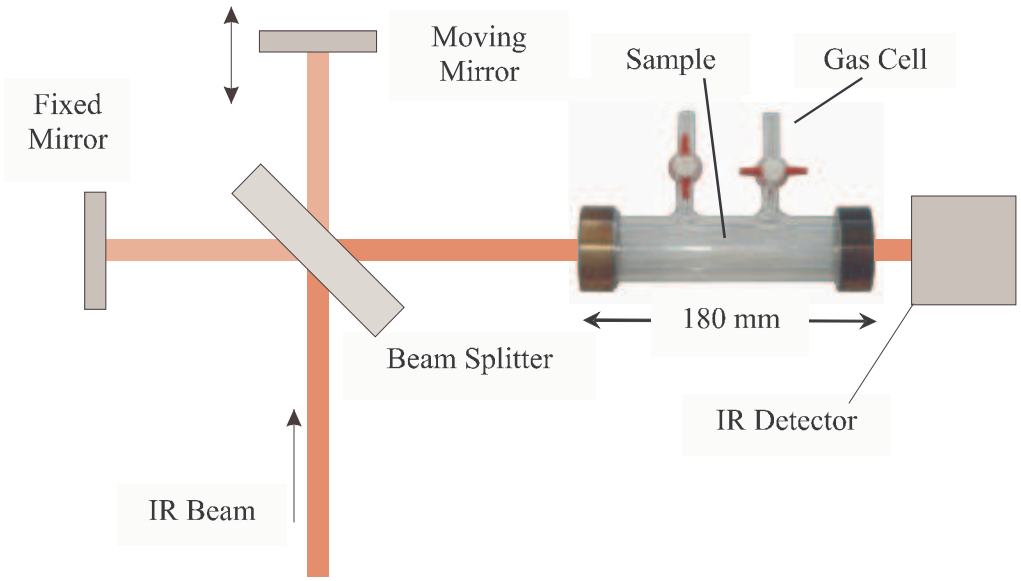

Figure 3.2 Schematic of the FTIR spectrometer, with Gas Cell overlaid.

Although detection at the ppm level is possible, a long path gas cell is required. The maximum path length available in a single pass cell on the FTIR spectrometer at the University of Canterbury Chemistry Department was 180 mm, well short of the length required for ppm resolution. This physical restriction is overcome by using a gas cell with mirrors that reflect the IR light many times through the cell. However, such a cell costs up to NZ$10 000 and was therefore out of the range of this project. FTIR was also inconvenient as gas samples required storage and analysis in batches at scheduled times.

3.1.6 Selected Ion Flow Tube Mass Spectrometer

The Selected Ion Flow Tube Mass Spectrometer (SIFT-MS), developed and operated by the University of Canterbury Chemistry Department, was used in the initial stages of the project. The apparatus had not previously been used to measure CO_2, but was adapted for the purpose by faculty. The technique involves generating specific precursor ions (N_2H^+ in the case of CO_2) which react with the compound of interest but not with other constituents of the gas sample. A quadrupole mass filter isolates the correct ions which are injected, with helium, into the ‘flow tube’. The sample gas is also injected into the flow tube, where the ions and target molecules react. A second

quadrupole mass filter and a particle multiplier counting system analyse the reactant and product ions, giving accurate measurements of analyte compound present. A schematic of the apparatus is included in Figure 3.3.

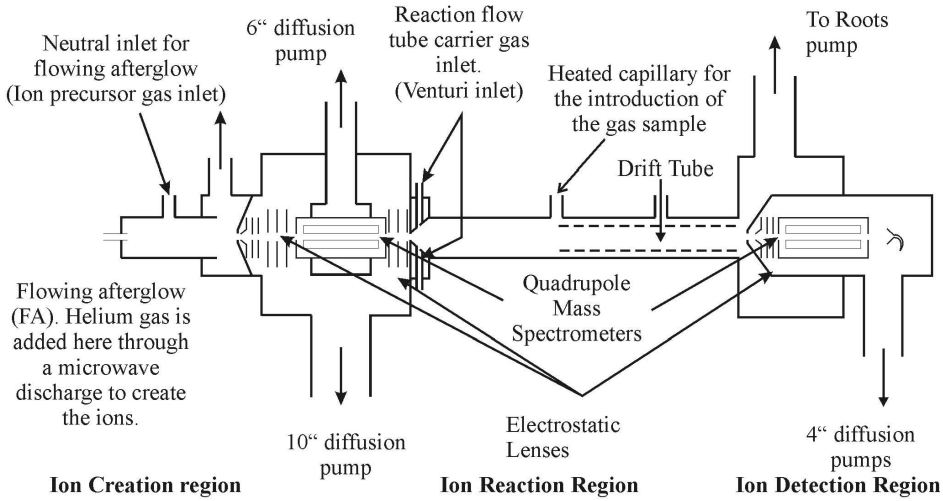

Figure 3.3 Diagram of SIFT-MS spectrometer.
University of Canterbury Chemistry Department.

The SIFT-MS is capable of measuring to part per billion accuracy for many organic substances. Initial testing indicated the technique is capable of very low ppm measurements of CO_2, but further investigation and calibration was required to enable reliable analyses. In particular, there may have been some interference from moisture in the samples, which caused the SIFT-MS technique to over estimate the CO_2 present. Experimentation showed that using a strong dehydrating agent, phosphorus pentoxide (P_2O_5) had no effect on the CO_2 concentration in the samples.

The setup, investigation and subsequent analyses with the SIFT-MS would incur some cost, since there were no other applications for ppm level CO_2 measurement identified. Due to the specific set up for analysing CO_2, analysis of large sample batches would be required with inherent sample capture and storage risk, and considerable inconvenience. Using the SIFT-MS and a calibration gas, mylar balloons were investigated as a storage device for gas samples, and found to have no effect on CO_2 measurements. Gas capture, transport and introduction to the analytical apparatus is possible with a degree of care.

3.1.7 Gas Chromatography

Gas Chromatography (GC) is a widely used industrial and laboratory analyses technique. GC entails the separation of gas and/or liquid components in a mixture, then analysis for the presence and quantity of each component. Analysis for CO_2 is possible by GC methods [45], but the exact resolution obtainable was undetermined.

A key advantage to this technique was the availability of a dedicated apparatus, a Shimadzu GC-9A Gas Chromatograph. Sample analysis was possible at any time, and there was no alteration or contamination of apparatus between samples. A schematic of the GC system is shown in Figure 3.4.

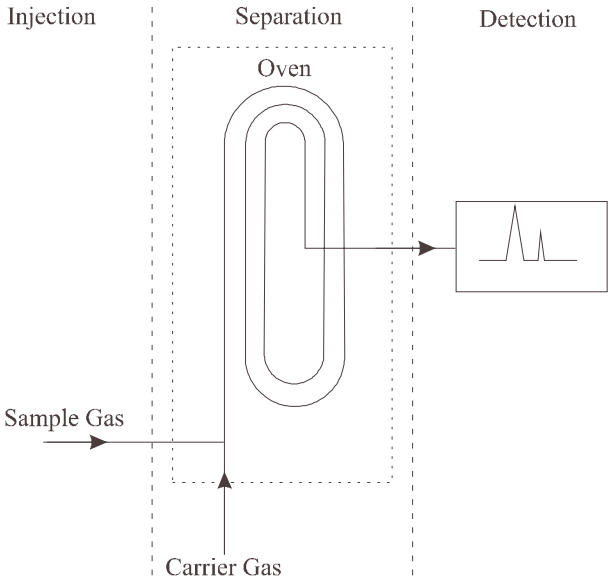

Figure 3.4 Simple representation of a gas chromatograph.
A gas sample is injected into the separation column, and sample components flow through a detector for analysis.

Detector Selection

There are many detection systems available for use in gas chromatography [46] [47] [48] [45], the thermal conductivity detector (TCD) and flame ionisation detector (FID) being amongst the most common [45]. The FID is very sensitive [48], however

CO_2 is one of the few gases to which almost no response is acquired [45] [48]. The TCD is the most universal detector, and is often applied to process control analysis [46] because it can detect such a wide variety of compounds, and is relatively simple, cheap and easy to use [48].

The TCD can detect inorganic gases (O_2, N_2, water vapour, CO_2), to which other detectors have little response [48] [45]. Although it is not generally considered a sensitive detector (the response to a change in measurand quantity is small), Guiochon [46] states low ppm accuracy can be obtained with appropriate conditions. The detector response can be amplified to give higher sensitivity for trace analysis [49]. The apparatus available to the project was equipped with a TCD detector.

Carrier Gas

The TCD requires a carrier gas at all times, to protect detector components from overheating, provide a reference signal, and carry the analyte gas. To gain sensitivity, the thermal conductivity of the carrier gas should be as different as possible to the gas(es) of interest. It is usual to use either hydrogen or helium as carrier gas due to their comparatively high thermal conductivities (Table 3.1, Verdin [47]). The TCD is considered a low sensitivity detector because, given the absolute value of thermal conductivities, the difference between carrier and analyte gases is always small [45].

Table 3.1 Thermal conductivities of selected gases at 100°C.

	Relative Thermal Conductivity	Thermal Conductivity (W/mK)
Air	1	0.024
Helium	5.55	0.135
Hydrogen	6.90	0.168
CO_2	0.70	0.017

Hydrogen is highly flammable and precautions must be taken to disperse the gas safely post analysis. For maximum sensitivity, it is desirable to keep the detector at the lowest possible temperature – just hot enough to avoid condensation of any sample components [50]. In humid air samples water has the highest boiling point, setting the minimum detector temperature at 100°C. A high current through the detector increases sensitivity, but this is counteracted by the risk of detector burnout or base line (datum) instability [50]. With helium carrier gas at low temperatures, the current allowable is approximately 10% higher than with hydrogen (Figure 3.5), and for this reason and ease of use, helium carrier gas was chosen for the experimental investigations.

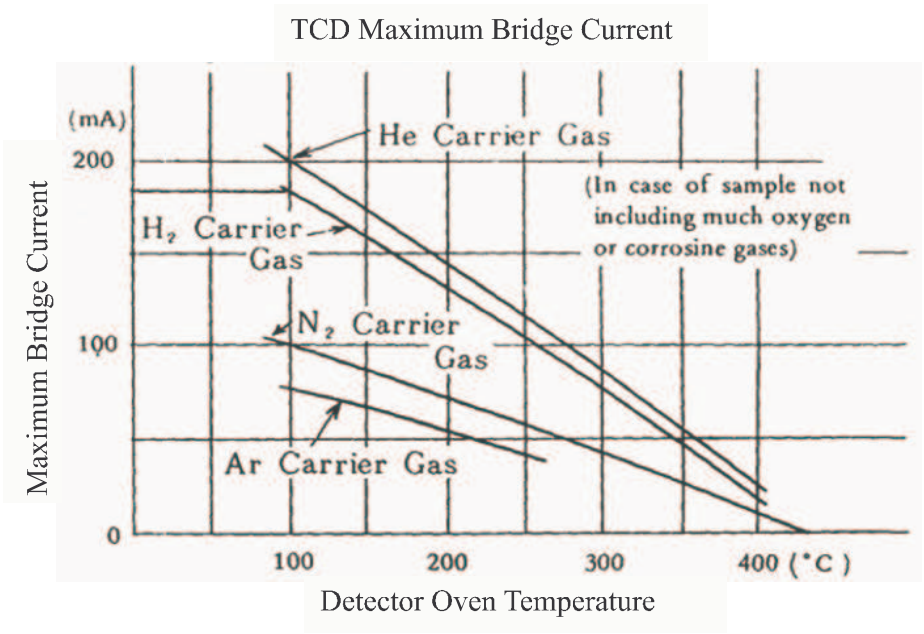

Figure 3.5 Detector temperature and current correlations for various carrier gases. From Shimadzu GC-9A Gas Chromatograph.

TCD

The TCD consists of four current carrying filaments connected in a Wheatstone bridge circuit, encased in an isothermal block of metal. Each filament has the carrier gas passing over it at precisely controlled temperature, pressure and flow rate. The TCD operates on the principle that each gas has a unique thermal conductivity; a gas

with a high thermal conductivity is capable of conducting more heat away from the filament than that with low thermal conductivity.

In equilibrium, the heat generated by each filament is equal to that dissipated by the carrier gas, and the filaments achieve a constant temperature and electrical resistance (a relatively easy property to measure). The balanced branches of the Wheatstone bridge generate a reference voltage or baseline. Any change to the system, such as a different gas flowing over a filament, causes a change in the rate of heat transfer, filament temperature and therefore electrical resistance. The Wheatstone bridge becomes unbalanced and a non-zero output results. In practice, two branches of the Wheatstone bridge have pure carrier gas flowing over them to provide a reference signal, while the remaining two branches are exposed to the carrier gas with sample components (Figure 3.6).

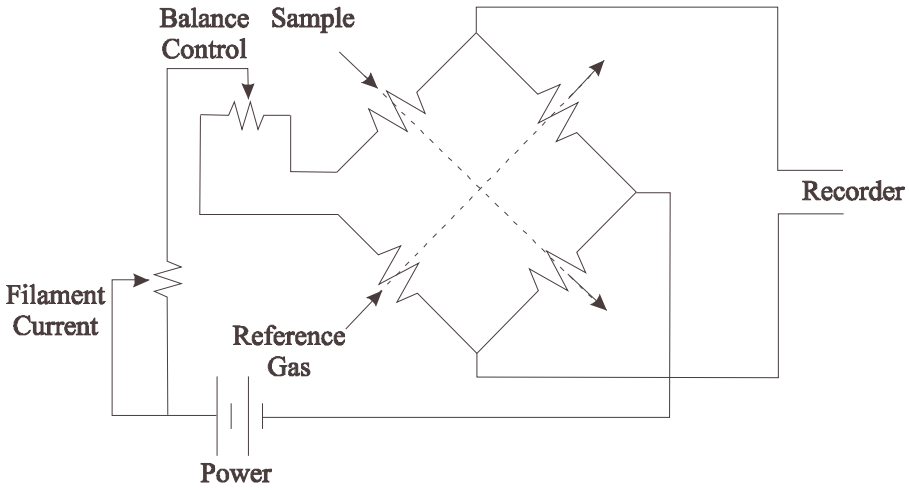

Figure 3.6 Diagram of TCD circuit and gas flows during analysis.

To gain maximum sensitivity to CO_2, it was necessary to run the TCD at maximum allowable current for the detector temperature, low carrier gas flow rate and small gas sample volume. This increased the load on the filaments since less heat was removed and the filaments ran at higher temperature. While increasing accuracy, these modifications also increased background noise, instability and the warm up period of the detector. This was significant for trace analyses as the noise due to operating parameters was large compared to the analyte response.

TCD filaments are corroded by oxygen in the sample gas, also causing instability [50]. The effect of this in practice was an offset in the baseline with each sample. Experiments confirmed the shift of datum had no effect on analytical results. At low temperatures, condensation of high boiling point components on the filaments is possible. With the detector at just 100°C, it is possible for water and traces of MEA vapour to condense. A regular bake out, an increase in detector temperature beyond the boiling point of any possible pollutants, overcame this [50]. Some instability, possibly attributable to condensation, was observed and a bake out was performed daily as part of the experimental method.

Column

A separation column segregates the gas mixture into components in order to identify and quantify specific compounds. In this way, only one component (mixed with the carrier gas) passes over the detector at a time. Separation of the sample gas is commonly performed by a packed column (Figure 3.7).

Figure 3.7 Photograph of a Porapak separation column.
2.5 metres in length.

Packed columns are metal tubes, about 4 mm outer diameter and several metres in length, filled with fine particles or packing. Packing properties are chosen specifically for the application, and cause the separation of the sample components by chemical interaction, physical impediment, or polarity interaction. A packed column exhibits a

characteristic retention time for different compounds – small molecules relative to the packing porosity may pass through almost unhindered (low retention time), while larger molecules can require several hours to work through the column. Similarly some molecules may interact more with the packing due to polarity or reactive groups and take longer to elute. Columns with different packing may be required in series to adequately separate components of interest [46].

The retention time of a particular compound is essentially a physical characteristic of the column and is constant at given operating conditions. Reference to literature and simple experiments with known gases can disclose the retention times for compounds of interest, and ensure adequate component separation. Ideally, all molecules of a particular component would elute from the separation column at the same time, but in reality a normal distribution occurs due to effects of molecular diffusion, sample introduction and mass transfer [47] [45].

Molecular diffusion of the sample within the column occurs in all directions, and axial diffusion (with respect to the column) results in a distribution of the component [47]. Sample injection occurs over a finite period, so the first molecules injected have a slight head start over the last ones, creating a spread [47]. Inappropriate packing or conditions can cause a similar effect, called tailing, due to retention characteristics of certain compounds. The aim when selecting a column packing is to separate the components, but also elute all of each component in as short a period as possible. Failure to achieve this results in a component eluting from the column over time, contributing to tailing, noise or base line instability.

Injecting too large a sample can overload a column. Samples less than 10 millilitres at atmospheric pressure are recommended, and while the exact volume is not crucial [50] [47], it is most important that the volume be repeatable [47]. Generally, a smaller sample provides benefits for both separation and detection [47]. The sample loop on the Shimadzu GC-9A was approximately 1 millilitre.

Lowering column temperature and carrier gas flow rate enhances the performance of a column [47]. Maximum column temperature is determined by the detector temperature, which is approximately 50°C warmer than the column [49]. As with the

detector, minimum column temperature is determined by the nature of samples introduced – too low a temperature will result in condensation of some components, or excessively long elution periods causing the column to become congested with traces of the component [47]. To achieve adequate sensitivity to CO_2 the oven temperature, 40°C, is well below the boiling point of water at the column pressure. This causes water to elute gradually from the column instead of as a well defined component over a finite period.

Back flushing, reversing the carrier gas flow once the components of interest have eluted, overcomes problems induced by bleeding or long elution time. Back flushing avoids a gradual change in column properties, or causing baseline instability as a heavy component elutes from the column [47]. However, the GC available to the project was not equipped for back flushing. An alternative is to regularly bake out the column by raising the temperature beyond the boiling point of any sample component. For the CDOCS project column bake outs were performed overnight, in conjunction with the detector bake out, so as not to interfere with analysis.

Packing

Porapak is a commercially available porous packing comprised of uniformly structured beads of distinct pore size, providing a large surface area in the column [50]. There are several types of Porapak – P, Q, R, S,T and N, all available in various mesh (bead) sizes. Types P and Q are non polar (as is CO_2), with type P having a larger pore size than Q. Type Q Porapak is the most versatile, used for separation of low molecular weight components (< 300 g/mole) [50]. Porapak Q can separate CO_2 from air and water, though the usual rapid elution of water [50] was not possible at the conditions imposed for the project. Two 2.5 m Porapak Q columns in series adequately separated CO_2 from air (N_2 and O_2) and water. The retention time for CO_2 in the series columns was five minutes.

Injection

The analyte gas sample is introduced to the column, which operates at strictly controlled temperature, pressure and gas flow rate. There are two ways to accomplish

sample introduction – manual injection with a syringe or automatic injection using mechanised valves. For manual injection, a syringe needle pierces a rubber or plastic septum and the plunger is depressed. The septum seals around the needle and reseals when the needle is withdrawn. Injection by syringe has obvious potential for variation between samples. The sample quantity and injection procedure (particularly speed of injection) is user specific, and may cause variation in results with even the utmost care. Therefore, the use of a syringe is not recommended for gas sample injection [46].

The Shimadzu GC was equipped with an automatic injection system of rotary style sample valves, schematically shown in Figure 3.8. Upon command, an electric motor actuates the valve from flushing to sampling position. The valve channels allow introduction of an appropriate volume of sample gas (approximately 1 millilitre), but most importantly the volume and injection dynamics are highly repeatable [46].

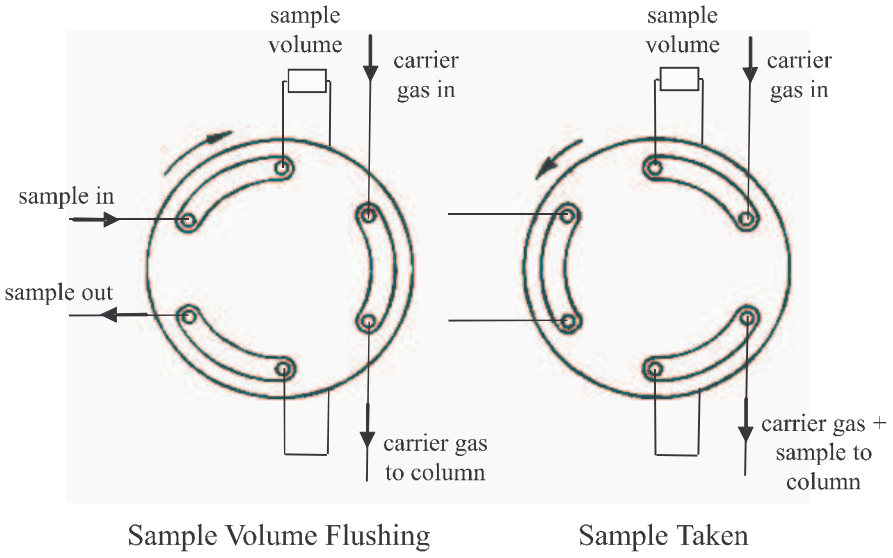

Figure 3.8 Six port rotary gas sample valve.
Flushing (left) and sampling (right) positions (Verdin [47]).

A diaphragm pump flushed the sample gas through the system for 90 seconds (equivalent to 4 times the entire sample system volume). To ensure constant sample pressure and good repeatability, the sample was then allowed to equilibrate to atmospheric pressure before injection into the separation column. Equilibration took

approximately twenty seconds [46], during which time it could be possible for air to diffuse into and contaminate the sample. A 5 m length of internal diameter 2 mm tubing upstream of the sample valve, and a 100 millilitre reservoir downstream, achieved a protective buffer against air contamination [46].

GC-TCD Parameters

The operating conditions for the GC and TCD during analysis and bake out are listed in Table 3.2 and Table 3.3 respectively.

Table 3.2 Gas chromatograph and TCD analysis parameters.

GC-TCD Parameter	Specification
Carrier Gas, flow	Helium (IG), 30 millilitres/minute
Primary Pressure	6 kg/cm^2
Sample Column	2 x 2.5 m Porapak Q in series
Reference Column	2.5 m Molecular Sieve
Column Pressure	1.4 kg/cm^2
Sample Volume	~ 1 millilitre
Detector	TCD
Detector current	190 mAmp
Detector Temperature	100°C
Oven Temperature	40°C
Injector temperature	100°C

Table 3.3 Gas chromatograph and TCD bake out parameters.

GC-TCD Parameter	Specification
Carrier Gas, flow	Helium (IG), 30 millilitres /minute
Primary Pressure	6 kg/cm^2
Sample Column	2 x 2.5 m Porapak Q in series
Column Pressure	1.4 kg/cm^2
Detector current	100 mAmp
Detector Temperature	200°C
Oven Temperature	180°C
Injector temperature	200°C

Results

The detector output is recorded with time as a graph (chromatogram) as shown in Figure 3.9. With knowledge of the separation column, each peak is attributable to a sample component by matching the retention time.

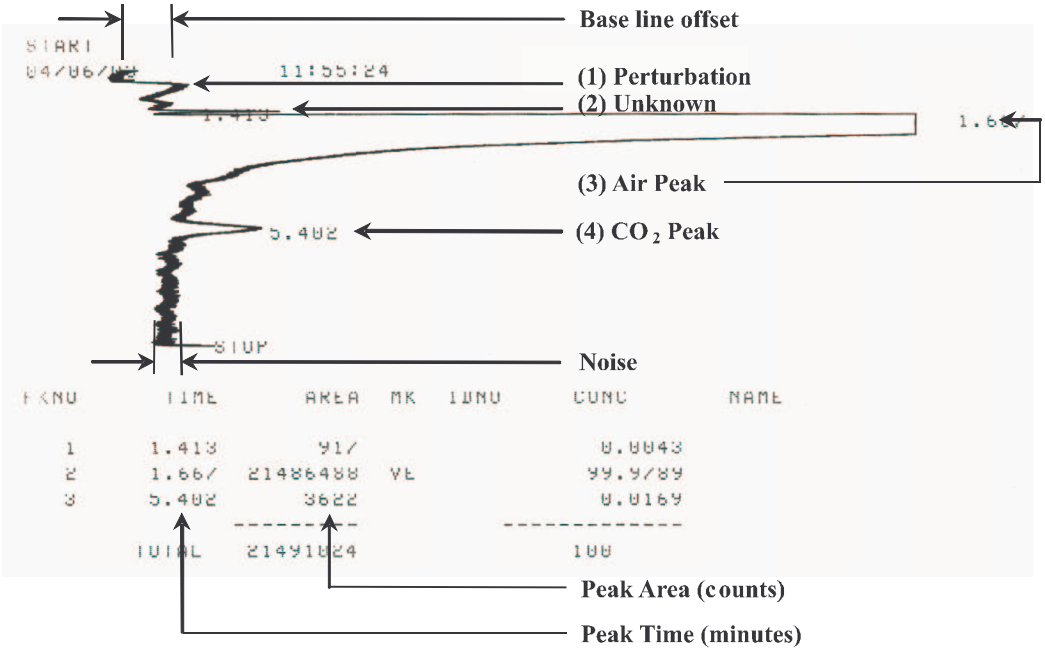

Figure 3.9 Typical chromatogram of a scrubbed air sample.

To obtain suitable response to low ppm CO_2 samples an instrumentation amplifier, with 1 kilohertz low pass filter, multiplied the TCD output by a factor of 10. The amplification increased peak size for integration but also base line noise. An electronic integrator quantified peak size or area, which is proportional to the quantity of component present. The GC 9A was equipped with a Shimadzu C-R3A Chromatopak recorder. This device prints the chromatograms and performs an electronic integration of the peaks, providing a peak area that can be correlated to CO_2 concentration.

Figure 3.9 is a typical chromatogram for analysis of CO_2 in scrubbed air under the conditions described and detailed in Table 3.2. Noise, due to high sensitivity, caused baseline distortion. Peak (1) is a perturbation peak from sample injection. Peak (2) is probably a trace component of air, but no attempt was made to identify it. The remainder of the air sample, nitrogen and oxygen, elute together and display some tailing (Peak (3)). By the time CO_2 elutes, five minutes after injection (Peak (4)), the baseline is sufficiently flat for analysis (and slightly offset due to oxygen effects on the filaments).

Following the chromatogram, the Chromatopak prints the peak times and integrated peak areas in units of ‘counts’. The CO_2 peak area was manually converted to a concentration (ppm) by reference to results from a standard sample. BOC Gases supplied a calibration gas containing 18.3 ± 0.2 ppm CO_2 in helium for this purpose (recipe number MB83229), analysed by FTIR with a long path gas cell.

There are many considerations for the accurate integration of peak area [48] and only a brief description is given here. The Chromatopak identifies a peak by its tangent slope varying with time faster than a preset rate (Figure 3.10(a)). Electronic programs are designed to cope with imperfect chromatograms including those with tailing, unresolved (overlapping) peaks and base line drift (Figure 3.10(b)-(d)). In general the Shimadzu apparatus achieved good separation, and any baseline drift was minimal compared to the CO_2 peak width. Table 3.4 contains specific details of the settings used for the C-R3A Chromatopak.

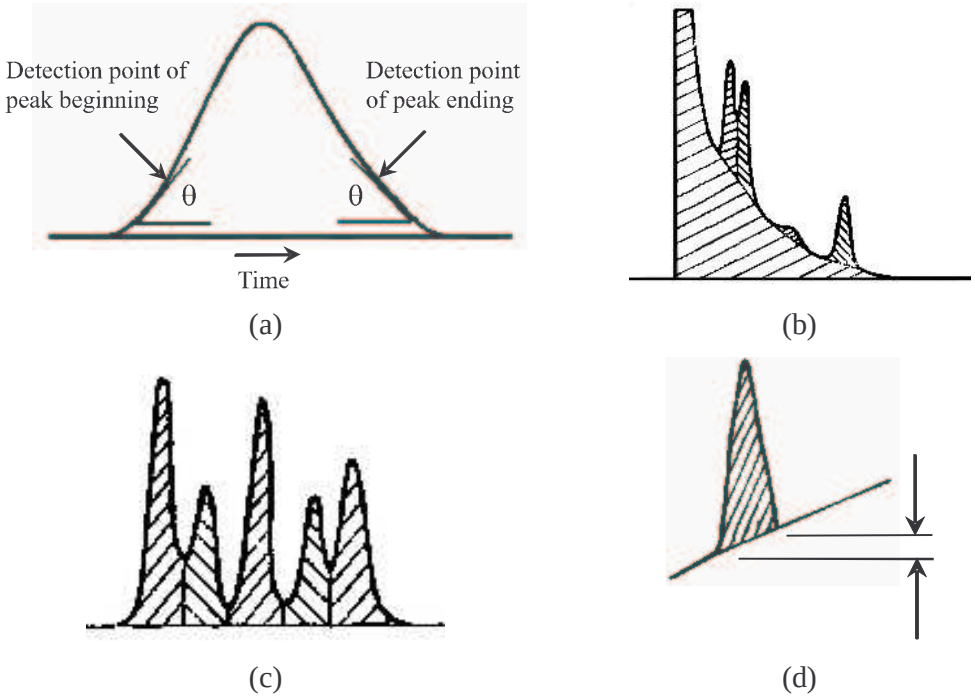

Figure 3.10 (a) Peak detection by analysis of slope, (b) Peak tailing with subsequent peaks on tail, (c) Unresolved (coincident) peaks and (d) Baseline drift.

From Shimadzu C-R3A Chromatopak instruction manual [51].

Table 3.4 Shimadzu Chromatopak processing parameters.

Chromatopak Parameter	Specification
Minimum Peak Width	10 seconds
Peak Detection Sensitivity	500 μV/minute
Degree of Baseline Drift	0 μV/minute
Minimum Peak Area	500 counts
Method	0041 – Area Normalisation

GC Uncertainty Analysis

Errors contributing to uncertainty can be divided into two categories, bias (or systematic) error and precision (or random) error [52]. Possible contributions to uncertainty in GC results were identified, separated into these groupings and evaluated.

Bias Error

For a set of measurements taken under identical conditions, bias error shifts the sample mean from the true value. The following factors contributed to bias error of the gas chromatograph:

Calibration

Results from the GC-TCD analyses relied solely on the calibration standard supplied by BOC Gases. If the standard was not accurate, all measurements derived from the GC were offset from the true CO_2 concentration. Given the stated accuracy of the standard (± 0.2 ppm) and the inability to verify accuracy by independent means, it is reasonable to assume calibration error was negligible. Further bias error due to the standard gas is possible if calibrations are performed intermittently over a long period. It is possible for the standard gas composition to change due to diffusion over time, hence BOC certify the standard for one year only. This error was also negligible since calibrations were deliberately performed within a one year time frame.

Interference

Constant electrical interference from sources such as laboratory lighting and the CDOCS air blower affected output because of the highly sensitive TCD operating parameters. The observed result of interference was a baseline datum shift, but for constant sources of interference, the error induced was negligible since a datum shift does not interfere with CO_2 peak integration.

Column Separation

Carbon dioxide elutes in a similar manner for every sample, assuming identical preparation and injection conditions. The retention characteristics of the column generate a normal distribution, causing a small quantity of CO_2, the very first and very last molecules to elute, to become lost in the baseline noise. It is reasonable to assume

this bias error was constant and negligible since analyses are comparative and all, including the calibration standard, were subject to the error.

Column Bleeding

Bleeding of the column packing is very unlikely at analysis temperature, but water and MEA bleeding is probable. The observed effect was a baseline drift of far greater period than the CO_2 peak. The result of the drift, with respect to the relatively short period CO_2 peak, was a datum shift, which does not affect peak integration.

Oxygen Effect on Filaments

The observed effect of filament exposure to oxygen is a stepwise datum shift as shown on Figure 3.9. The shift occurs prior to CO_2 elution, so the CO_2 peak is resolved on a flat baseline with no effect on quantification. Datum shifts accrued during multiple analyses, but the nightly TCD bake out counteracted the effect.

Precision Error

Precision errors result in random variations in repeated analyses, giving rise to the common normal distribution of sample data about a sample mean.

Instrument Insensitivity

Precision error arises when the instrument does not give adequate response to the measurand. This error source is likely to be significant for a GC TCD measuring low ppm CO_2 concentrations. The thermal conductivities of gases are of similar magnitude, physically restricting the sensitivity of the detector. It is for this reason that the GC TCD was operating at the absolute limit of sensitivity, resulting in instability and noise.

Helium Control

GC and TCD components are designed to accurately control the pressure, flow and temperature of the carrier and sample gases. However, especially at trying conditions such as used for the project, some variability is inevitable. The contribution to overall uncertainty was deemed small compared to the chief errors in the system.

Sample Technique

Assuming highly repeatable sample volume and injection by the mechanical valves, the largest variation in the sample technique was the pressure in the sampling system prior to injection. Sample pressure affects the volume of sample introduced and therefore the quantity of CO_2 detected. Following flushing, the gas sample equilibrated to atmospheric pressure for 20 seconds, established by a balance between pressure equalisation and the risk of sample contamination by diffusion. As recommended by Guiochon [46] and found by experiment, 20 seconds was adequate for pressure equalisation resulting in good repeatability. The day to day variation in atmospheric pressure was negligible, causing the quantity of CO_2 to vary by less than the resolution of the apparatus.

Detector Control

The TCD is accurately controlled to maintain constant temperature (± 0.1°C) and current flowing in the filaments. The GC and TCD are designed specifically for this purpose so the error is minimised. Some variation in temperature and current is unavoidable, but negligible for this application.

Interference

As well as interference bias error, precision errors resulted when electrical devices in the laboratory were turned on or off during analysis. For example the diaphragm pump, which flushed air through the sample loop, caused a sharp spike in the chromatograph if turned on or off during recording. This did not affect analysis in practice since the pump was turned off before sample injection, but other devices in the laboratory had a similar effect and sometimes occurred at less opportune times.

Because they are very sharp, interference peaks have a very small integrated area and do not contribute significantly to error. However a datum shift due to interference, coinciding with the CO_2 peak, affects quantification of CO_2 and results of this kind were discarded.

Peak Processing

Significant precision error occurred at peak integration due to baseline noise. Amplification aggravates noise but was necessary to provide adequate sensitivity. The error induced was random but within a small range of magnitudes, related to the width of the baseline. The peak area error diminishes as the analyte CO_2 concentration, and peak size, increase.

Resolution

Resolution refers to the smallest detectable change in the measurand. Under ideal conditions, the resolution of the TCD for CO_2 was approximately 5 ppm. However this pertains to measurements in the order of 100 ppm (with appropriate calibration standard), as opposed to 20 ppm. At higher CO_2 concentration the response amplification can be reduced and aforementioned errors greatly diminished. At low ppm measurements the resolution deteriorates as precision errors escalate.

Relative Error

Precision errors are the main contributor to uncertainty. From 27 repeated measurements at nominally identical conditions, the estimated sample mean, x_m, based on the 18 ppm gas standard was 1854 counts, or 100 counts per ppm. The standard deviation, σ, was 288 counts or 2.9 ppm. The error in the estimated mean is represented by Eq 3.5 where N is the number of samples, 27 [52].

$$\begin{aligned} error &= \frac{\sigma}{\sqrt{N}} = 55\,(\text{counts}) \\ &= 0.6\,(\text{ppm}) \end{aligned} \tag{3.6}$$

The standard deviation is also the estimated error in each individual measurement (statistical error), ± 2.9 ppm. Relative error is a more useful measure of uncertainty over the range of concentrations encountered. For the 18 ppm standard samples, the relative error was

$$\text{Relative Error} = \frac{\sigma}{x_m} \times 100\% = 16\% \tag{3.7}$$

This corresponds to an error of 60 ppm at atmospheric CO_2 concentration, based on the 18 ppm gas standard. If desired the error at atmospheric or other concentrations can be greatly reduced by calibration with a more appropriate gas standard.

Accuracy

Accuracy is a combination of both precision and bias errors, and reflects the measurement system's ability to indicate the true value of the measurand. Bias errors for the Shimadzu apparatus and application were negligible because the error effectively cancelled out due to the comparative nature of the analyses. The largest errors were precision errors, particularly from lack of sensitivity and, related to this, the peak processing. The percent accuracy of the instrument is reflected by the relative error according to Eq 3.7 [52], equal to 84 %.

$$\% \text{ Accuracy} = 100\% - \text{Relative Error} \tag{3.8}$$

The linearity and range of the detector were not fully investigated since the most valuable results were from the very low ppm analyses. However, the instrument detected atmospheric concentration, an order of magnitude higher than the calibration range, with reasonable accuracy as calculated above. This indicates that atmospheric CO_2 concentration, 380 ppm, was just within the linear range of the detection system.

3.2 High Concentration Carbon Dioxide Detection

Analysing gas flow from the regenerator in real time enables easy identification of improvements to regenerator conditions, and gives a quantitative measure of CO_2 evolved. Several industries use CO_2 detection and monitoring in the percent range, as expected from the regenerator.

3.2.1 Infra Red Detection

The most common technique for CO_2 monitoring is infra red detection. As with FTIR, the analyser exploits the characteristic absorption of infra red energy by the target gas. Following calibration of the analyser, the amount of CO_2 in a sample is determined by comparison with a reference signal. The difference from FTIR is in data collection and conversion. FTIR collects all wavelengths simultaneously, and processes the signal (performs a Fourier Transform), making FTIR fast and capable of much more accurate measurements. For percent measurements though, infra red detection is well established. Commercial units are widely available to continuously read the CO_2 concentration in an atmosphere.

A Draeger Polytron IR CO_2 detector (Figure 3.11) was used to monitor the CO_2 concentration in the regenerator off gas. The detector has a gas permeable filter, allowing surrounding air to enter the optical path of the instrument. A liquid crystal display continuously presents the CO_2 concentration as a ppm or percent value. Like the GC, the main advantage for this project was the availability of a dedicated analyser.

Figure 3.11 Draeger Polytron IR CO_2 detector.
Commercially available unit used for high concentration CO_2 analyses.

The Polytron is calibrated at the time of purchase. Although documentation states a measurement range from 0-2000 ppm, the zero point calibration must be performed with gas containing 'less than 50 ppm' CO_2. The detector cannot therefore be used to measure very low levels of CO_2. This was reinforced by inaccurate ambient CO_2 measurements (frequently around 650 ppm). This error becomes insignificant for high concentration measurements (stated repeatability less than 0.05 volume percent) such as those from the regenerator, to which the device is more suited.

3.3 MEA Analysis

3.3.1 Gas Chromatography

Monitoring of MEA concentration, loading and pH is important to identify the state of a solution and the effects of changing concentration. In principle, gas chromatography is capable of measuring all of the components in solution, and with good accuracy given the high concentrations. In practice however, it was not possible to separate the component peaks with common columns available.

It is also theoretically possible to use the same GC as for gas sampling, but the operating parameters and warm up period required prohibited this. The GC operating temperature must be higher than the boiling point of all components, to ensure

samples remain in the gaseous phase, and to speed elution. Therefore the GC operating temperature for liquid analyses (boiling point of MEA 170°C) is far higher than for gas analyses (boiling point of water 100°C) and long warm up and cool down periods are required. Experiments showed that alternating between amine and gas samples affects the CO_2 concentration results, presumably due to residual MEA in the column. For these reasons, an independent GC would be necessary.

3.3.2 Nuclear Magnetic Resonance

Liaw [53] investigated the use of Nuclear Magnetic Resonance (NMR) to identify compounds in monoethanolamine/monoethyleneglycol/water/carbon dioxide ($MEA/MEG/H_2O/CO_2$) solutions. NMR spectroscopy analyses the radio frequency of energy given off by atomic nuclei, which is dependent on the atomic arrangement around the nuclei. Specific atomic arrangements in a molecule can be targeted, allowing analysis for elected compounds.

Liaw concluded that the chemical species in the $MEA/MEG/H_2O/CO_2$ system are identifiable and quantifiable to good accuracy. The technique was used extensively by Liaw, and some samples were processed for this project. However, the complexity of the technique restricted its service to experienced operators, and the available apparatus (University of Canterbury Chemistry Department) was in high demand. Exact analysis was not required for this project and a more convenient and timely technique was preferable.

3.3.3 Titration

Titration of MEA solution with acid (HCl [23] or H_2SO_4 [30]) and indicator (methyl red or methyl orange [38]) gives the molar concentration present with relative ease. This technique yields accurate results for fresh solution (no CO_2 exposure), but slightly underestimates the MEA concentration for carbonated solutions. HCl reacts only with free MEA in solution, not MEA bound to CO_2 but still regenerable (carbamate). However the amount of carbamate is relatively small below 0.35 loading [54] so the effect is minimal.

This technique is adequate for monitoring the state of solution, with the added benefit of simple, dedicated apparatus. For this project 2.5 millilitres of solution was titrated with 0.1 molar HCl and methyl red indicator. Up to 21 millilitres of HCl was required to neutralise the MEA, depending on solution history.

Loading of an MEA solution can be determined by heating a solution in the presence of excess $BaCl_2$. Carbon dioxide evolves at the elevated temperature and reacts to form a precipitate, $BaCO_3$. Titration of either the precipitate or filtrate with HCl and methyl orange gives the concentration of uncarbonated amine in the original sample. A second titration, of the unprecipitated sample, is also performed, and the difference in amine concentration yields the CO_2 content [55] [30]. For the absorber, little additional knowledge would be gained from the loading and, given the complication of the measurement, the technique was not pursued. An approximate loading could be back calculated from the volume of scrubbed gas and moles of MEA used if necessary.

3.3.4 pH Meter

A second simple technique to monitor the MEA solution is pH determination by an Orion Research 701A/digital Ionalyzer from the Department of Chemical and Process Engineering, University of Canterbury. The pH value of a solution is the negative log of its hydrogen ion concentration:

$$pH = -\log[H^+] \tag{3.9}$$

The Ionalyzer measures pH by comparing the potential of the unknown solution to that of a known reference potential. The voltage ratio, which changes proportionally with H^+ concentration, is measured, converted to a pH measurement by the Nernst equation, and shown on a liquid crystal display. The Ionalyzer uses a combination electrode, housing the reference and sensing electrodes in the same body for quick and easy measurement. The electrode was calibrated with, and stored in, a solution of known pH.

Chapter 4

COMPONENT EMBODIMENT

In chapter 4 a literature review of the apparatus selected to perform the CO_2 absorption process is presented. The effects of various operating parameters are described, and the selection of chemicals comprising the absorptive solution considered. Material selection for a prototype system is discussed, and developmental prototype CDOCS components described in detail. Theoretical energy requirements of the prototype apparatus are calculated.

4.1 Apparatus Concepts

From concept matrices for the absorber and regenerator, the packed bubble column apparatus were chosen (Figure 4.1(a) and (b)). The columns provide gas liquid interaction to aid absorption and regeneration at low and high temperature respectively.

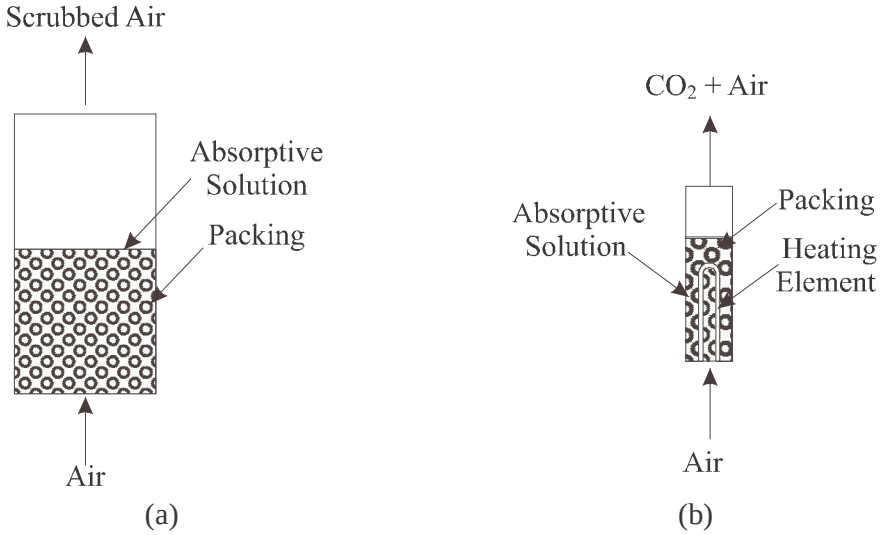

Figure 4.1 (a) Absorber concept and (b) Regenerator concept.

Due to the differences from processes described in literature [44] [35] [40], characterisation of the apparatus was required in order to define performance and determine design relations. Initially the two system components, absorber and regenerator, were evaluated independently.

4.2 Absorber

4.2.1 Column

Bubble columns are used increasingly for absorption with chemical reaction [40]. In its simplest form, a bubble column contains a volume of liquid and some method of injecting a continuous gas stream into it. Bubbles of gas are released and move through the liquid under buoyancy forces, during which time absorption, desorption or reaction occurs.

Research indicates that bubble columns are very simple, low cost and compact while providing high interfacial area and mass transfer between the gas and liquid phases [40] [56] [57]. Bubble columns are especially useful when a large residence time (contact time between gas and liquid) is required [40]. Other relevant advantages of bubble columns are the ability to handle solids, absence of moving parts [57], good heat transfer rates [39] and no complicated sealing [58], which is of particular benefit for an MEA system.

4.2.2 Bubble Dynamics

The injection of bubbles into liquid provides the necessary interaction between gas and liquid to enable absorption to occur. The success of the operation is most dependent on bubble size, interaction and residence time. The bubble rise velocity depends mostly on liquid properties and bubble size (smaller bubbles have slower rise velocity) [56]. Operation and performance is generally independent of gas properties [59] [39] [56] and column operating pressure [59]. However when absorbing from lean gas streams (as is the case of CO_2 from air) the gas side resistance to mass transfer is significant [58] [44] [40].

4.2.3 Packing

Filling the bubble column with low volume, high surface area packing offers several benefits. Packing prevents bubble coalescence and controls the maximum bubble size, thereby increasing interfacial area [60]. Reduced coalescence gives smoother operation at high gas flow rates. Unpacked columns are prone to excessive vibration caused by violent manipulation of the liquid phase by large gas bubbles [61]. Packing and related hydrodynamic affects contribute negligible pressure drop compared to the liquid head in the column [62] [56]. Packing also increases the gas hold up, or time it takes for the gas to rise through the liquid, by physical hindrance and by maintenance of smaller bubble size in the absence of coalescence [63].

Figure 4.2 shows three generic packing types of relevance. All are commonly available and, though not designed for the purpose, suitable as bubble column packing. The most effective packing, such as Pall rings, provide small average bubble size with minimal liquid volume displacement.

(a) (b) (c)

Figure 4.2 Packing elements for bubble column reactors.
(a) 20 mm diameter plastic Raschig ring, (b) 15 mm diameter stainless steel Pall ring, (c) 25 mm diameter polyethylene Pall ring.

4.2.4 Flow regimes

There are three commonly recognised flow regimes in bubble columns. The bubble (or homogeneous) regime exists at low flow rates (<0.05 m/s [58] [56]). Uniform, individual bubbles or swarms of bubbles rise through the liquid [61], as shown in

Figure 4.3(a). The churn turbulent or recirculating regime [40], at high flow rates (> 0.1 m/s [56]), exhibits turbulence and high liquid recirculation (Figure 4.3(b)). High flow rates (>0.5 m/s, [63]) in relatively small diameter columns induce slug flow (Figure 4.3(c)), whereby bubbles coalesce and adhere to the walls of the column [58] [40], rising as large single bubbles. Industrial columns operate in the churn turbulent regime, which is most useful for gas liquid interaction and high gas throughput [57] [40]. Columns less than about 0.07 metres in diameter do not adhere to the described behaviour [63].

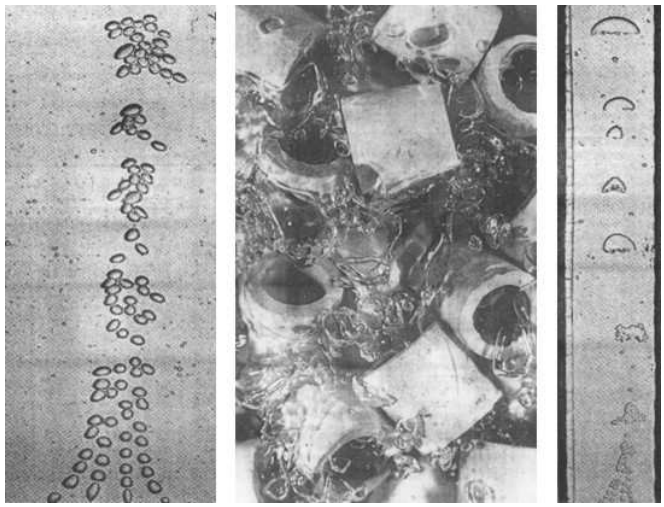

(a) (b) (c)

Figure 4.3 Visualisation of flow regimes.
(a) Homogeneous [64], (b) Churn turbulent [62] and (c) Slug flow [64].

4.2.5 Design

While a body of work exists on the properties and design of bubble columns, scaling is difficult due to hydrodynamic conditions changing with size [40] [58] [57]. It is generally accepted that the length to diameter ratio should be maintained between 3 and 12 to develop a churn turbulent flow and avoid slug flow, which is detrimental to the absorption process [59] [56]. Between these limits, the column diameter has little effect on absorption [59]. Superficial gas velocity, the volume flow rate of gas divided by column cross sectional area, may be used as a criterion for scaling [59] [56].

For high flow rates in the churn turbulent regime (> 0.1 m/s [56]), the gas injection method, or sparger, is of little importance [39] [59]. Optimising pressure drop gives rise to simply using an open tube to inject the gas [59]. In this regime, a liquid flow up the centre of the column is induced by the gas, and a matching return flow rate of liquid exists down the walls of the column [40].

The key disadvantage of the packed bubble column is the pressure required to feed gas into the bottom of the liquid pool [57] [58]. For this reason, the liquid depth should be minimised by design. By raising the injection point and adding additional liquid the absorber can contain a greater volume of solution, increasing longevity without increasing pressure drop. In the churn turbulent regime the solution below the injection point is completely mixed in the absorber.

4.3 Regenerator

4.3.1 Column

The purpose of regeneration is to reduce the partial pressure of CO_2 in the MEA solution to less than the partial pressure of CO_2 in the scrubbed gas, thus maintaining a driving force for absorption. The regenerator supplies the sensible heat required to bring the solution to temperature plus the heat required to reverse the CO_2 - amine reaction (85 kJ/mole at low loadings [17]). In industry the scrubber is always part of a bigger system [22] so regeneration is performed with a large packed column using steam generated from waste heat.

Curnow [65] reported the use of a packed bubble column for regeneration of CO_2 in MEA-MEG aqueous solutions. Regeneration was achieved at comparatively low temperatures (from 80°C) and atmospheric pressure by providing gas-liquid surface area and generating turbulence in the column.

4.3.2 Bubble Dynamics

CO_2 evolution is limited by the desorption rate at the gas-liquid interface. This rate can be maximised using a packed bubble column with inert gas injection, which reduces the liquid and gas side resistance to diffusion. A maximum gas flow rate exists, beyond which no increase in desorption rate or total regeneration is achieved [65].

4.3.3 Liquid Flow

The regenerator requires a constant flow of solution for continuous operation. The emulsion formed by forcing a large air flow rate through a liquid column generates a small pressure head, ΔP, due to gravity (Figure 4.4). By connecting a tube from the side of the absorber, within the emulsion depth, to the bottom of the absorber a low resistance path is provided for gravitational feed of solution (as opposed to down the column walls [40]).

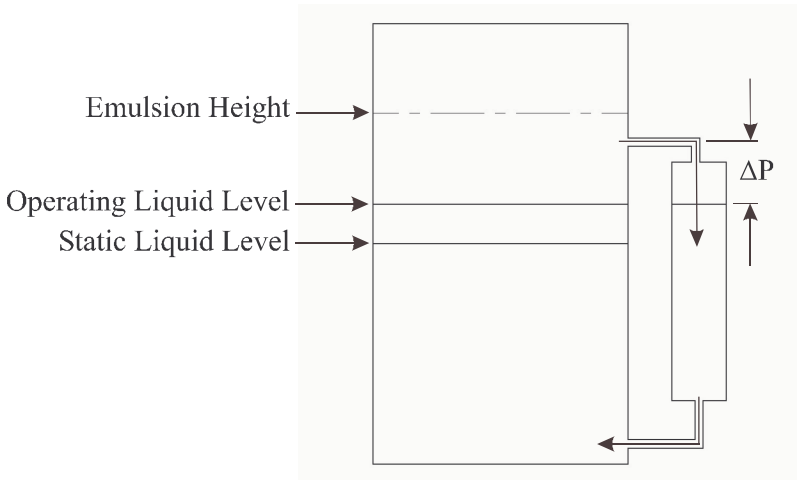

Figure 4.4 Liquid and emulsion levels of the packed bubble column. Resulting gravity feed to external tube.

The flow rate is controllable to ensure adequate residence time for heating and CO_2 evolution. The operating level in the regenerator, located within the vertical bounds of the tube, is equal to that in the absorber. [39]

4.3.4 Design

Since a bubble column type continuous regenerator has never been studied, the residence time required to ensure regeneration was found empirically. Similarly, the flow rate of solution required through the regenerator was estimated based on analysis from first principles. Figure 4.5 represents the molar flow of CO_2 through the absorber ($\overline{A}_{CO_2}$) and regenerator ($\overline{R}_{CO_2}$) at time t.

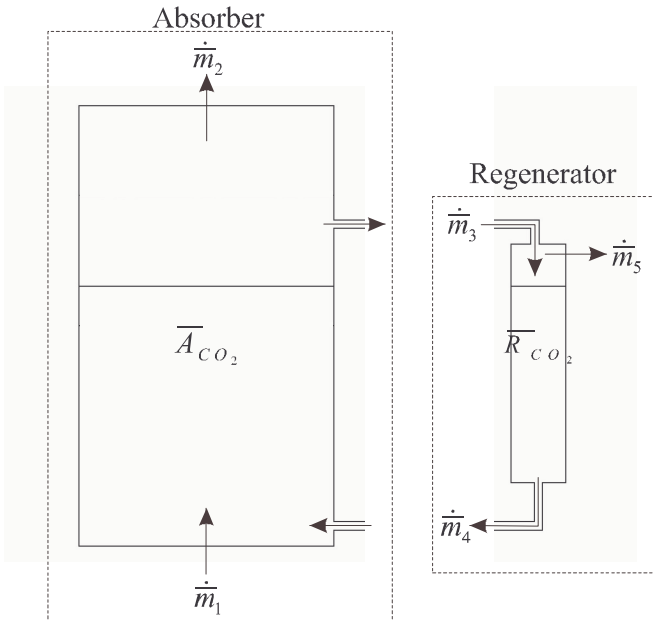

Figure 4.5 Molar flow rates of CO_2 through absorber and regenerator.

Absorption and regeneration were approximated as isothermal processes, which was reinforced experimentally. Due to the large air flow rate, the absorber temperature was dictated by the temperature of the air being scrubbed. Heat input to the regenerator was electronically controlled to maintain a set temperature.

Considering a CO_2 mole balance in the absorber, the rate of change with time of CO_2 in the absorber (moles/s) is:

$$\frac{d\overline{A}_{CO_2}}{dt} = \dot{\overline{m}}_1 - \dot{\overline{m}}_2 - \dot{\overline{m}}_3 + \dot{\overline{m}}_4 \qquad (4.1)$$

$\dot{\overline{m}}_1$ is the known molar flow rate of CO_2 within the air entering the absorber, $\dot{\overline{m}}_2$ the molar flow rate of CO_2 in the scrubbed air, and $\dot{\overline{m}}_3$ and $\dot{\overline{m}}_4$ are the regenerator feed and return CO_2 molar flow rates respectively. Similarly, the rate of change with time of CO_2 in the regenerator (moles/s) is:

$$\frac{d\overline{R}_{CO_2}}{dt} = \dot{\overline{m}}_3 - \dot{\overline{m}}_5 - \dot{\overline{m}}_4 \tag{4.2}$$

$\dot{\overline{m}}_5$ is the molar flow rate of regenerated CO_2 expelled from the system. The quantity of CO_2 actually absorbed, $\dot{\overline{m}}_1 - \dot{\overline{m}}_2$, is dependant on the apparatus and chemical solution properties, such as the number of moles of active MEA present ($\overline{M}_{MEA}$), loading and pH. To account for varying parameters, an absorption efficiency ε_A was established.

$$\varepsilon_A = \text{f(solution properties, apparatus)} \tag{4.3}$$

The molar flow rate of CO_2 in the scrubbed air exiting the absorber (moles/s) is thus given by

$$\dot{\overline{m}}_2 = (1 - \varepsilon_A)\dot{\overline{m}}_1 \tag{4.4}$$

It has been suggested [34] that significant absorption capacity is lost by MEA solutions following regeneration, due to degradation and formation of stable compounds. The loss may be as high as 40% after the first regeneration, but less than 2% upon subsequent regeneration. As with absorption, the regeneration of a solution is dependant on the solution properties and the regenerator apparatus. Furthermore it is improbable that every molecule of reacted MEA heated would be regenerated. Therefore a regenerator efficiency, ε_R, is introduced, representing the fraction of reacted MEA regenerated in a single pass.

$$\varepsilon_R = \text{f(solution properties, apparatus)} \tag{4.5}$$

The molar flow rate of CO_2 remaining in the return flow to the absorber (moles/s) is given by

$$\dot{\bar{m}}_4 = (1-\varepsilon_R)\dot{\bar{m}}_3 \tag{4.6}$$

At steady state, the rate of CO_2 absorption must be equal to the rate of regeneration and the net change in CO_2 concentration within the absorber and regenerator ($\frac{d\bar{A}_{CO_2}}{dt}$ and $\frac{d\bar{R}_{CO_2}}{dt}$) is zero. Eq 4.1 can then be rewritten as

$$\dot{\bar{m}}_1 - \dot{\bar{m}}_2 = \dot{\bar{m}}_3 - \dot{\bar{m}}_4 \tag{4.7}$$

From Eq 4.4,

$$\dot{\bar{m}}_1 - \dot{\bar{m}}_2 = \dot{\bar{m}}_1 - (1-\varepsilon_A)\dot{\bar{m}}_1 = \varepsilon_A \dot{\bar{m}}_1 \tag{4.8}$$

Similarly from Eq 4.6,

$$\dot{\bar{m}}_3 - \dot{\bar{m}}_4 = \dot{\bar{m}}_3 - (1-\varepsilon_R)\dot{\bar{m}}_3 = \varepsilon_R \dot{\bar{m}}_3 \tag{4.9}$$

Substituting the results of Eq 4.8 and Eq 4.9 into Eq 4.7, and rearranging for the unknown flow of CO_2 to the regenerator, $\dot{\bar{m}}_3$,

$$\dot{\bar{m}}_3 = \frac{\varepsilon_A}{\varepsilon_R}\dot{\bar{m}}_1 \tag{4.10}$$

$\dot{\bar{m}}_3$ represents the molar flow rate of CO_2 through the regenerator, at steady state conditions, to ensure constant molar concentrations within each apparatus ($\frac{d\bar{A}_{CO_2}}{dt} = \frac{d\bar{R}_{CO_2}}{dt} = 0$). With regard to the chemical solution, this is equivalent to the rate of regeneration being equal to the rate of absorption, and must be correlated to the

flow of solution through the regenerator, $\dot{\bar{m}}_{solution}$ (moles/second), which is of practical importance.

$\dot{\bar{m}}_3$ is related to the flow of MEA by the reaction product, carbamate. Up to 2 moles of MEA are required to absorb one mole of CO_2. Then

$$\dot{\bar{m}}_3 = \frac{\dot{\bar{m}}_{carbamate}}{2} \tag{4.11}$$

The molar flow rate of CO_2 is thus related to a flow of liquid. Rearranging for $\dot{\bar{m}}_{carbamate}$ and substituting from Eq 4.10:

$$\dot{\bar{m}}_{carbamate} = 2\frac{\varepsilon_A}{\varepsilon_R}\dot{\bar{m}}_1 \tag{4.12}$$

Assuming complete mixing in the absorber, the solution flow contains a proportion of free and reacted (carbamate) amine,

$$\dot{\bar{m}}_{MEA} = \dot{\bar{m}}_{free} + \dot{\bar{m}}_{carbamate} \tag{4.13}$$

It is not possible to remove only reacted MEA molecules for regeneration. The volume flow rate of solution required to deliver a sufficient molar flow rate of reacted MEA to the regenerator varies with the quantity of reacted MEA in solution. When the solution is fresh, a small amount of reacted MEA is distributed throughout, so a large volume is heated in order to regenerate a small amount of MEA. Conversely, if the solution is highly loaded, a large proportion of reacted MEA is regenerated in the same volume. At steady state, the fractions of free and reacted MEA remain constant and may be represented as

$$\dot{\bar{m}}_{free} = x\dot{\bar{m}}_{MEA} \tag{4.14}$$

And

$$\dot{\bar{m}}_{carbamate} = (1-x)\dot{\bar{m}}_{MEA} \tag{4.15}$$

x is the proportion of free moles to total moles of MEA in the absorber, and has a significant bearing on the scrubbing ability of the solution. This relationship is used to determine the fraction *x*. The total number of moles of MEA in the absorber, $\overline{M}_{MEA}$, is found by carefully mixing solution to appropriate proportions and measuring the quantity added to the absorber. The proportion of free moles, $\dot{\bar{m}}_{free}$, remaining after a given period of scrubbing to the desired level of CO_2 is found by measuring the CO_2 concentration in the scrubbed air over the period of interest, and calculating the number of moles of CO_2 absorbed. This corresponds to the number of moles of MEA reacted (allowing 2 moles MEA per mole CO_2), so the fraction of free MEA is easily found. Substituting $\dot{\bar{m}}_{carbamate}$ from Eq 4.12 into Eq 4.15:

$$\dot{\bar{m}}_{MEA} = 2\frac{\varepsilon_A}{\varepsilon_R}\frac{\dot{\bar{m}}_1}{(1-\mathrm{x})} \tag{4.16}$$

The flow of solution to the regenerator is comprised of three components, MEA (including both free and reacted molecules), MEG and water. Combining the molar flow of MEG and water into the parameter $\dot{\bar{m}}_{other}$,

$$\dot{\bar{m}}_{solution} = \dot{\bar{m}}_{MEA} + \dot{\bar{m}}_{other} \tag{4.17}$$

If the solution composition is known, the molar fraction of MEA, $\bar{f}_{MEA}$, is known and

$$\dot{\bar{m}}_{MEA} = \dot{\bar{m}}_{solution} \times \bar{f}_{MEA} \tag{4.18}$$

Back calculating from Eq 4.18 to find the total flow of solution

$$\dot{\bar{m}}_{solution} = \frac{\dot{\bar{m}}_{MEA}}{\bar{f}_{MEA}} = 2\frac{\varepsilon_A}{\varepsilon_R}\frac{\dot{\bar{m}}_1}{(1-\mathrm{x})\bar{f}_{MEA}} \tag{4.19}$$

The molar flow rate of solution fed to the regenerator is converted to a meaningful volumetric flow rate (m^3/s) by the solution molar weight ($M_{solution}$) and density ($\rho_{solution}$).

$$Q_{solution} = \dot{\bar{m}}_{solution} \frac{M_{solution}}{\rho_{solution}} \tag{4.20}$$

$$Q_{solution} = 2 \frac{\varepsilon_A}{\varepsilon_R} \frac{\dot{\bar{m}}_1}{(1 - x)\bar{f}_{MEA}} \frac{M_{solution}}{\rho_{solution}} \tag{4.21}$$

Factors affecting the outcome of the analysis include vapour loss and degradation. However it is impossible to predict these values *a priori* and the analysis serves as an initial estimation for experimental work. As described above, the disadvantage of the continuous flow regenerator is the inability to select or control the makeup of solution regenerated. The result of this is energy waste in heating non regenerable MEA or compounds, and unnecessary exposure of MEA to heat, increasing degradation.

4.4 Chemical Solution Selection

4.4.1 Absorption

The most common MEA solution used in industry is around 15 wt% due to corrosion of plant, which is directly proportional to MEA strength. Corrosion is not relevant to the scrubber system due to materials selection. For AFC scrubber applications, regeneration energy is less abundant than in large plants. It is desirable to put as much energy as possible into carbonated MEA as opposed to water, which is heated to no avail during regeneration [66] [31].

The reaction kinetics between MEA and CO_2 are fast. Chemistry factors affecting absorption are temperature, alkalinity (pH) [17], availability of free MEA [38] and diffusion [67]. Increasing MEA concentration in solution increases alkalinity and the rate of absorption [33]; however as seen in Figure 4.6 the effect is not linear and, extrapolating over 50 wt% MEA, the increase in pH becomes small for increases in MEA concentration.

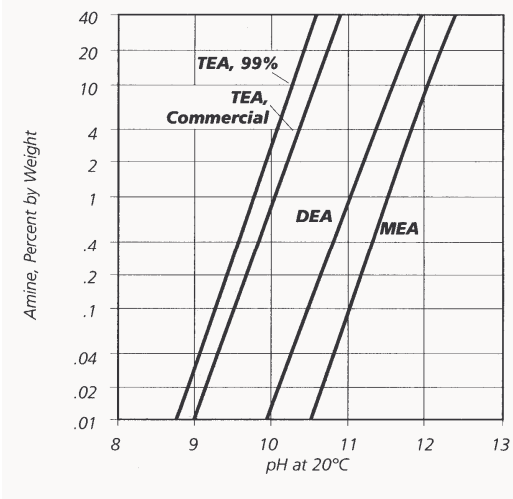

Figure 4.6 Change in solution pH with amine concentration.
Note the non linear y axis (Dow Chemicals [68]).
MEA = Monoethanolamine, DEA = Diethanolamine, TEA = Triethanolamine

Furthermore, Figure 4.7 shows that for a given loading (moles CO_2 absorbed per mole of amine) the vapour pressure of CO_2 is greater over stronger solutions.

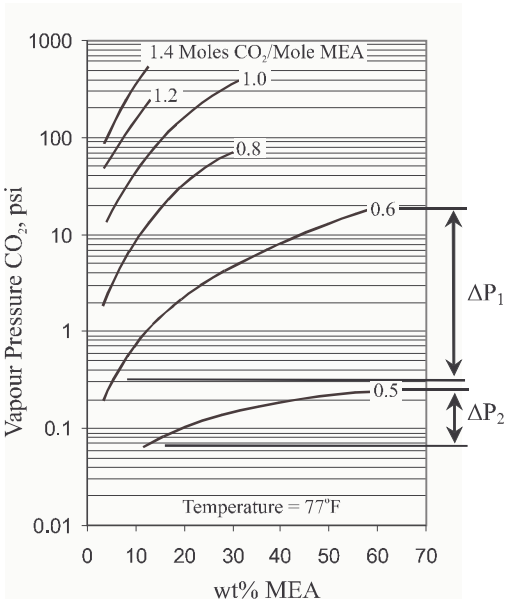

Figure 4.7 Carbon dioxide vapour pressure with MEA concentration and loading.
The change in vapour pressure with concentration reduces with decreasing loading [17].

Although higher MEA concentration solutions do not achieve as high a loading for a given partial pressure of CO_2, it is not expected (Table 4.1) that the scrubber will achieve loadings as high as those shown in Figure 4.7.

Table 4.1 Solubility of CO_2 in 30 wt% MEA solution.

The solution loading (mole ratio CO_2 : MEA) decreases as the CO_2 partial pressure decreases. At 25ºC, 0.06 kPa = 592 ppm [23].

25ºC		60ºC		100ºC		120ºC	
P_{CO_2}	**Mole Ratio**	P_{CO_2}	**Mole Ratio**	P_{CO_2}	**Mole Ratio**	P_{CO_2}	**Mole Ratio**
19936	1.25	19893	1.11	19812	0.94	17723	0.86
9973	1.17	9959	1.03	9871	0.86	9770	0.78
2996	1.04	2977	0.88	2899	0.71	2804	0.64
297	0.81	282	0.64	376	0.59	422	0.47
55.1	0.65	34.1	0.57	39	0.42	47	0.35
2.8	0.54	2.01	0.44	1.43	0.17	2.3	0.12
0.06	0.44	0.06	0.20	0.14	0.057	0.098	0.025
0.0021	0.21	0.0043	0.056	0.0072	0.012	0.002	0.0033

Figure 4.7 shows that for a given loading, the difference in equilibrium partial pressure of CO_2 between low and high MEA concentration decreases as the loading decreases (i.e. $\Delta P_1 >> \Delta P_2$). Extrapolating this trend, a line corresponding to 0.3 loading is almost horizontal - there would be little difference in the partial pressure of CO_2 with the solution be it 10 or 50 weight percent.

Overall therefore, increasing MEA concentration increases the scrubbing capacity (by the presence of more moles of amine) as well as raising the absorption rate by increasing alkalinity, while not appreciably affecting CO_2 partial pressure over the solution.

As seen in Figure 2.3 (MEA – CO_2 chemical system), water plays an important role in the absorption process, permitting ionisation of reactants, hydrolysis of carbamate and setting an upper limit to MEA strength. As is often the case, the selection of MEA concentration was somewhat subjective [17] [35], though based on the above observations. A 50 wt% MEA solution was deemed a reasonable compromise between MEA strength, water content and likely performance. This selection was

supported by data from DeMontigny *et al* [38], investigating up to 50 wt% solutions to determine performance. Other factors to consider were cost, vapour pressure of the solution, boiling and freezing temperatures, and solution physical properties.

4.4.2 Regeneration

Hook [7], Yeh [31] and Curnow [65] state that MEA regeneration can be achieved below 100°C, in contrast to the usual pressurised steam regeneration method most common in industry. An MEA regeneration method without steam or boiling was proposed, reducing energy consumption and liquid losses. To avoid boiling, a solution with a boiling point of well over 100°C was required, allowing for localised heating that may occur when solution is in direct contact with a heating element.

The boiling point of a 50/50 wt% MEA/H_2O mixture is barely over 100°C, despite the high boiling point of MEA, so a chemical additive was considered. An obvious choice was a glycol, which is used to raise the boiling point and lower the freezing point of coolant in internal combustion engines. Monoethyleneglycol (MEG) was used in some CO_2 absorption plants as a dehydrator (the glycol-amine process [17] [21]), indicating that its presence is not detrimental to absorption chemistry.

Yeh [31] investigated improvements to the amine scrubbing process, including the use of glycol instead of water in solution to reduce regeneration energy cost. Yeh reported that glycol reduces the absorption rate of CO_2 by MEA, but due to having low vapour pressure may be a suitable diluent for atmospheric operations. Furthermore, data reported by Song *et al* [69] suggests that although CO_2 solubility in MEA/H_2O/glycol systems generally decreases with increasing glycol concentration, at very low CO_2 partial pressures (<10 kPa) the solubility actually increases over the comparable MEA/H_2O system. Data was acquired down to approximately 4 kPa (compared to atmospheric CO_2 partial pressure 0.04 kPa). Subsequent investigation by Liaw [53] revealed that glycol did not adversely affect MEA - CO_2 chemistry, as asserted by Song and Kohl.

Figure 4.8 displays the experimentally determined boiling points of solutions containing 50 wt% MEA, the balance a mixture of water and monoethyleneglycol (MEG). MEG increases the boiling point of solutions in approximately linear proportion to weight percent. The glycol concentration selection was aided by ensuring at least 1:1 mole ratio of MEA and water, in an effort to maintain adequate ionic strength in solution. Furthermore, sufficient water is necessary to saturate the glycol, a hygroscopic chemical, to avoid dehydration of the air and a subsequent increase in solution volume.

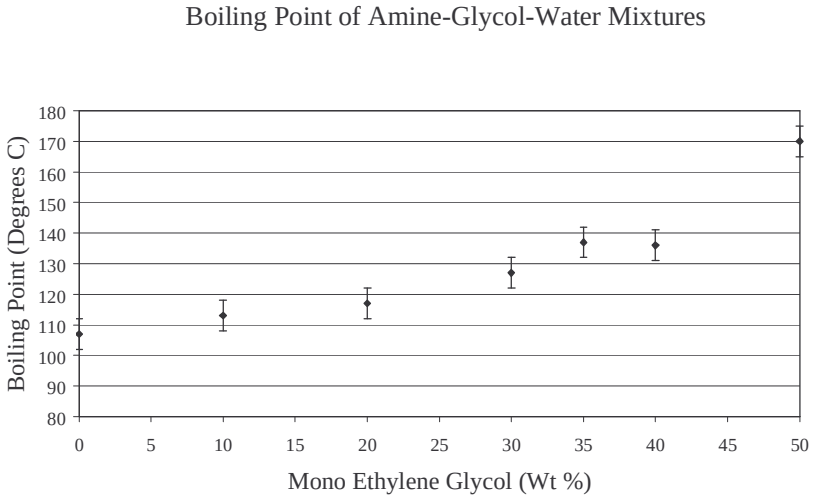

Figure 4.8 Investigation of boiling points for various chemical solutions. All solutions are 50 wt% MEA, wt% glycol indicated, balance water.

The final experimental solution was set at 50/35/15 weight percent, or 37/25/38 mole percent, MEA/MEG/H_2O with a boiling point of approximately 135°C. This mixture is referred to as the standard solution. The boiling point allows a suitable buffer for the maximum expected regeneration temperature of 120°C. Regeneration at over 126°C achieves no desorption rate enhancement, while the rate of MEA degradation increases significantly [70]. A further advantage of glycol addition is that glycol has a lower specific heat than water (2.4 compared to 4.2 kJ/kgK) and therefore requires less energy to elevate its temperature.

4.4.3 Physical Properties

Physical properties of the solution affect behaviour in packed bubble columns [40]. Increasing surface tension increases coalescence [39] and bubble size [56], and therefore decreases interfacial area [59] [56]. MEA and glycol serve to increase the viscosity of solution, as does increasing the CO_2 loading of MEA [71]. Increasing viscosity can enhance the interfacial area because of increased stability of the bubble dispersion and lower coalescence [56] [59], however molecular diffusion through the liquid is reduced [59] [56] [72]. The onset of the churn turbulent flow regime occurs at lower superficial gas velocities as solution viscosity increases [57].

As well as the usual considerations such as species diffusion, mixing and interfacial area, the height of emulsion (or froth) generated is important for the CDOCS scrubber. Experiments with the concept column showed that blowing air through liquid generates an emulsion, effectively providing a pressure head that can be tapped to provide flow through a regenerator. Of the chemicals in solution, water provides the highest level of emulsion, due to relatively low viscosity. MEA and glycol, which share similar properties, have much higher viscosities (almost 20 times water) that act to damp the motion of the liquid, so suppressing emulsion [17]. The surface tension of these chemicals is approximately 7/10 that of water, making little impression.

A small addition of surfactant or detergent drastically lowers the surface tension of a solution. Low surface tension solutions tend to form films, and maintain smaller bubble size [56], resulting in decreased bubble rise velocity [40] [58]. These effects contribute to emulsion formation; however the presence of surface impurities (surfactant) could hinder mass transfer [56]. A surfactant could increase emulsion height to feed a regenerator if necessary, but the effect on chemistry requires investigation. Emulsion height also depends on the liquid depth and air flow rate, the combination of which must generate a churn turbulent regime in order to maximise the emulsion.

Density of solution is important for determining pressure head. MEA and MEG have similar densities to water (density range 1000-1100 kg/m^3), and the overall solution density is little more than pure water, 1040 kg/m^3 (Appendix 3).

4.5 Materials Selection

MEA is a highly alkaline chemical (pH ~12.5), and increasingly corrosive at elevated temperature and high CO_2 loading [23]. Chemical attack from MEA can result in mechanical failure of some metals, rubbers and plastics, particularly at stress concentrations. Table 4.2 gives a generic MEA compatibility rating for several common construction and sealing materials. It is unclear whether the ratings apply to hot MEA solution as well as at ambient temperature.

Table 4.2 Monoethanolamine material compatibility.
Cole Parmer [73] plus additions (*) by author.

Material	Compatibility	Material	Compatibility
304 stainless steel	A- Excellent	Polypropylene	B- Good
316 stainless steel	A- Excellent	PVC	D- Severe Effect
Cast iron	A- Excellent	LDPE	C- Fair
Aluminium	B- Good	Acetal (Delrin®)	D- Severe Effect
Brass	D-Severe Effect	EPDM	B- Good
Bronze	A- Excellent	Natural rubber	B- Good
Copper	D- Severe Effect	PTFE (Teflon®)	A- Excellent
Titanium	B- Good	Neoprene	D- Severe Effect
Carbon graphite	A- Excellent	Viton®	D- Severe Effect
ABS plastic	B-Good*	Buna N (Nitrile)	B- Good
Polycarbonate	D- Severe Effect*	Epoxy	A- Excellent
Acrylic	D- Severe Effect*	Silicone	B- Good
Nylon	A- Excellent	732 RTV Sealant	A- Excellent*

The ratings are indicative of long term compatibility - a D rating does not indicate that the material will be instantly dissolved by MEA. It is possible to use some materials with a D rating, but they may suffer damage in the long term or affect the chemical solution. Examples are PVC tubing which becomes brittle, especially at high

temperature exposure to MEA, and copper, which causes MEA solution to turn deep blue.

Due to the physical size of industrial installations, it is generally not economical to use completely resistant materials such as stainless steel. Therefore MEA concentrations are maintained at relatively low levels (up to 15 wt%) to reduce the corrosion of steel plant. For the prototype scrubber however, 316 stainless steel was chosen for relative ease of manufacture and availability. This selection removed any possibility of corrosion or its effects, which may include changing the absorption characteristics of MEA solutions during experimentation.

Complete stainless steel construction may prove prohibitive to economical manufacture in the long term. Extensive testing of a prototype Acrylonitrile Butadiene Styrene (ABS) plastic absorber revealed no sign of degradation, chemical attack, or structural weakening. Long term exposure to MEA showed no swelling of the plastic or the chemical weld used to join plastic components. The effect of MEA on ABS was investigated at near ambient temperatures only (up to 40°C). Due to the increasingly corrosive nature of hot MEA, for longevity and safety the regenerator was constructed from stainless steel. ABS does not have a high tolerance to UV sunlight, so requires protection in service.

4.6 Developmental Prototype

4.6.1 Absorber

For the 6 kW AFC system, the volumetric flow rate of air to be scrubbed is 40 m^3/hr. To ensure the churn turbulent flow regime prevailed in the absorber, a superficial gas velocity of at least 0.1 m/s is required [56], equating to a column diameter of 376 mm. Due to limited capability of the available blower, an air flow rate of 20 m^3/hr was used extensively for prototype development, corresponding to a maximum column diameter of 266 mm. The superficial gas velocity with 266 mm diameter and 40 m^3/hr air flow rate is still within the churn turbulent regime.

The absorption column was fabricated from spiral welded stainless steel tube with an internal diameter of 254 mm and 2 mm wall, giving an averaged superficial gas velocity of 0.20 m/s for 40 m^3/hr or 0.11 m/s for 20 m^3/hr flow rate. A 3 mm plate welded circumferentially forms the base of the absorber. A schematic of the experimental apparatus is given in Figure 4.9.

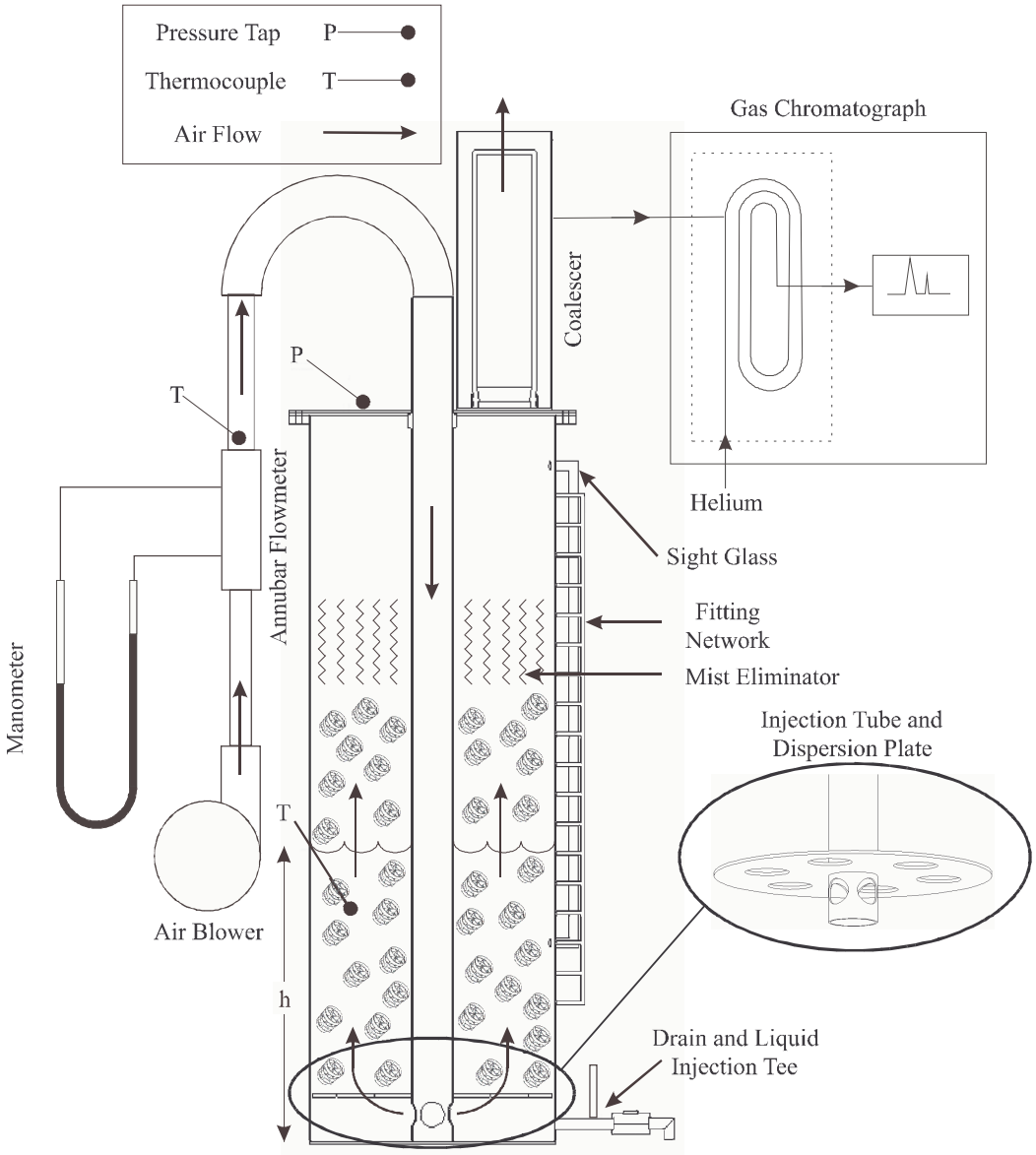

Figure 4.9 Developmental prototype absorber, main body sectioned.

Air was supplied by an Electrolux 333 centrifugal blower, voltage controlled by a Variac W20 (240V, 8A). The blower supplied 40 m^3/hr air at up to 500 mm solution

depth. The air flow rate was measured by a 1.049" Dietrich Standard Corp Annubar Flow meter station (model 713-316SS) in conjunction with a Wilh. Lambrecht KG Gottenger type 655 inclined manometer at an inclination of 1:2. The manometer fluid fluctuated about the average reading by ± 2 scale divisions (± less than ½ m^3/hr at 20 m^3/hr flow rate) with fluctuations in the bubble column. The calibration curve for the annubar flow meter is included in Appendix 4.

Air was injected near the bottom of the column through a stainless steel tube of inside diameter 40 mm. For accurate location, the tube rested on the base of the absorber, and four equally spaced radial holes of diameter 25 mm permitted air injection (detail view in Figure 4.9). Only a small fraction of the injection holes actually allowed egress of air due to pressure and buoyancy forces, therefore the injection depth was taken to be 40 mm above the base of the column. To aid radial bubble dispersion in the column, a distribution plate was fixed to the injection tube just above the radial holes. The distribution plate also supported the packing above the injection point, with wire mesh resting on the plate to stop packing elements from falling through the dispersion holes.

Random packing elements were poured into the column, to a height of 600 mm, after placement of the injection tube. Care was taken to centrally locate the injection tube during filling, to enable positioning of the lid. A 150 mm strip of Wire Mesh Industries Pty Ltd PSA10 mist eliminator mesh (Figure 4.10) was rolled into a cylinder and placed above the packing. The mesh fitted neatly around the injection tube and inside wall of the column to consolidate larger solution drops and mist carried with the air stream. Pressure drop across the mesh was negligible compared to the liquid pressure head. The column was capped with a 3 mm plate which sealed around the injection tube and column flange with an O-ring and 3 mm gasket respectively. A pressure tap for monitoring the pressure in the top of the column was attached to the cap.

Figure 4.10 Single layer of woven mesh mist eliminator.

Scrubbed air exited the column through a diameter 70 mm hole in the cap. A Pall Corporation Seprasol Liquid/Gas coalescer, diameter 70 mm by 260 mm long, housed in a stainless steel tube of 100 mm diameter, adjoined the cap. The Pall coalescer has a metal core for mechanical strength, surrounded by a pleated proprietary filter similar to that found in automotive oil, fuel and air filters (Figure 4.11). The filter material is chemically treated to lower the surface energy of liquid and encourage coalescence, wrapped in light plastic mesh to aid drainage of coalesced liquid, and finally surrounded by a polymeric outer wrap to reduce re-entrainment. The pleated filter material absorbs moisture which increases the pressure drop across the coalescer.

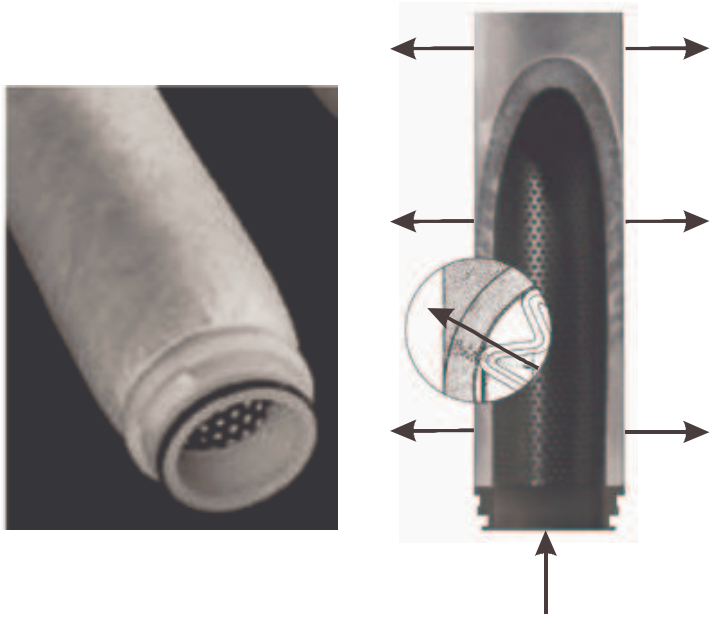

Figure 4.11 Pall Corporation Seprasol Liquid/Gas Coalescer.

Isometric and sectioned views. Gas/aerosol mixture enters the coalescer axially (vertical arrow), liquid particles as small as 0.1 micrometres are coalesced so only gas passes through the coalescer wall (horizontal arrows).

The coalescer is capable of removing droplets down to 0.1 micron diameter, and added a pressure drop of between 0.5 and 2 kPa, depending on how much liquid had been absorbed during operation. Exhaust air was expelled to atmosphere outside the laboratory. A hole in the coalescer housing allowed extraction of samples for GC analyses; the GC sample tube was inserted and withdrawn as required, and the hole plugged when not in use.

The column has 18 barbed ABS fittings of internal diameter 4 mm at regular intervals of 30 mm, starting at 140 mm from the bottom of the absorber. The barbs were connected with ABS tees and clear PVC tubing. The fittings allowed visual observation of the emulsion height in the absorber with each liquid depth and air flow rate combination. The fitting network worked on the same principle as the regenerator flow; the solution emulsion caused a small, visible flow through the highest fitting reached. The approximate error in emulsion depth was ± 10 mm. A sight glass fitted to the column enabled visualisation of the static liquid level and the operating level.

A ball valve at the bottom of the column acted as a drain. A tee on the column side of the valve enabled gradual injection of liquid by a TPS Easy-FLOW Variable Speed Peristaltic Dosing Pump. The peristaltic pump fed the tee via a PVC tube, accurately controlling the volume and rate of liquid addition.

4.6.2 Regenerator

To avoid any material incompatibility with hot MEA solution, all components of the regenerator were stainless steel. Absorber operating parameters constrained the inlet and outlet positions of the regenerator, and thus the height of the regenerator and heating element. A chemically resistant Incoloy 230 V/500 W immersed heating element was supplied by B.J. Cocksedge of Wellington New Zealand, and is shown in Figure 4.12. Power consumption was monitored with a YEW 2433-12 AC power meter from Yokogawa Hokushin Electric.

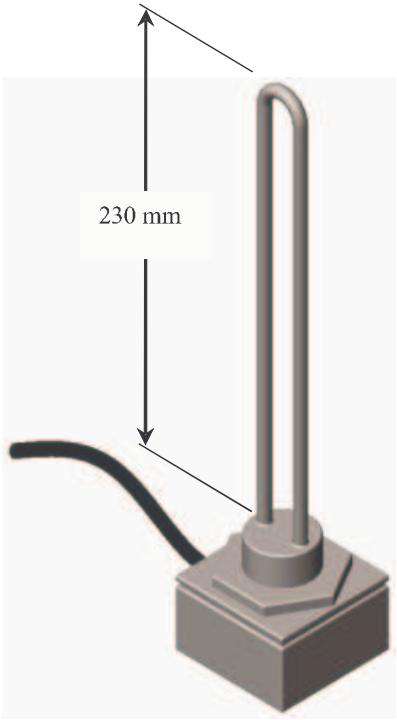

Figure 4.12 Immersed 500 W heating element.
Located within developmental regenerator apparatus.

The element was fixed to a 1¼" BSPF boss, and for ease of construction and alteration, the regenerator was assembled from compatible fittings and pipe. The column body (OD 60, ID 53 mm tube with BSP threaded ends) was attached to the element with a BSP socket and 2" reduction fitting, and sealed at the top with a cap (Figure 4.13). This gave the regenerator a working volume, at any instant, of 0.5 litres with 300 mm solution depth in the absorber.

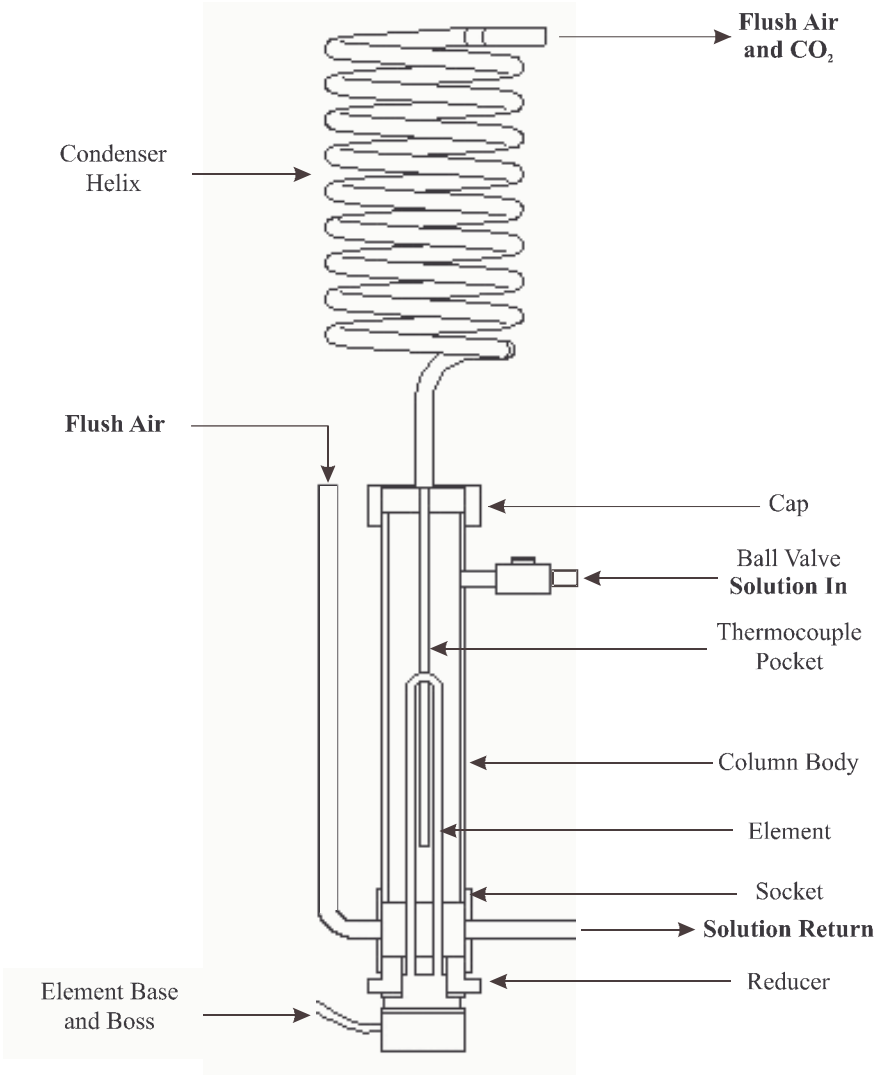

Figure 4.13 Developmental prototype regenerator.
Packing material, woven stainless steel mesh wrapped around the element, not shown.

Regenerator flush air was supplied by an in house compressed air line, regulated to provide 4 litres/minute as measured by a Comweld Group Medical Products eziflow

medical flow meter. A water bath humidified the air prior to injection into the bottom centre of the regenerator column, by means of a Swagelok fitting and ½" tube. Air and CO_2 from the regenerator exited through a Swagelok fitting in the cap followed by a ½" tube condenser helix with forced convection, to condense water and MEA vapour leaving the regenerator. Condensed fluid was able to run down the helix and deposit in the regenerator.

The regenerator column was filled with PSA10 mist eliminator mesh, tightly rolled around the heating element and fitting tightly in the column body to avoid air channelling at the wall. This acted as a packing material, providing smaller bubbles than would be possible with 15 mm diameter Pall rings.

Temperature control in the regenerator was achieved by an RKC PID phase angle controlled output device with a type K thermocouple. Due to the corrosive nature of hot MEA solution, a 250 mm ¼" tube, sealed at one end and filled with thermodynamic paste, enveloped the thermocouple. The tube extended into the regenerator through a Swagelok fitting in the column cap. The PID controller restricted power input to avoid burning solution in contact with the element.

The regenerator accepted solution from the absorber through a ball valve, which controlled the flow rate, and solution was free flowing from the regenerator to the bottom of the absorber. The regenerator was sized according to the analysis detailed in section 4.3.4, which resulted in Eq 4.21, reproduced below.

$$Q_{solution} = 2\frac{\varepsilon_A}{\varepsilon_R}\frac{\dot{\bar{m}}_1}{(1-\mathrm{x})\bar{f}_{MEA}}\frac{M_{solution}}{\rho_{solution}} \tag{4.21}$$

$\dot{\bar{m}}_1$ is the molar flow rate of CO_2 in the atmospheric air being scrubbed. The atmospheric concentration of CO_2 is 380 ppm, or 0.038% by volume. For the 40 m^3/hr flow rate required by the 6 kW AFC, the volume flow rate of CO_2 is

$$V_{CO_2} = \frac{40}{60^2}\times 0.038\% = 4.22\times 10^{-6}\ (\mathrm{m}^3/\mathrm{s}) \tag{4.22}$$

Assuming ideal gas behaviour, the molar flow rate of CO_2, $\dot{\bar{m}}_1$, is

$$\dot{\bar{m}}_1 = \frac{P_{atm} V_{CO_2}}{RT} = 1.715 \times 10^{-4} \text{ (moles/s)} \tag{4.23}$$

Where P_{atm} is 101.325 kPa, R is the universal gas constant, 8.314 J/moleK, and T is 300 Kelvin. The solution molecular weight ($M_{solution}$) and density ($\rho_{solution}$) are known, equal to 44.96 grams/mole and 1040 kg/m^3 respectively (Appendix 3). Similarly, $\bar{f}_{MEA}$ is known from the solution chemical composition (37 mole% MEA) and is equal to 0.37.

The proportion of free to total MEA in the absorber, *x*, was determined by experiment, detailed fully in section 5.1.2. The experiment showed that the concentration of CO_2 exiting the absorber (ppm), in the absence of regeneration, increased linearly with the volume of air scrubbed, according to the relationship in Eq 4.24.

$$CO_2 = 0.07 \times [\text{m}^3 \text{ air scrubbed}] \tag{4.24}$$

Carbon dioxide removal of 95% (380 down to 20 ppm) or better was achieved up to 285 m^3 air scrubbed (at atmospheric pressure and 300 K). Although this result pertains to an air flow of 20 m^3/hr, the quantity of CO_2 in 285 m^3 of air is constant and the air flow rate has a small influence on absorption. For simplicity, it is convenient to assume an average of 10 ppm escaped for the entire period. Converting this to the volume of CO_2 absorbed at atmospheric pressure and 300 K:

$$\begin{aligned} V_{CO_2} &= 285 \times 0.037\% \\ &= 0.105 \left(\text{m}^3\right) \end{aligned} \tag{4.25}$$

Using the ideal gas law with P_{atm} = 101.3 kPa, R = 8.314 J/moleK and T = 300 K, the number of moles (n) of CO_2 absorbed from 285 m^3 of air is

$$n = \frac{P_{atm} V_{CO_2}}{RT} = 4.3 \,(\text{moles}) \tag{4.26}$$

Still assuming two moles of MEA are required to absorb one mole of CO_2, 8.6 moles of reacted MEA, carbamate, were formed over the period considered. The absorber initially contained 17 litres of standard solution, equivalent to 145 moles of fresh MEA. Therefore the proportion of fresh to total moles of MEA is

$$x = \frac{145 - 2(4.3)}{145} = 0.94069 \tag{4.27}$$

This fraction of fresh MEA results in scrubbing to 20 ppm CO_2 or less from atmospheric air. The absorber and regenerator efficiencies, ε_A and $\varepsilon_{R,}$ are set conservatively at 0.5. Applying the above values to the variables in Eq 4.21 gives:

$$Q_{solution} = 2\frac{0.5}{0.5}\frac{\left(1.715\times10^{-4}\right)}{(1-0.94069)0.37}\frac{0.04496}{1040} = 6.76\times10^{-7}\ (\text{m}^3/\text{s}) \tag{4.28}$$

Finally, converting to litres per hour for a meaningful solution flow rate

$$Q_{solution} = 1000\times(60)^2\times6.76\times10^{-7} = 2.43\,(\text{litres/hr}) \tag{4.29}$$

The analysis shows that approximately 2.5 litres/hour of solution must be fed to the regenerator during steady state operation, to maintain satisfactory performance. This value bears a high degree of uncertainty due to assumptions made, particularly concerning the absorber and regenerator efficiencies. At 2.5 litres/hour flow rate of solution, the apparatus provided an average residence time of 12 minutes.

4.6.3 Blower

The blower for the AFC system air supply is of particular importance because it runs continuously, representing a significant parasitic power load and reliability concern. As well as being capable of supplying the maximum required air flow at maximum

system pressure, the blower must be controllable and run efficiently over a range of operating conditions. AFC systems typically generate anywhere from 12 to several hundred volts DC power (0.8 volts per cell), and for most applications this is converted to useful DC or AC voltage, specific to the situation. The power supply for the blower is therefore flexible and is specific to system design.

Ametek Technical and Industrial Products produce unique low voltage brushless DC motors and centrifugal blowers specifically for developing fuel cell technology. Brushless motor technology has the advantages of high efficiency, spark-free and maintenance-free operation, high reliability and long service life. Electronic control allows fast response to changing flow demand caused by a varying load on the fuel cell.

A feature of the Ametek range is relatively high pressure from small devices. The AFC system pressure and flow requirements were in a range not accommodated by either traditional blowers, which tend to be very high flow rate and very low pressure, or pumps and compressors with very high pressure and low flow rate. For the 6 kW AFC system under consideration, the system pressure was comprised of the following components:

Table 4.3 Contributions to supply pressure required of blower.

Fuel Cell Inlet Pressure	5.9 kPa	(Zetek Power PLC)
Absorber Liquid Head	3.4 kPa.	(350 mm liquid depth)
Absorber Auxiliaries	1 kPa	(Estimated for coalescer and piping)
Total Supply Pressure	10.3 kPa.	(41" H_2O)

The fuel cell inlet pressure is the recommended pressure to the fuel cell stacks brought about by operating conditions in the system. It is greater than the pressure drop across the stacks themselves, which is up to 2 kPa. The 6 kW AFC system requires a maximum air flow rate, corresponding to full output, of 40 m^3/hr. This is equivalent to

23.5 normal cubic feet per minute (NCFM), and must be supplied at the total supply pressure, 10.3 kPa.

Figure 4.14 shows the performance curve for a suitable two stage bypass blower from Ametek, model 116639. The 120 volt DC blower has a diameter of 150 mm, length of 160 mm and electronic speed control. To cope with varying pressure and flow rate demands from an AFC system, the blower has a dedicated fan to cool electronics, as opposed to using the working air. From the supplied performance graph, the blower is capable of over 10 kPa (41" H_2O) at 11.8 litres/s (25 NCFM). Full specifications of the blower are included in Appendix 5.

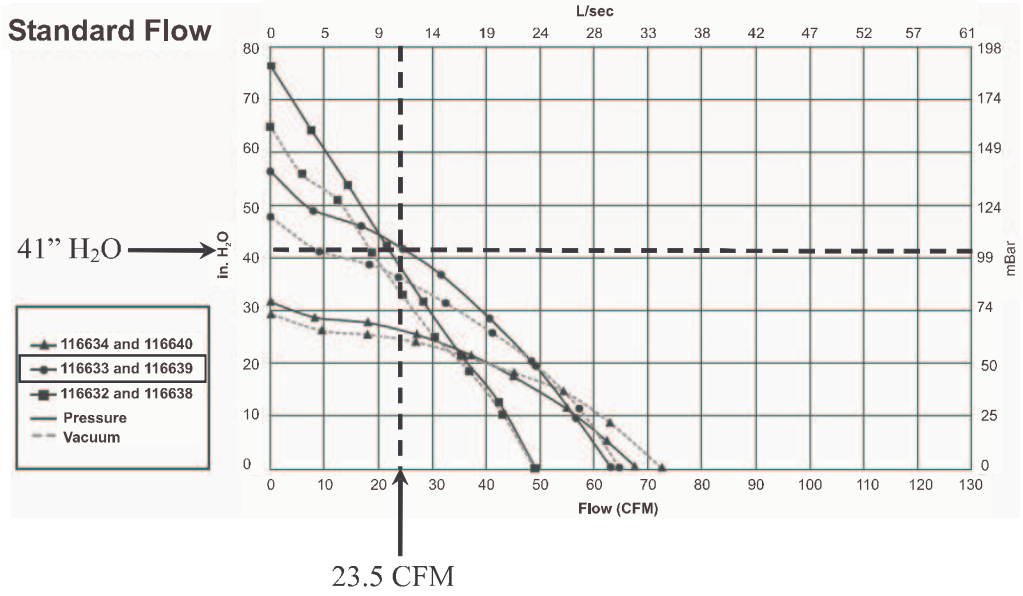

Figure 4.14 Blower performance graph for Ametek 116639.

Ametek make several capable models in various voltage and power ratings. The 116639 is the lowest voltage model available to meet requirements, but ultimately selection would rest with AFC system designers to best meet individual system needs. Ametek also have a custom design capability which may be useful for mass produced systems.

The cost of the 116639 blower through Australian agent Ross Brown Sales was over NZ$1200 with an eight week delivery period from the USA, warranting an alternative

air supply. The only common blower capable of both the required pressure and flow for experimental purposes was a vacuum cleaner. An Electrolux 333 was capable of supplying 20 m^3/hr at up to 5 kPa (500 mm liquid depth) continuously, and 40 m^3/hr at the same pressure for short periods (several hours). A Variac voltage controller enabled flow regulation at various pressures. The increased load and power requirement at 40 m^3/hr caused the vacuum cleaner to overheat if run for extended periods. Although vacuum cleaners are not designed to run continuously for weeks on end, the Electrolux was quite capable of meeting experimental requirements providing brushes were maintained and replaced.

4.6.4 Experimental Apparatus Energy Requirements

Blower

The selected Ametek blower has a 120 volt input and is rated at 250 W, a nominal rating at a mid range operating point. The blower draws a maximum current of 5 amps, and therefore maximum power of 600 W. Blower power varies directly with air density (Ametek Catalogue), which varies directly (assuming the ideal gas law applies) with pressure. Power therefore increases approximately linearly with pressure on the performance graph, Figure 4.14. Exact power consumption can only be determined by experiment, but assigning a nominal offset power for losses, friction and inertial effects of 100 W, there is a 500 W variation in power over 15 kPa variation in pressure, or 33 W per kilopascal. Therefore, at 10 kPa, the blower would use approximately 430 W.

The same model blower is necessary to meet pressure and flow requirements of the 6 kW AFC system without the CDOCS. In this case, approximately 7 kPa is required for the fuel cells and soda lime scrubber, corresponding to 320 W power consumption.

Regenerator

A resistive heating element supplies energy to bring the flows of solution and flush gas to regeneration temperature, and provides the heat of reaction to evolve CO_2. The thermodynamic boundary and calculated or estimated parameters for the system are

defined in Figure 4.15. The calculations include assumptions that the mass flow rate of CO_2 evolved is negligible compared to mass flow rate of solution, and CO_2 evolves at regeneration temperature so does not require further energy input.

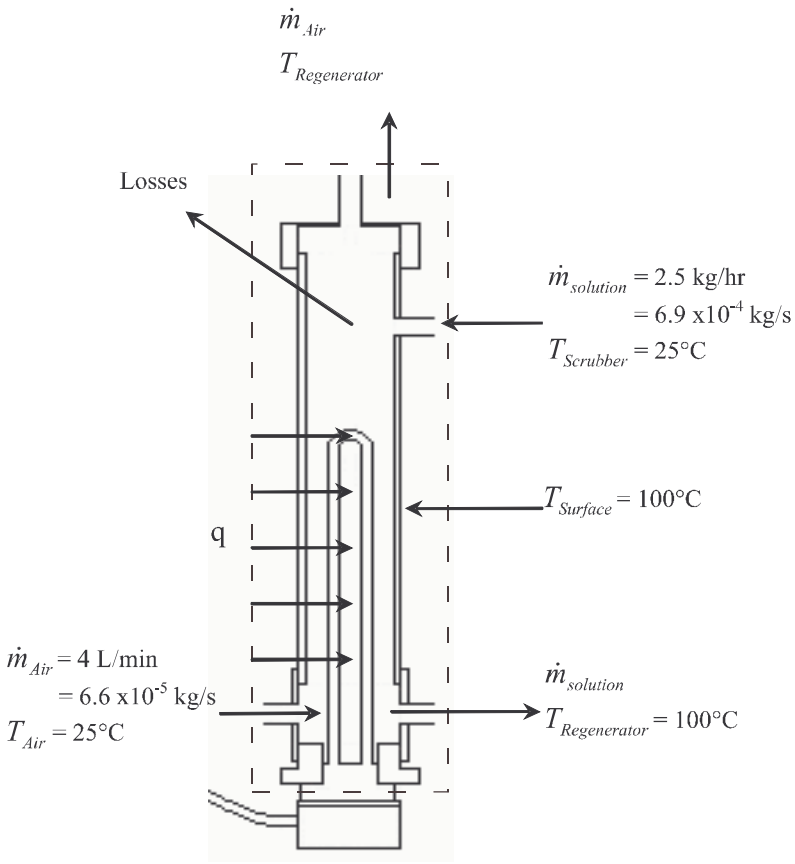

Figure 4.15 Model for thermodynamic analysis of regenerator.

Solution Sensible Heat

Raising the solution flow to regeneration temperature requires a significant portion of regenerator energy (W) according to Eq 4.30.

$$q = \dot{m} c_p \Delta T \tag{4.30}$$

Specific heat, c_p, for the standard solution was estimated from the law of mixtures [74] in Eq 4.31, where chemical properties are found in Appendix 3. This corresponds well with available data on similar solutions [17] [75].

$$\begin{aligned} c_{p_{(Solution)}} &= 0.37c_{p_{(MEA)}} + 0.25c_{p_{(MEG)}} + 0.38c_{p_{(H_2O)}} \\ &= 0.37(2780) + 0.25(2400) + 0.38(4200) \\ &= 3180\,(\text{J/kgK}) \end{aligned} \tag{4.31}$$

Assuming a temperature change from 30 to 100°C regeneration temperature,

$$\begin{aligned} \Delta T &= T_{regenerator} - T_{Scrubber} \\ &= 100 - 30 \\ &= 70^{\circ}\text{C} \end{aligned} \tag{4.32}$$

Then

$$\begin{aligned} q &= 6.9\times10^{-4}\times3180\times70 \\ &= 154\,(\text{W}) \end{aligned} \tag{4.33}$$

Energy consumption increases in direct proportion to the solution flow rate and temperature difference.

Heat of Reaction

Heat of reaction for the MEA - CO_2 system is in the range 72-85 kJ/mole CO_2 absorbed or desorbed [31] [17]. From section 4.6.2, 0.56 moles of CO_2 evolve per hour at steady operating conditions. Rounding to 80 kJ/mole heat of reaction, and converting to moles CO_2 per second,

$$\begin{aligned} q &= moles CO_2 / s \times J / mole \\ &= 1.6\times10^{-4}\times80\times10^{3} \\ &= 13\ (\text{W}) \end{aligned} \tag{4.34}$$

Flush Gas Sensible Heat

The regenerator also warms the flow of flush gas to regeneration temperature as it travels through the column. Assuming the air to be saturated with water at ambient temperature and pressure (T_{Air} = 25°C, P_{atm} = 101.325 kPa), the partial pressure of

water vapour in the air ($P_{sat,\ 25°C}$, P_{atm}) is 3169 Pa. The specific humidity, ω, is defined as the mass of water vapour per unit mass dry air [76]. Applying the ideal gas equation to both gases, the relationship becomes:

$$\begin{aligned}\omega &= \frac{0.622P_{sat}}{P - P_{sat}} \\ &= \frac{0.622 \times 3169}{P_{atm} - 3169} \\ &= 0.02\end{aligned} \tag{4.35}$$

The mass flow of water vapour is then

$$\begin{aligned}\dot{m}_{Vapour} &= 0.02\dot{m}_{Air} \\ &= 1.33 \times 10^{-6}\ \text{(kg/s)}\end{aligned} \tag{4.36}$$

Heat input to the saturated air is given by Eq 4.37, where $c_{p(Air)}$ is 1005 J/kgK.

$$q = \dot{m}_{Air} c_{p\,(Air)} \Delta T + \dot{m}_{Vapour} \Delta h_g \tag{4.37}$$

The enthalpy of water vapour is approximately equal to

$$h_g \approx 2501 + 1.82T\ \text{(kJ/kg)} \tag{4.38}$$

Where T is in degrees Celsius [76]. Then the enthalpy change from $T_{Scrubber}$ to $T_{Regenerator}$ is:

$$\begin{aligned}\Delta h_g &\approx 1.82(T_{Regenerator} - T_{Scrubber}) \\ &= 136\ \text{(kJ/kg)}\end{aligned} \tag{4.39}$$

Finally, the heat input to the flush gas is

$$\begin{aligned} q &= \dot{m}_{Air} c_{p(Air)} \Delta T + \dot{m}_{Vapour} \Delta h_g \\ &= 5 + 0.2 \\ &= 5.2 \ \text{(W)} \end{aligned} \tag{4.40}$$

Losses

To minimise heat loss the regenerator should be insulated with glass fibre insulation. Glass fibre can withstand service temperatures of over 250°C, and has a thermal conductivity of 0.05 W/mK [77]. The regenerator was modelled as a one dimensional (radial direction) steady state conduction problem, thereby neglecting loses from the ends and thermal resistance of the regenerator tube itself. The problem setup is shown in Figure 4.16.

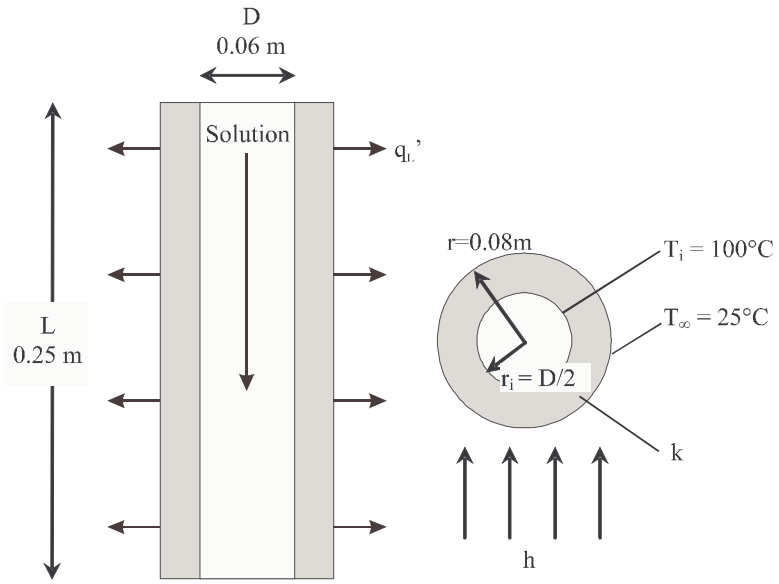

Figure 4.16 Problem setup and parameters for regenerator insulation calculation.

First checking for a critical insulation radius, R_{cr}, where h = 10 W/m^{2}K [77]:

$$\begin{aligned} R_{cr} &= \frac{k}{h} \\ &= 0.005\,(\text{m}) \end{aligned} \tag{4.41}$$

$R_{cr} < r_i$, therefore any addition of insulation reduces heat lost from the regenerator.

Thermal resistance is predominantly a combination of conductive and convective components, which are combined to the total resistance per unit length, R'$_{tot}$:

$$R'_{tot} = \frac{ln\frac{r}{r_i}}{2\pi k} + \frac{1}{2\pi r h} = 3.1 + 0.2\,(\text{mK/W}) \tag{4.42}$$

The rate of heat transfer per unit length is then

$$q_L' = \frac{T_\infty - T_i}{R'_{tot}} = -23\,(\text{W/m}) \tag{4.43}$$

For a length of 0.25 m the heat loss through the insulation is approximately 6 W. The losses increase modestly with parameters that may vary in service. For example, taking a high loss case of 50 mm insulation, T_∞ = -10°C, T_i = 130°C, h = 20 W/m^{2}K, all else being equal, the energy loss is 10 W.

Total Regenerator Energy Requirement

Summing the contributions calculated, the estimated total energy required by the regenerator is:

Solution Sensible Heat	154 W
Heat of Reaction	13 W
Flush Gas Sensible Heat	5 W
Losses	6 W
Total	**178 W**

Chapter 5

EXPERIMENTAL CHARACTERISATION

In Chapter 5 theoretical relationships are established to describe the absorption process and aid absorber optimisation. The developmental prototype components are then characterised experimentally. Component performance and the relationship of key parameters for the absorber and regenerator are investigated. The performance of existing scrubbing technology used for AFC systems, soda lime, is experimentally evaluated.

5.1 Absorber

5.1.1 Effect of Solution Depth on Scrubbing Performance

Liquid depth is a key parameter for bubble columns because this defines the gas feed pressure to be supplied by the blower. Feed pressure represents a parasitic power load on the system and must be minimised for efficiency. The scrubbing process, for the control volume of an individual bubble, is shown in Figure 5.1.

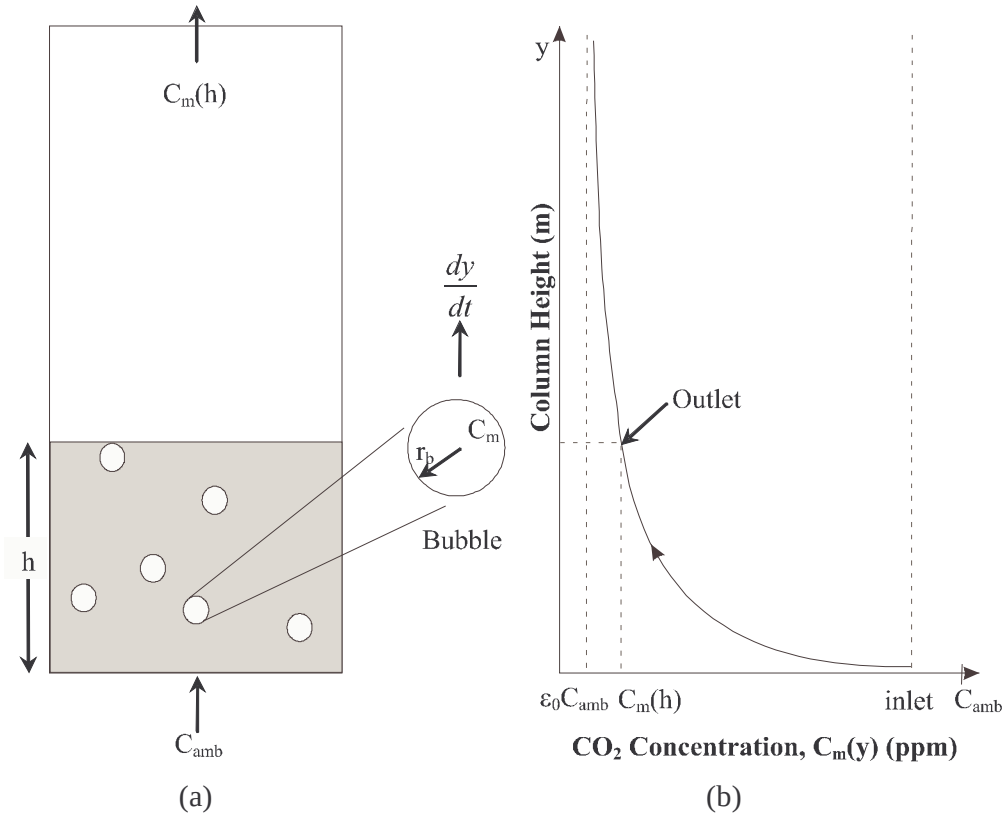

Figure 5.1 (a) Air bubbles rise through solution in a packed bubble column and (b) Variation in CO_2 concentration with height.

Air enters the column with ambient CO_2 concentration, C_{amb} (moles/m^3). An air bubble of radius r_b (m), surface area A_b (m^2) and volume V_b (m^3) moving upward through the absorbent solution has a mean CO_2 concentration C_m (moles/m^3) at height y (m). A minimum possible CO_2 concentration of $\varepsilon_0 C_{amb}$ (moles/m^3) is achieved by a given solution, where ε_0 (%) corresponds to the equilibrium solubility for the system at a given temperature and pressure. The bubble moves with velocity u_b (m/s) from y = 0 to y = h, the depth of solution.

Residence time, t_r (s), representing the time a gas bubble is in contact with the absorbent liquid, is a function of the air volume flow rate, Q (m^3/s), the fluid depth, h (m), and the column cross sectional area, A_c (m^2). The superficial gas velocity, u_g (m/s), is defined as the air volume flow rate divided by the column cross sectional area.

$$t_r = \frac{hA_c}{Q} = \frac{h}{u_g} \tag{5.1}$$

The mean CO_2 concentration in the gas is a function of height at any instant, and consequently a function of residence time. Considering a CO_2 mole balance on a bubble travelling upward from height y to y+dy:

$$\{\text{mols in bubble at y}\} = \{\text{mols in bubble at y} + \text{dy}\} - \{\text{mols absorbed}\}$$

$$\{C_m(y)V_b\} = \left\{C_m(y)V_b + \frac{dC_m(y)}{dy}\cdot dyV_b\right\} + \{C_m(y)V_b kA_b dt\} \tag{5.2}$$

where k ($1/m^2s$) is the mass transfer rate coefficient for the given solution and conditions. Rearranging and collecting terms:

$$\frac{dC_m}{C_m} = -kA_b dt \tag{5.3}$$

The CO_2 concentration in the air bubble can be normalised, using $\varepsilon_o C_{amb}$ as a reference point, to account for the equilibrium CO_2 concentration over the particular solution used. Accordingly, $C_m(y)^*$ is defined as:

$$C_m(y)^* = C_m(y) - \varepsilon_0 C_{amb} \tag{5.4}$$

Substituting variables and integrating over the process from inlet to outlet gives:

$$\int_{\text{inlet}}^{\text{outlet}} \frac{dC_m^*}{C_m^*} = -\int_0^{t_r} kA_b dt \tag{5.5}$$

The CO_2 concentration in air is reduced by exposure to an MEA surface. The absorption arising from passing air across MEA is designated ε_i (%), and thus the inlet condition for Eq 5.5 is:

$$C_m^* \Big|_{inlet} = \varepsilon_i C_{amb} - \varepsilon_0 C_{amb} \tag{5.6}$$

The upper limit of integration represents the concentration value at height y = h, which by Eq 5.1 is directly proportional to t_r. Thus the outlet condition is:

$$C_m^* \Big|_{outlet} = C_m(t_r) - \varepsilon_0 C_{amb} \tag{5.7}$$

Evaluating the integral gives:

$$\frac{C_m(t_r) - \varepsilon_o C_{amb}}{\varepsilon_i C_{amb} - \varepsilon_o C_{amb}} = \exp(-kA_b t_r) \tag{5.8}$$

$$C_m(t_r) = (\varepsilon_i - \varepsilon_o) C_{amb} \exp(-kA_b t_r) + \varepsilon_o C_{amb} \tag{5.9}$$

Equation 5.9 shows an exponential relationship between the CO_2 concentration exiting the absorber and the residence time (or depth); the following experimental results verified this relationship and allow empirical determination of process and chemical parameters.

Maintaining a constant gas flow rate of 20 or 40 m^3/hr, the absorber liquid depth was varied in 50 mm increments. The absorber was initially filled to capacity with fresh standard solution, and volumes of liquid drawn off after analysis at each depth increment. Emulsion contributes to residence time, so at each depth and flow combination, the level of emulsion was measured.

Performing experiments within a relatively short period ensured the absorption potential of the MEA solution did not change appreciably. The absorber was run for ten minutes between depth changes, to allow the system to reach steady operating conditions before exhaust gas analysis for CO_2 content. Measurements were performed with the GC-TCD. Results of the experiments are shown in Figure 5.2.

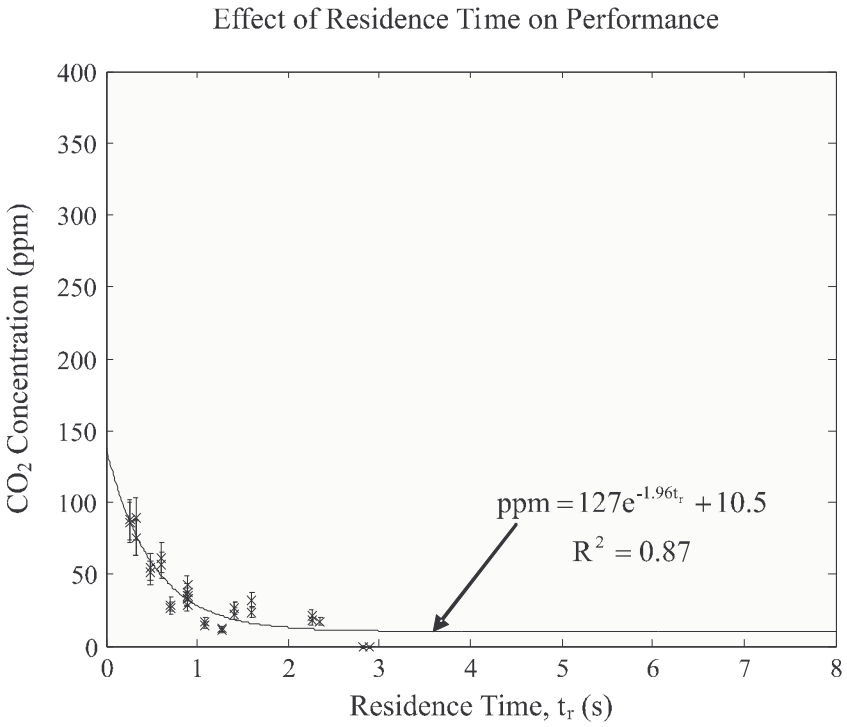

Figure 5.2 Effect of residence time on scrubbing performance.
Residence Time = Liquid Depth x Column Area/Air Flow Rate. 20 and 40 m^3/hr air, standard solution, depth 50-500 mm plus emulsion depth.

The behaviour predicted from the rising bubble model is commensurate with the performance of the absorber. Since residence time is directly dependent on solution depth, the results are representative of the effect that solution depth has on scrubbing performance (provided a churn turbulent flow regime is maintained).

A packed bubble column filled with a given solution of MEA has a lower limit for CO_2 scrubbing represented by $\varepsilon_0 C_{amb}$. From the best fit equation (Figure 5.2) and Eq 5.9, $\varepsilon_0 C_{amb}$ is 10 ppm for 50 wt% MEA solution. By extrapolating to zero residence time, the surface exposure concentration, $\varepsilon_i C_{amb}$, is 137 ppm. This value is indicative of the scrubbing performance gained by simply blowing an air stream over the MEA solution considered, for example through a packed column where the packing surface is wetted but there is no bubble-liquid mixing.

The exponential behaviour of the column aids design of the liquid height for a desired scrubbing system. Practically, scrubbing is considered complete when the CO_2

concentration has been reduced from ambient concentration to within 2% of that possible for the solution.

$$C_m(t_{r98\%}) = 0.02(C_{amb} - \varepsilon_0 C_{amb}) + \varepsilon_0 C_{amb} \tag{5.10}$$

Given the equilibrium solubility of a solution, the scrubbing curve data is used to determine $t_{r98\%}$. For the 50 wt% solution in Figure 5.2, $C_m(t_{r98\%})$ = 18 ppm and $t_{r98\%}$ = 1.44 seconds, corresponding to a liquid depth of 160 mm for 20 m^3/hr or 320 mm for 40 m^3/hr air flow rate (excluding depth of emulsion).

Figure 5.2 applies only to fresh 50 wt% solution. As a solution absorbs CO_2, the quantity of active MEA and absorption potential progressively decrease, so the performance of a used 50 wt% solution eventually resembles that of a fresh 45 wt% solution, then 30 wt% as the solution approaches a steady operating state. This is demonstrated in Figure 5.3.

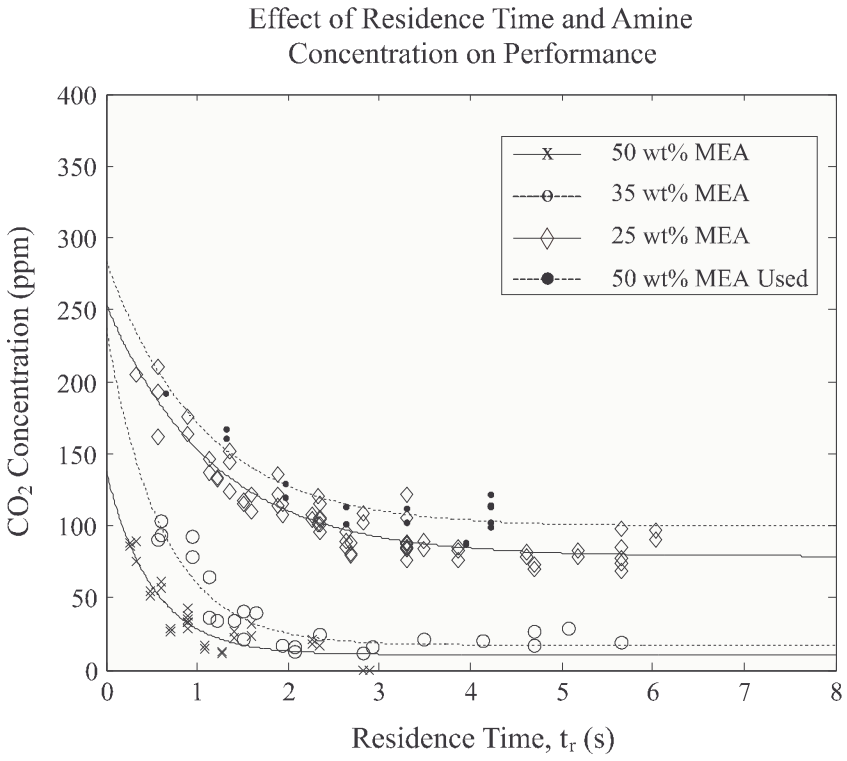

Figure 5.3 Effect of amine concentration on scrubbing performance.

Figure 5.3 shows performance of three fresh solutions of varying MEA concentration. The lower limit of performance, at large t_r, increases from 10 to 79 ppm CO_2 as MEA concentration decreases from 50 to 25 wt%. The fourth data set ('50 wt% MEA Used') represents the performance of a solution originally composed of 50 wt% MEA. The used solution had scrubbed a significant volume of air prior to the experiment, thus reducing the quantity of free amine and absorption ability. The estimated solution composition, from titration of a solution sample, was 20 wt% and the limiting CO_2 concentration correspondingly high at 100 ppm.

5.1.2 Absorption Performance without Regeneration

A long term experiment was performed to investigate absorber performance without regeneration. The absorption characteristics of the solution over time have not been described in literature. In particular, it was not clear whether the solution strongly absorbs CO_2 up to a breakthrough point, or the CO_2 escaping gradually rises with time in a linear, quadratic or exponential fashion.

The absorption performance experiment employed 17 litres of solution (300 mm depth) and 20 m^3/hr air flow, providing a residence time of 3.5 seconds including the 80 mm depth of emulsion. Carbon dioxide content in the exhaust air was monitored by GC-TCD, and a small sample of solution was drawn from the column periodically for pH measurement and MEA concentration analyses by titration. Due to evaporative loss in the exhaust stream, a peristaltic pump added 0.5 litres of water to the absorber per day to maintain the correct liquid depth. Figure 5.4 shows a compilation of CO_2 concentrations in scrubbed air from two experiments.

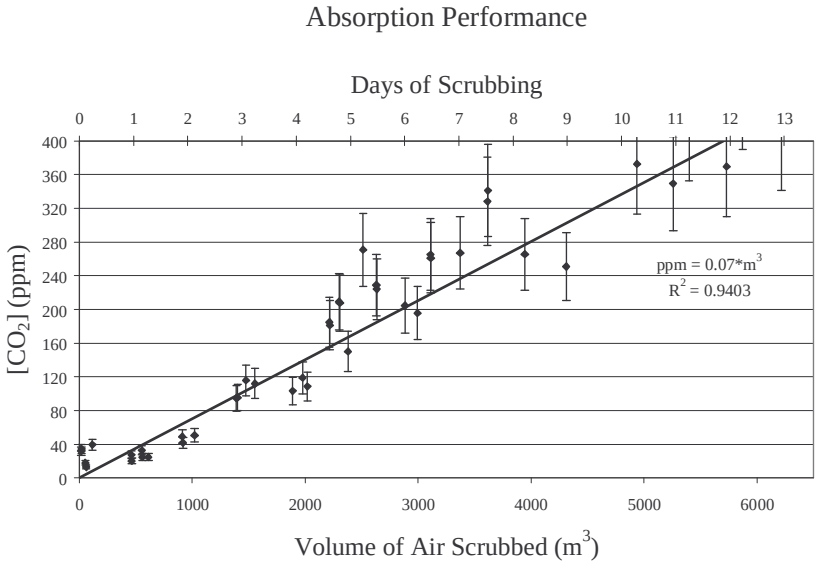

Figure 5.4 Absorption performance with standard solution.
300 mm static depth and 20 m^3/hr air flow rate.

The concentration of CO_2 escaping the absorber increased linearly with the volume of air scrubbed, up to atmospheric concentration. Weight percent MEA and solution pH, shown in Figure 5.5(a) and (b) respectively, were monitored by titration and pH meter to establish the relationship between solution properties and performance.

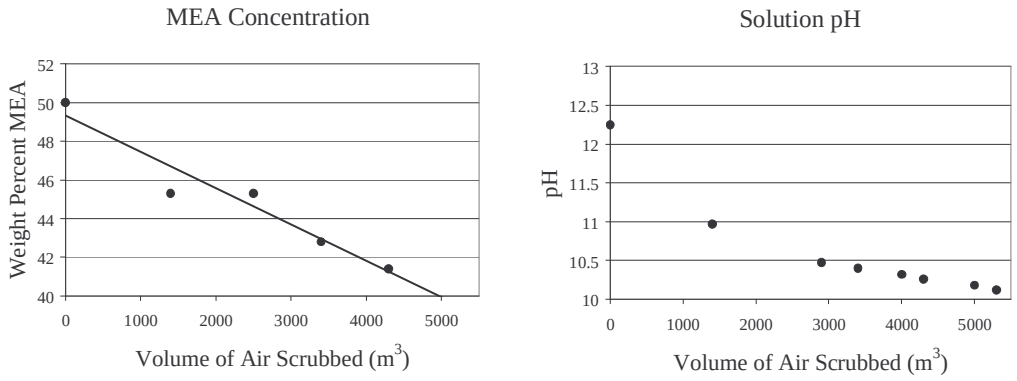

(a) (b)

Figure 5.5 (a) Change in MEA concentration and (b) Change in pH of solution during absorption experiment.

The titrated weight percent MEA is not an exact measure, but an approximately linear relationship existed between MEA concentration and the volume of air scrubbed. This could be expected for constant absorption throughout the experiment (a horizontal line on Figure 5.4), however as illustrated in Figure 5.6, the gross CO_2 absorption rate (moles absorbed/unit time) decreased as the experiment progressed.

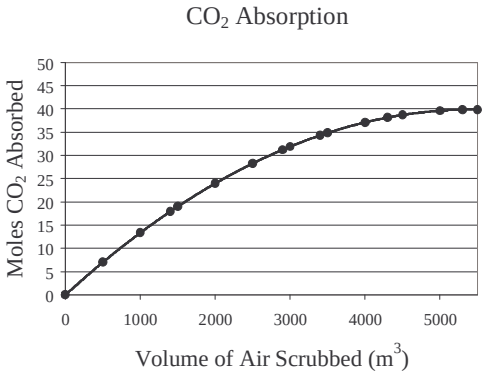

Figure 5.6 Cumulative quantity of CO_2 absorbed during absorption experiment.

Other processes that could have enhanced the conversion rate of active MEA in the latter stages were degradation and equilibrium reaction changes that occur with loading and pH.

pH is one of several factors controlling the absorption rate of the system, and depends on MEA concentration. A logarithmic variation was expected due to the (simplified) definition

$$pH = -\log[H^+] \tag{5.11}$$

At high pH, as for 50 wt% MEA solution, a small addition of H^+ ions causes a disproportionately large drop in pH value. Though there is some distortion due to the non linear absorption of CO_2, Figure 5.5(b) displays the negative log relationship.

Over the range of values considered, the linear absorption characteristic displayed in Figure 5.4 is the net effect of changing CO_2 absorption, weight percent MEA and pH. The absorption performance case provided a benchmark of performance for the absorber, against which the performance of the regenerator was evaluated.

5.1.3 Effect of Packing on Scrubbing Performance

Packing greatly enhances performance of a bubble column, but commercial packing units such as Pall rings are expensive (approximately NZ$20 per litre in small quantities) and could prohibit the economic success of the scrubber. The following experiments evaluated each of the three random packing elements described in section 4.2.3.

The absorber was filled with the selected packing and run with 10 L of fresh standard solution at 200 mm depth. A residence time of 2.3 seconds, including an emulsion depth of 50 mm, was established with a 20 m^3/hr air flow. The GC-TCD was used to repeatedly sample scrubbed air for CO_2 content, the results of which are shown in Figure 5.7.

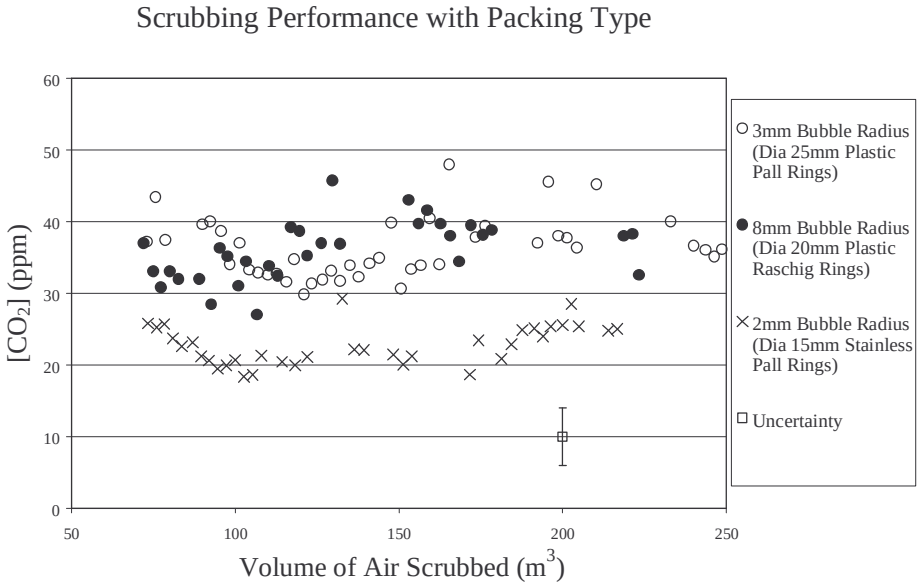

Figure 5.7 Influence of packing media on performance.

The relatively low liquid depth was chosen to improve GC-TCD measurement accuracy – the results do not represent the best scrubbing performance obtainable from the absorber. Compared to the other packing elements, 15mm diameter Pall rings enhanced performance slightly (approximately 4%). Visual observation

indicated that the smaller Pall rings maintained a smaller average bubble size, and therefore larger total interfacial area and better performance. Although the 25 mm diameter Pall rings are considerably larger than the Raschig rings, the more complex internal structure maintained a smaller bubble size, and no appreciable difference in performance was observed.

Stainless steel Pall rings have the advantage of a very high surface area to volume ratio due to fabrication from sheet metal (Table 5.1). Both ceramic and plastic Raschig or Pall rings have thicker walls and therefore displace more absorbent liquid. In other respects, the packing varieties showed similar performance, including pressure drop, gas hold-up, turbulent mixing and resistance to channelling.

Table 5.1 Physical properties of packing materials.

	$\frac{\text{Surface Area}}{\text{Displacement Volume}}$	Relative Surface Area per Litre of Packing
Stainless Steel diameter 15 mm Pall Rings	5.9	1
Plastic diameter 20 mm Raschig rings	1.1	0.8
Plastic diameter 25 mm Pall rings	1.7	0.7

5.2 Investigation of Soda Lime Performance

A point of reference for scrubbing alternatives was required to evaluate the absorber for AFC application. The most common scrubbing method for AFC's is soda lime absorbent, however the exact performance of soda lime was not found in literature. One kilogram of Panreac indicating soda lime was supplied by Scientific Supplies Ltd Auckland New Zealand, for a scaled experiment (Figure 5.8), based on absorber dimensions from Zetek, a fuel cell manufacturer.

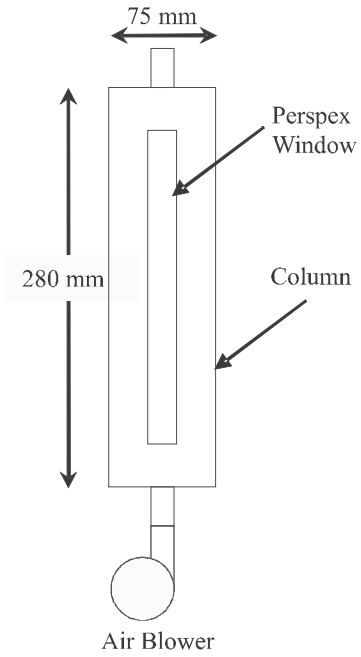

Figure 5.8 Experimental soda lime apparatus.

An air flow rate of 2 m^3/hr was sufficient to maintain similarity in residence time, gas velocity and mass of soda lime. Soda lime scrubbing performance over time was monitored by GC TCD analysis for CO_2 in the exhaust air (Figure 5.9). The level of indicator colour change is the only measure of exhaustion available in practice, so was also recorded.

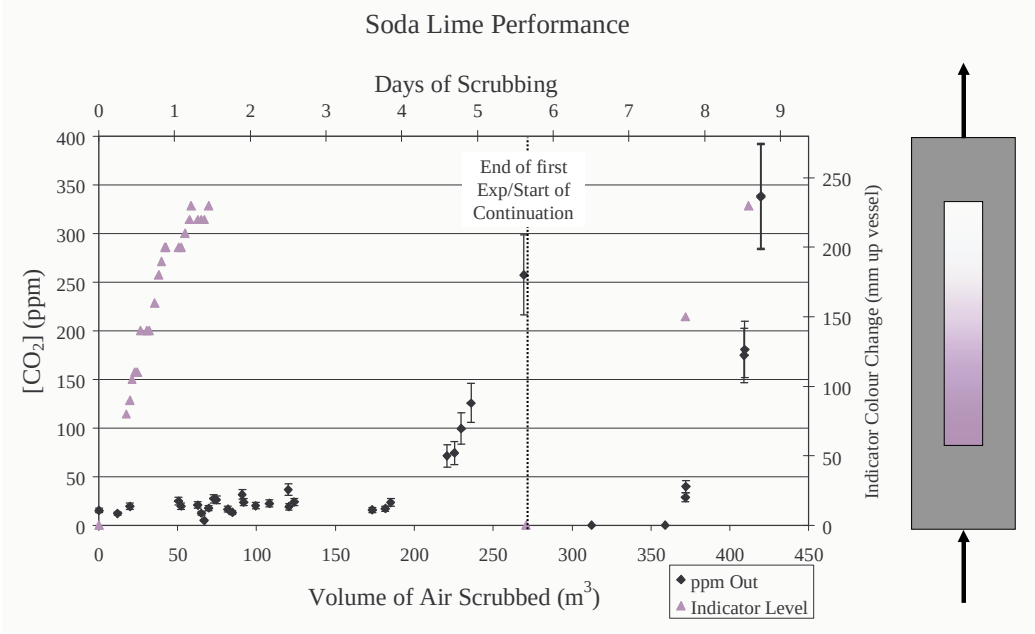

Figure 5.9 Scaled soda lime apparatus performance.

In contrast to MEA solution, the soda lime absorbed CO_2 very strongly up to a breakthrough point, beyond which the CO_2 escaping increased dramatically. The indictor colour change was a poor measure of exhaustion, grossly underestimating the absorption ability. One kilogram of soda lime was capable of scrubbing 180 m^3 of air from 380 to approximately 20 ppm CO_2. For the 6 kW AFC system, requiring air at 40 m^3/hr, this corresponds to 25 kWh generation per kilogram of soda lime. This value lies between the extremes found in literature of 135 and 0.4 kWh (section 2.1.2) and matches the estimated value for the Eneco Ltd fuel cell.

Literature indicated that due to the diffusion step in the soda lime-CO_2 reaction, soda lime which appears to be exhausted will absorb more CO_2 following a period of rest. During the rest, CO_2 continues to diffuse deeper into each granule, replenishing the reactive components near the surface.

The performance of exhausted soda lime, rested for 12 weeks in a sealed container, is included in Figure 5.9. During the rest period, the soda lime returned to the original off white colour, and was subsequently capable of further absorption to very low levels. However, longevity was greatly reduced (less than 50% capacity compared to fresh state), and the indicator colour change was of no practical use. This pattern repeats several times, each with a reduction in capacity compared to the last.

5.3 Investigation of Regenerator Performance

The performance characteristics of the small packed bubble column regenerator were investigated. Some insight into the effect of operational parameters was gained by experimenting with a custom made glass reaction vessel of diameter 70 mm. Filled with Pall rings, the vessel acted as a packed bubble column (Figure 5.10). Half a litre of standard solution was loaded with CO_2 by adding dry ice, to achieve a loading of 0.5 moles CO_2 per mole MEA. The CO_2 absorbed was measured by weighing the solution before and after absorption.

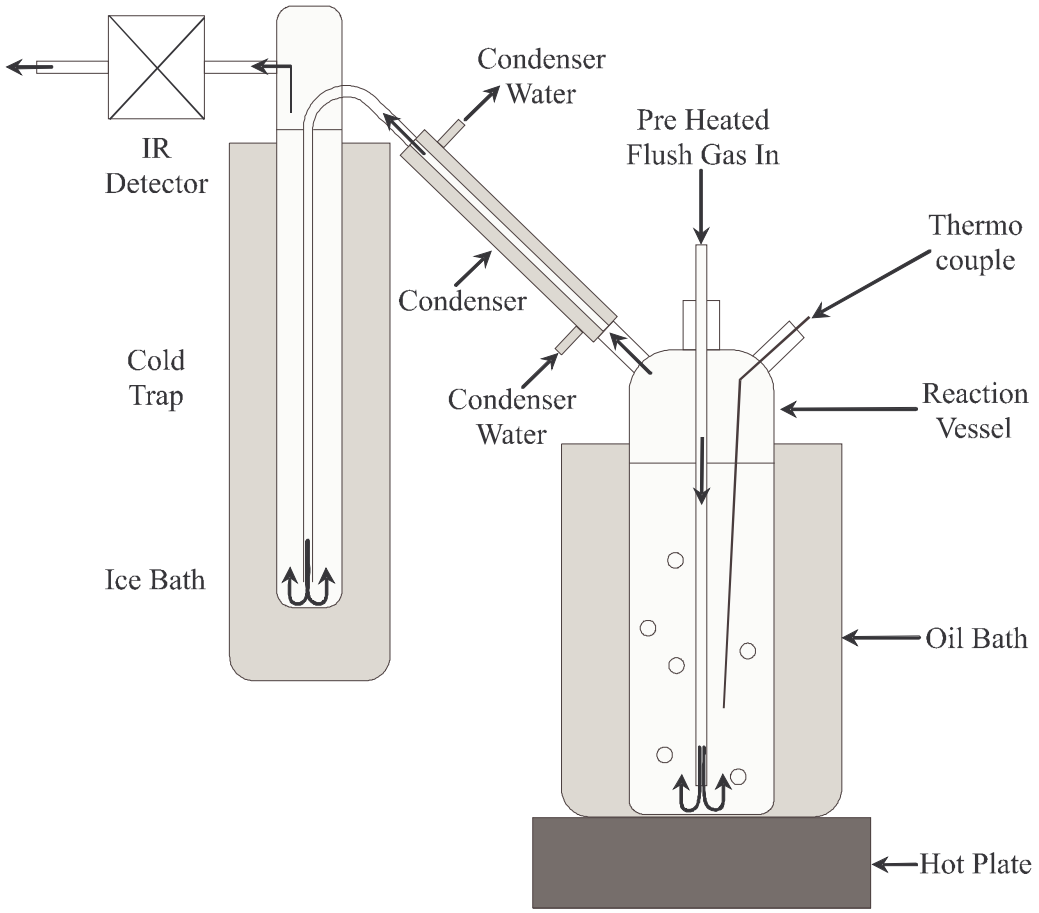

Figure 5.10 Schematic of regenerator characterisation apparatus.
Packing in reaction vessel not shown.

An oil bath was used to heat the standard solution to regeneration temperature and preheat nitrogen or air (the flush gas) to 30°C before being blown over or through the solution. Entrained vapour was removed by a condenser and a water-salt-ice cold trap, and the gas analysed for CO_2 content with the Draeger Polytron IR detector. The oil bath was preheated to the target temperature prior to the experiment. The solution, initially at room temperature, was placed in the bath, resulting in a temperature gradient during the experiment. The temperature gradient and variation in solution properties during regeneration resulted in a characteristic CO_2 evolution profile. Typical temperature and evolution profiles are shown in Figure 5.11.

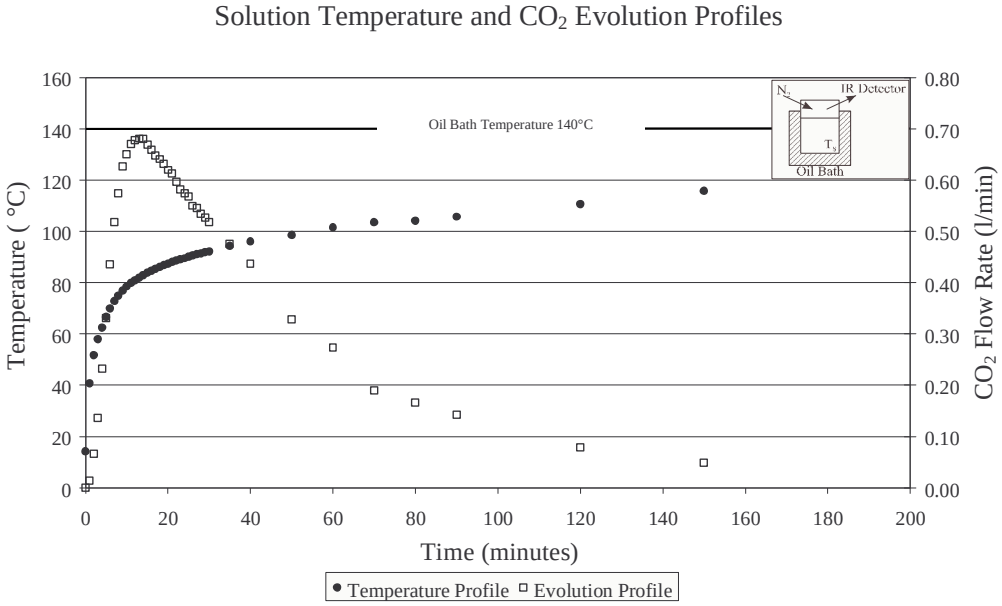

Figure 5.11 Typical solution temperature and CO_2 evolution profile during regenerator prototype experiments.

Target temperature 140°C, 6.8 litres/minute nitrogen flow rate.

Figure 5.11 corresponds to an oil bath temperature of 140°C with nitrogen injected into the solution. The solution temperature remained well below the oil bath temperature throughout the experiment due to a cooling effect from flush gas flow. To enable comparison of experiments at various oil bath temperatures, an approximation to the actual regeneration temperature was taken as the temperature at 100 minutes. A large flow rate of CO_2 was evolved initially, at relatively low temperatures. The dynamics of the regeneration process which result in this profile are discussed in section 5.3.7.

5.3.1 Effect of Temperature on Regeneration with Nitrogen Surface Flush Gas

The regeneration achieved by blowing 6.8 litres/minute nitrogen over the surface of the solution at various temperatures is shown in Figure 5.12. The y axis parameter, percent CO_2 regenerated, refers to the cumulative CO_2 evolved as a percentage of that initially absorbed.

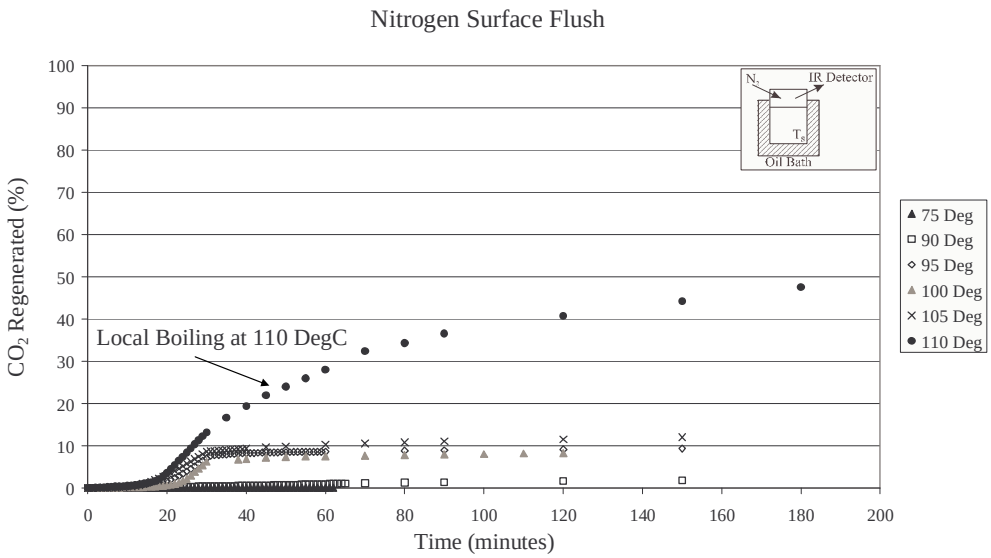

Figure 5.12 Regeneration achieved by blowing 6.8 litres/minute nitrogen across the liquid surface in a reaction vessel at various solution temperatures.

All temperatures achieved regeneration, but the effectiveness varied greatly. Local boiling occurred for the 110°C case, corresponding to a relatively high level of regeneration. Results showed that to accomplish a practical level of regeneration with gas blown over the surface, the solution must be at or near its boiling point (approximately 135°C). Vapour produced by boiling provided gas bubbles with significant surface area and of low CO_2 partial pressure to aid nucleation and evolution.

5.3.2 Effect of Temperature on Regeneration with Nitrogen Injection Flush Gas

A 7 litres/minute flow of nitrogen was preheated in an oil bath to 30°C, then injected into the solution to simulate the beneficial conditions provided by boiling. The residence time of the flush gas in solution was approximately 4 seconds. The impact of varying regeneration temperature with gas injection is shown in Figure 5.13.

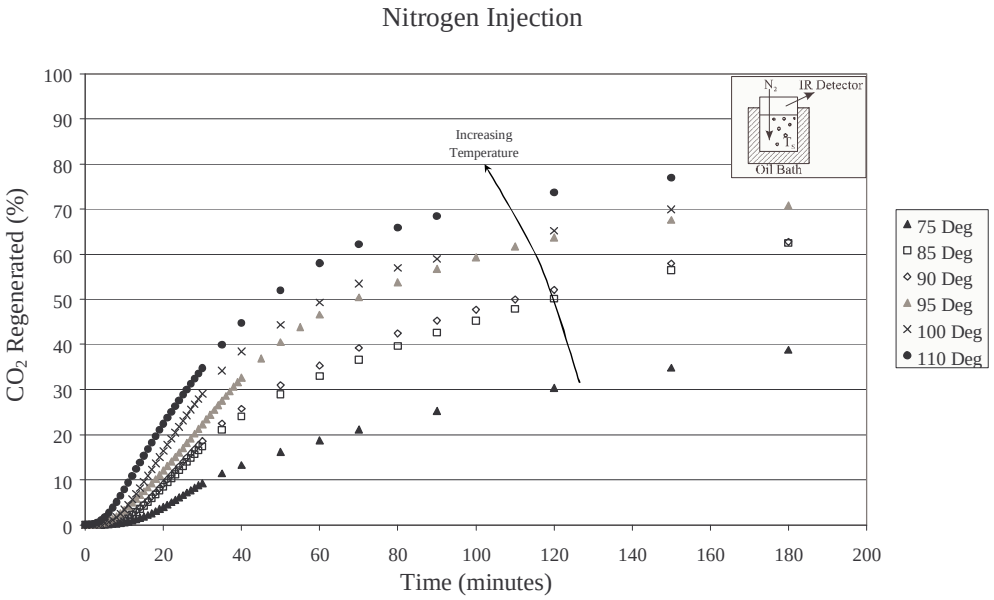

Figure 5.13 Regeneration achieved by injecting 7 litres/minute nitrogen into the solution, as per a bubble column, at various temperatures.

Inert gas injection through the heated solution induced a similar mechanism to boiling - the gas bubbles helped evolve and flush away CO_2 from the solution by increasing surface area and creating bubbles of gas with low CO_2 partial pressure. In comparison to gas flowing over the surface of the solution, injection achieved much faster regeneration, and to a greater degree (higher final percent regenerated) at lower temperature.

5.3.3 Effect of Varying Flush Gas Flow Rate on Regeneration with Nitrogen Injection

The effect of flush gas flow rate was investigated by varying the nitrogen flow rate from 2 to 10 litres/minute. Flush gas was injected into identical solutions at 90°C and monitored for CO_2 content by the Draeger IR CO_2 detector. Results are shown in Figure 5.14.

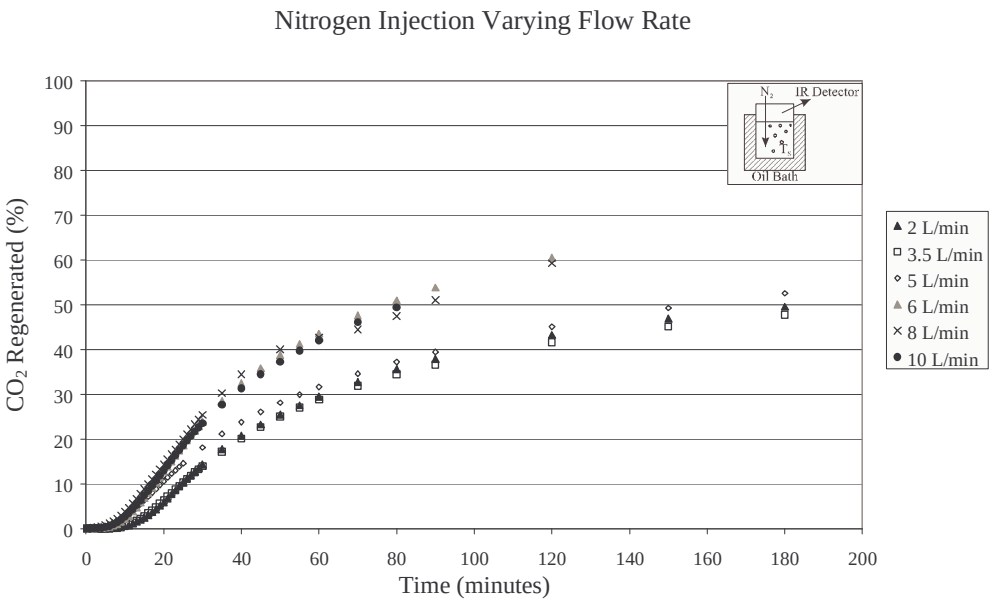

Figure 5.14 Effect of nitrogen flow rate on regeneration at 90°C with gas injection.

Figure 5.14 shows two groupings of flow rates in the ranges 0-5 litres/minute and 6-10 litres/minute, where the higher flow rates resulted in more complete regeneration. An emulsion similar to that in the absorber was observed at higher flow rates (superficial gas velocity > 0.03 m/s), indicating that the churn turbulent flow regime prevailed. For lower flow rates, the flow resembled the homogeneous regime. Mixing, and resultant gas liquid interaction, is therefore an important function of the regenerator, and a turbulent regime is desirable. The superficial gas velocities specified for the absorber (churn turbulent regime at $u_g > 0.1$ m/s) do not apply due to the very small diameter of the regenerator vessel.

5.3.4 Effect of Air Flush Gas on Regeneration with Injection

At elevated temperature, oxygen reacts with MEA to form degradation compounds, affecting the performance of the solution. The use of nitrogen flush gas ensured the effect of one parameter at a time was evaluated by avoiding oxidative degradation. However, nitrogen (or any processed gas) is impractical for the AFC application. The effect of using 5 litres/minute air, rather than nitrogen, as the flush gas is represented in Figure 5.15. Results from repeated runs are presented, plus an equivalent nitrogen run for comparison.

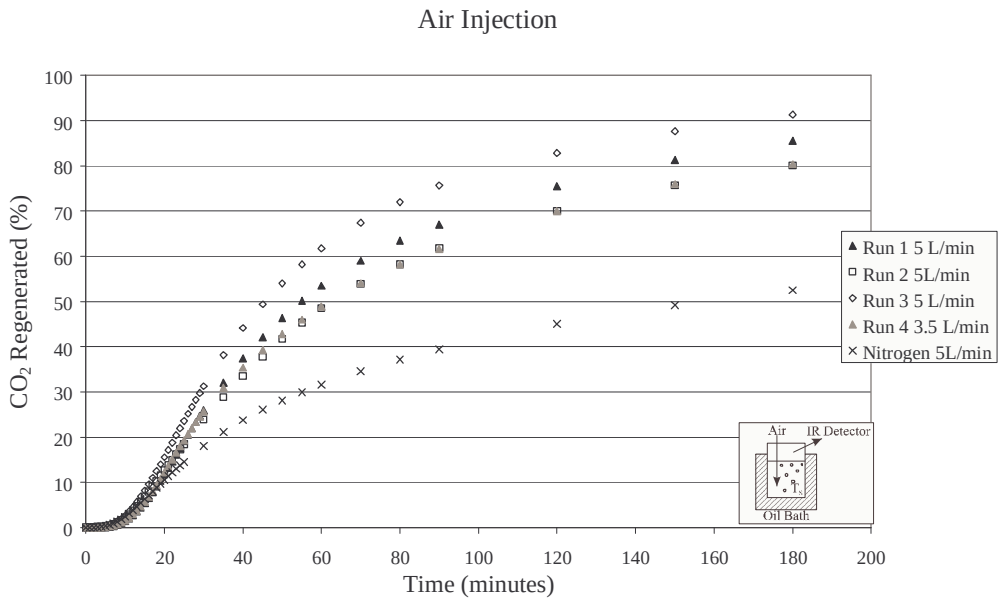

Figure 5.15 Regeneration achieved with air injected into the MEA solution. All data sets correspond to a regeneration temperature of 90°C.

The use of air as flush gas markedly improved regeneration performance. No explanation for this phenomenon has been determined. Upon exposure to oxygen, the MEA solution turned from clear to yellow during the experiment, a phenomenon also noted during the absorption performance experiment. The discolouring is believed to be a result of oxidative degradation since no discernable colour change was observed with nitrogen as flush gas.

5.3.5 Effect of Multiple Regeneration with Nitrogen Injection

Amines are used primarily because of the ability to cyclically absorb and desorb CO_2. The reaction is not completely reversible and the degree of regeneration can vary, with as much as 40% capacity loss on regeneration reported. To investigate the cycling ability of the standard solution, a single batch was repeatedly loaded with CO_2 and regenerated using nitrogen flush gas.

The quantity of CO_2 absorbed and evolved at each cycle resulted in the cumulative performance in Figure 5.16. The degree of regeneration achieved is dependent on the

state of the solution, including the CO_2 loading. To reflect this, the y axis parameter, percent CO_2 regenerated, was determined by adding the quantity of CO_2 remaining in solution from the previous regeneration, to the quantity subsequently reabsorbed.

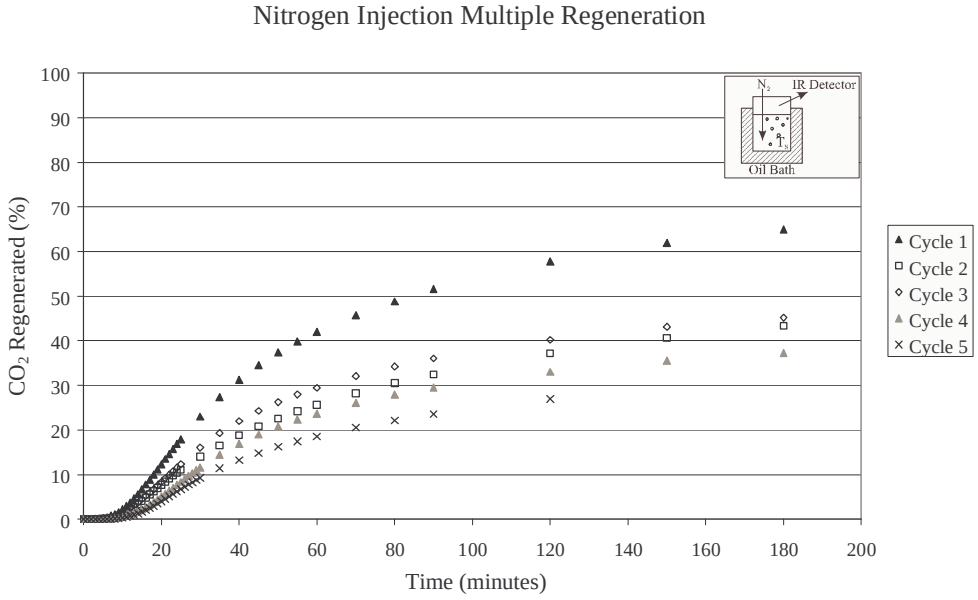

Figure 5.16 Multiple regeneration of standard solution at 90°C, nitrogen flush gas. Nitrogen flow rate 5 litres/minute.

A large loss of capacity is evident after the first regeneration, as suggested in literature. This is due to the initial formation of stable products formed by the MEA - CO_2 reaction, which are irreversible. Subsequent regenerations showed a gradual decline in percent regeneration, most likely due to the formation of degradation compounds and further stable compounds with changing solution loading and pH.

5.3.6 Effect of Multiple Regeneration with Air Injection

The effect of air on the cycling ability of amine solutions was not found in literature since the regeneration apparatus and method had not previously been investigated. Figure 5.17 displays results from five regeneration cycles.

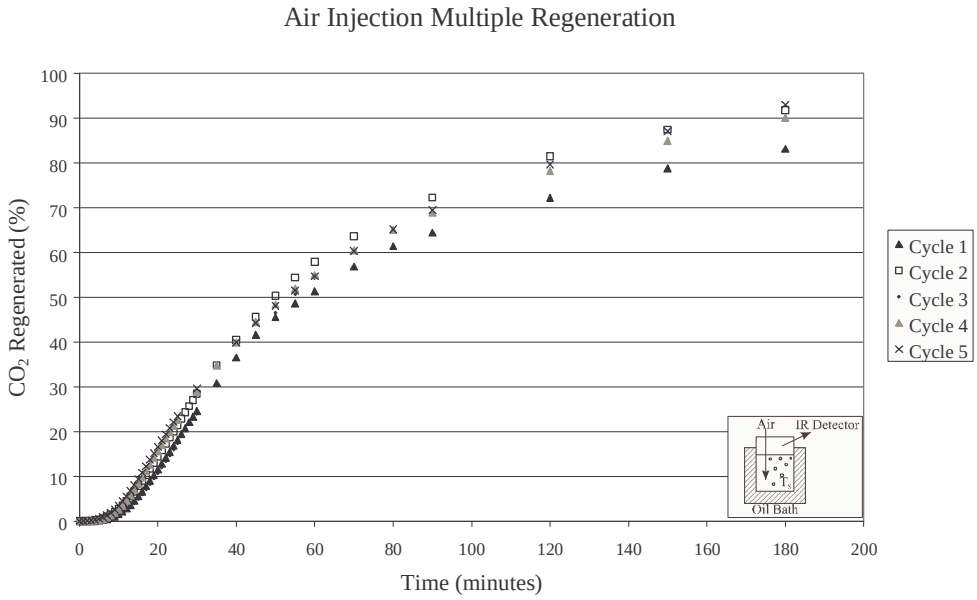

Figure 5.17 Multiple regeneration of standard solution at 90°C, air flush gas. Air flow rate 5 litres/minute.

Using air as the flush gas improved regeneration performance in general. The initial loss of capacity did not occur, and the solution maintained similar regeneration performance for all five cycles. No information regarding the use of air for regeneration was available and no reason for the improved performance is postulated. The solution developed a darker shade of yellow with each regeneration, indicating a build up of unknown reaction products. These aspects of regeneration require further investigation to develop a full understanding.

The solution in the CDOCS system will operate in a continuous regeneration process, as opposed to the batch process investigated. However, the results indicated that the solution will undergo several regenerations without detrimentally affecting absorption, even in the presence of oxygen. In industry, an MEA solution performs thousands of cycles before replacement, lasting for two years or more.

5.3.7 Investigation of Evolution Rate

The regeneration rate (moles CO_2 evolved per unit time) must be as high as possible to maximise the effectiveness of the regenerator and avoid holding the solution at

temperature for an extended period. There are three independent variables affecting the regeneration rate. The solution temperature and loading have a strong influence on the rate and the degree of regeneration achievable, attributable to changing the chemical equilibrium of the MEA - CO_2 system. Both parameters unavoidably changed with time during regeneration experiments. Flush gas flow rate also influences regeneration, but to a lesser degree.

A three dimensional graph (Figure 5.18(a)) represents all three regeneration parameters, providing insight to the optimum conditions for effective regeneration and comparison to the likely operating point of the prototype CDOCS system. Independent variables, temperature and loading, are plotted on the x and y (horizontal) axis, and the evolved CO_2 flow rate divided by the flush gas flow rate on the z axis. The figures include a typical air regeneration run for comparison. Figure 5.18 (b) and (c) give views of the x-z and y-z axes respectively.

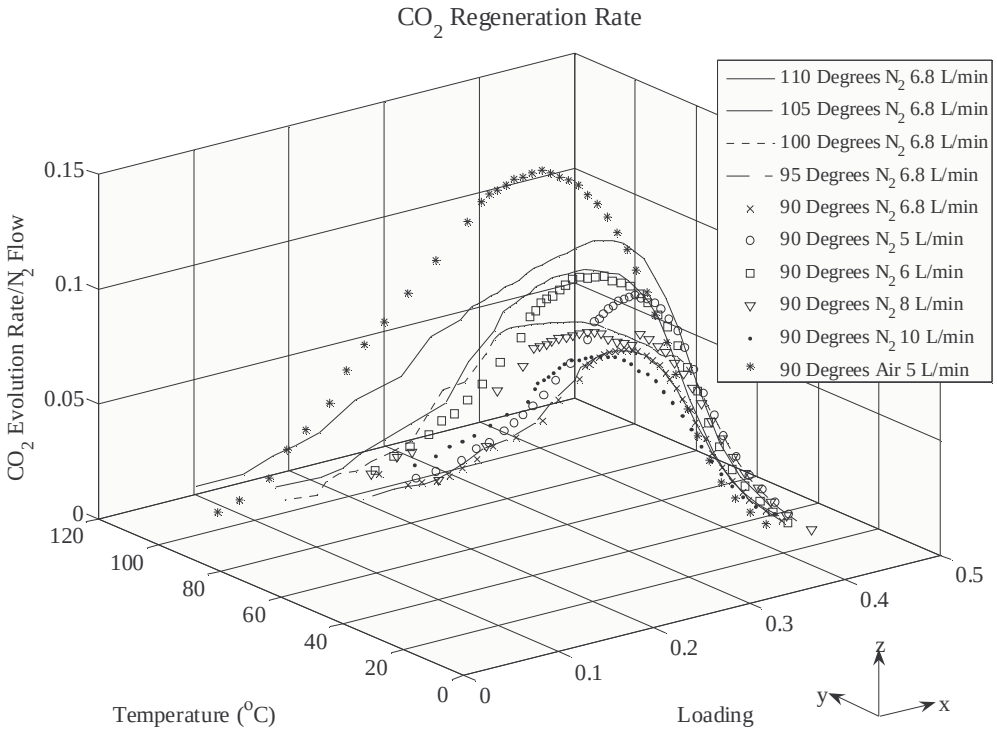

(a)

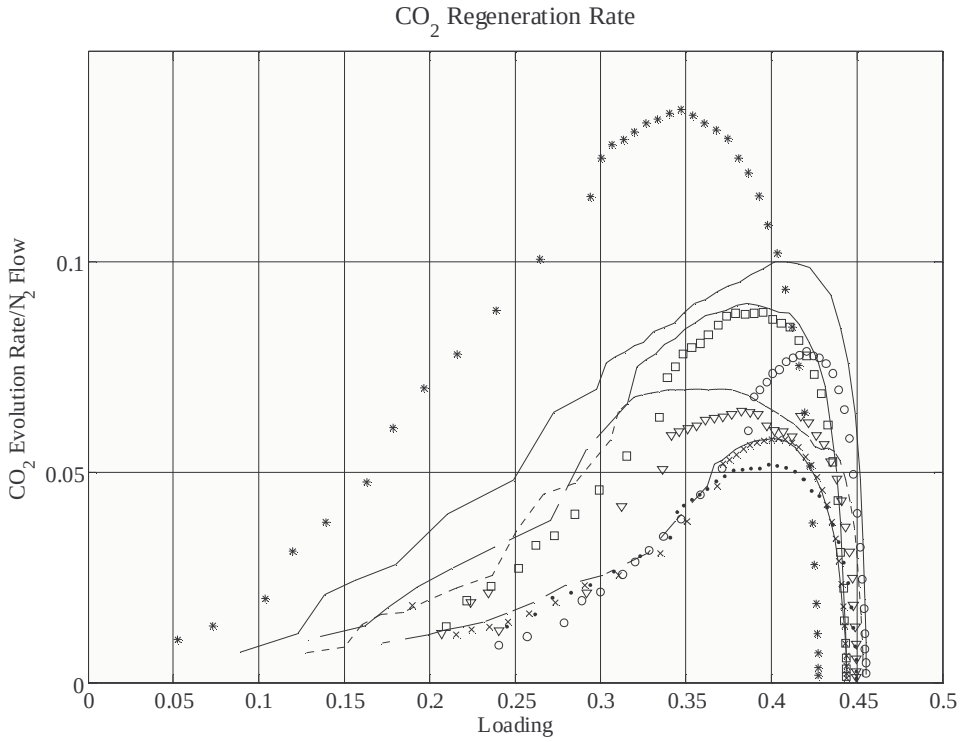

(b) x-z view

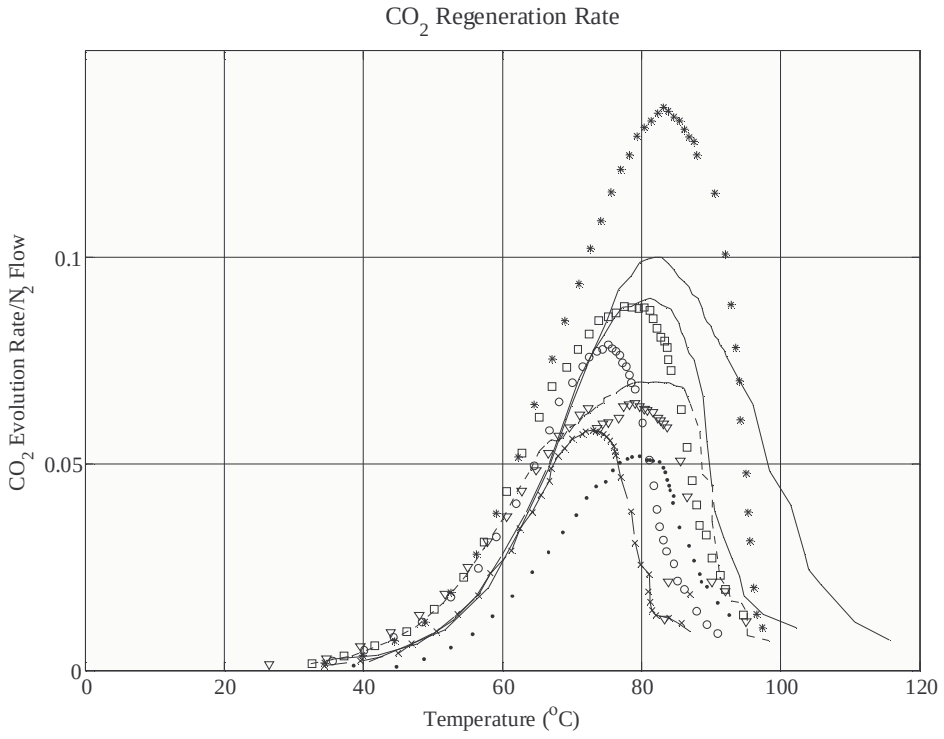

(c) y-z view

Figure 5.18 Representation of three inseparable factors affecting regeneration.

Figure 5.18 shows that evolution of CO_2 was achieved at high loading, even at relatively low temperature (60°C). The highest evolution rates were achieved at high loading (0.4 +) and temperatures at or above 80°C. Air regeneration followed the same trend as nitrogen, but gave higher evolution rates and peaked at slightly lower loading. Due to the inability of the oil bath to warm the solution quickly, no data at high loading and high temperature are presented, but very high evolution rates are expected for these conditions.

Evolution at high loading and low temperature is a result of the vapour liquid equilibrium between CO_2 and MEA. At high loading, a large concentration (partial pressure) of gaseous CO_2 may exist in equilibrium with that absorbed. A low partial pressure of CO_2 in the gas phase was maintained by flushing evolved CO_2 away, sustaining a driving force for CO_2 evolution. The driving force increases at elevated temperature because the vapour pressure of CO_2 increases at a much faster rate than the vapour pressure of the solution.

High loading is not desirable for low ppm CO_2 scrubbing, so the operating point for the prototype system is likely to lie somewhere in the low to medium loading range, 0.2-0.3, and 100°C solution temperature. Under experimental conditions this would achieve a CO_2/N_2 evolution rate of approximately 0.1. Assuming a 5 litres/minute flush gas flow rate and applying the ideal gas equation, approximately 1 mole/hour CO_2 would be evolved, compared to 0.3 moles/hour absorbed at 20 m^3/hr air flow rate.

5.3.8 Investigation of Regeneration with Low CO_2 Loading

Regeneration becomes more difficult as loading decreases due to low CO_2 partial pressure and increasing stability of reaction products. Solutions with low loading were investigated to determine if regeneration still occurs using the bubble column apparatus and air flush gas (3.5 litres/minute). Figure 5.19 and Figure 5.20 show the evolution rate and total regeneration for solutions with 0.5, 0.25 and 0.15 loading. For the 0.5 loading experiment, the air flow rate was 5 litres/minute.

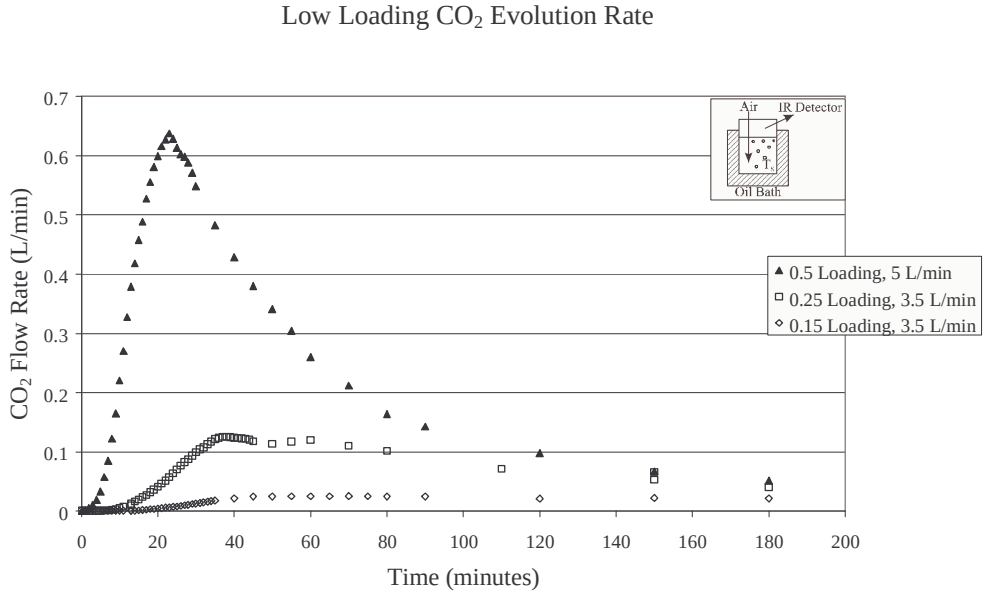

Figure 5.19 Evolution of CO_2 at 90°C for various solution loadings.

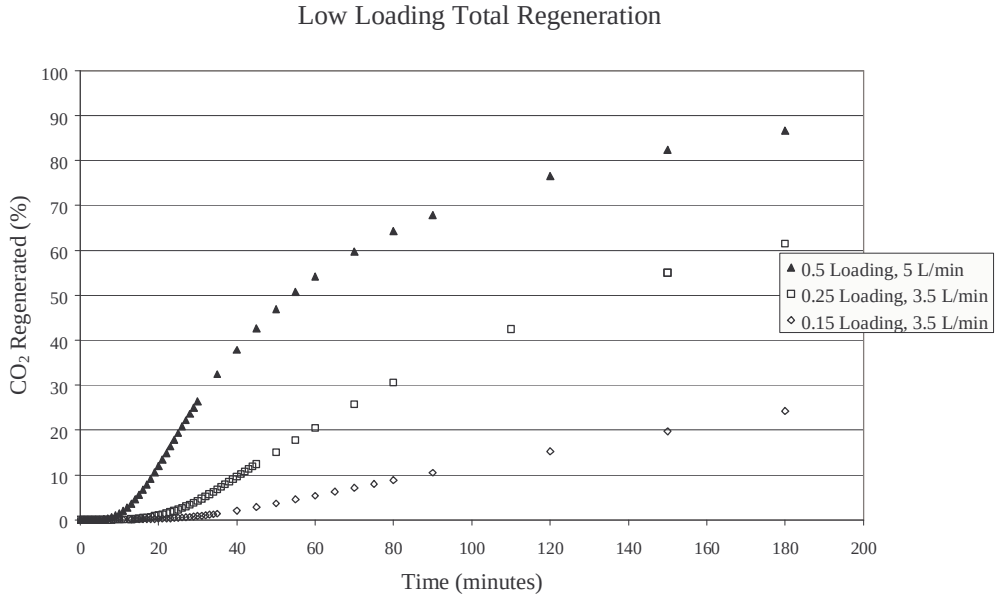

Figure 5.20 Total regeneration of CO_2 at 90°C for various solution loadings.

Figure 5.19 shows that carbon dioxide evolved from the solutions with low loading (0.15 and 0.25) but at a much slower rate, as expected from Figure 5.18, than that with higher loading of 0.5. The total regeneration achieved was also lower due to the larger proportion of stable reaction products to regenerable products in comparison to

a fully loaded solution. The experiments confirmed that solutions with lower loading are more difficult to regenerate due to lower CO_2 vapour pressure and more stable reaction products.

Chapter 6

SCRUBBER SYSTEM EMBODIMENT

The components required for integration of the absorber and regenerator apparatus are described and analysed in chapter 6, including a heat exchanger and pressure equalising valve. Resolution of difficulties encountered on commissioning the system are described, and the complete CDOCS prototype system presented.

6.1 Regenerated Solution Heat Exchanger

Regenerated solution feeds directly into the bottom of the CDOCS absorber where it meets a solution-air mixture. Due to the large volume flow rate, the incoming air controls the temperature in the absorber, and the energy from the regenerator flow is of little consequence. However, rejecting heat from the regenerated solution is advantageous since hot MEA does not absorb CO_2 and reacts adversely with oxygen.

The amine solution circulates through the regenerator by gravity feed. This leaves very little pressure head or space to accommodate a traditional heat exchanger. Neither copper nor aluminium is compatible with MEA, so material compatibility also poses a significant problem for common heat exchangers, particularly if standard units or manufacturing methods are desired to reduce cost.

A simple method of heat exchange by a stainless steel helix was designed to reduce the regenerated solution temperature to 40ºC. Although stainless steel is not a good heat conductor, it is the only material guaranteed to withstand the conditions imposed. A 12.5 mm outside diameter tube was formed into a helix with constant fall, providing a large surface area for forced convection heat exchange within the space and pressure restrictions. The following analysis determines the length of tube required (Figure 6.1).

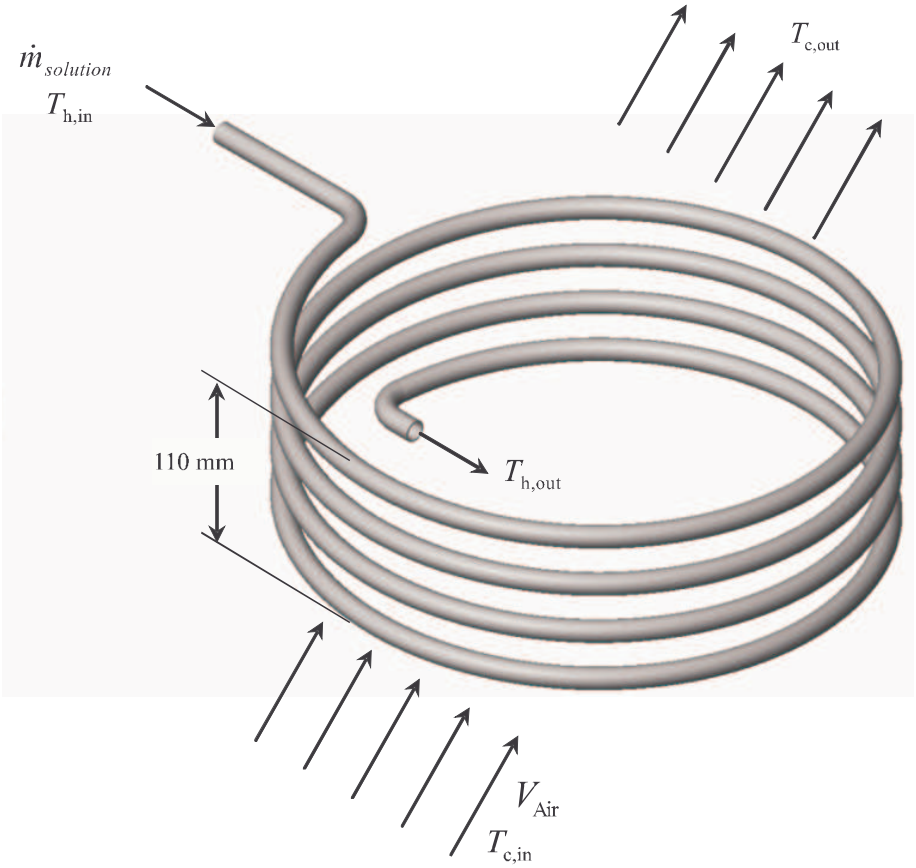

Figure 6.1 Thermodynamic model for solution cooling helix calculations. Tube outside diameter D_0 = 12.5 mm, inside diameter D_i = 9.5 mm.

6.1.1 Helix Heat Exchange Model

Assuming constant specific heat (c_p) values over the temperature ranges, the heat transfer from the exchanger is

$$q = \dot{m}_{solution} c_{p(solution)} \left(T_{h,out} - T_{h,in} \right) \tag{6.1}$$

$\dot{m}_{solution}$ is the MEA solution mass flow rate to the regenerator (6.9×10^{-4} kg/s) found in section 4.6.2, and $c_{p(solution)}$ is 3180 J/kgK (section 4.6.4). $T_{h,in}$ and $T_{h,out}$ are the solution inlet (100ºC) and outlet (40 ºC) temperatures respectively. Substituting these values into Eq 6.1:

$$q = 6.9\times10^{-4}(3180)(100-40) = 131(\text{W}) \tag{6.2}$$

This energy must be transferred to the air flowing over the helix:

$$q = \dot{m}_{Air} c_{p(Air)} \left(T_{c,out} - T_{c,in}\right) = 131(\text{W}) \tag{6.3}$$

$\dot{m}_{Air}$, equal to 0.049 kg/s, was calculated from the density of air at the measured temperature ($T_{c,in}$ = 25ºC), velocity (V_{Air} = 2.1 m/s) and swept area of the cooling fan. Rearranging for $T_{c,out}$, the outlet temperature of the air, with $c_{p(Air)}$ = 1005 J/kgK [77]:

$$\begin{aligned} T_{c,out} &= \frac{q}{\dot{m}_{Air} c_{p(Air)}} + T_{c,in} \\ &= 27.7 \ (^{\circ}\text{C}) \end{aligned} \tag{6.4}$$

The surface area required for heat exchange can be found from

$$q = UA\Delta T_{log\,mean} \tag{6.5}$$

Where

$$A = \pi D_o L \tag{6.6}$$

U is the overall heat transfer coefficient (W/m^2K), L the length of tube required (m) and D_o the tube outside diameter (m). The log mean temperature difference, $\Delta T_{log\ mean}$, is approximated by

$$\Delta T_{log\,mean} = F\Delta T_{lm,crossflow} \tag{6.7}$$

Where F defines the relationship between the log mean temperature and $T_{lm,crossflow}$, the approximation obtained by assuming counter flow conditions [77]. For the current analysis, the function F is very close to unity and the log mean temperature is defined by

$$\Delta T_{log\,mean} = \frac{\left(T_{h,in} - T_{c,out}\right) - \left(T_{h,out} - T_{c,in}\right)}{ln\left(\frac{T_{h,in} - T_{c,out}}{T_{h,out} - T_{c,in}}\right)} = 36.5\ (^{\circ}C) \tag{6.8}$$

Since the total energy transferred is low, the temperature gradient across the exchanger wall is very low, and thin wall conditions with negligible resistance to heat transfer are assumed. In this case the overall heat transfer coefficient is [77]

$$U = \frac{1}{\left(\frac{1}{h_i} + \frac{1}{h_o}\right)} \tag{6.9}$$

h_i and h_o are respectively the internal and external convection heat transfer coefficients (W/m^2K). The internal fluid (solution) convection heat transfer coefficient is

$$h_i = \frac{\overline{Nu}_{solution} k_{solution}}{D_i} \tag{6.10}$$

$\overline{Nu}_{solution}$, the Nusselt number, generally depends on the Reynolds number of the flow, $Re_{solution}$

$$Re_{solution} = \frac{V_{solution} D_i}{\nu_{solution}} \tag{6.11}$$

The velocity of solution, $V_{solution}$, inside the tube is found from the mass flow rate, $\dot{m}_{solution}$, and internal diameter of the tube, D_i, and is equal to 0.01 m/s. Solution viscosity , $\nu_{solution}$, is approximated from Dow Chemicals data [68] for 50 wt% MEA aqueous solution at 100°C, equal to 7.6×10^{-7} m^2/s. The Reynolds number is then 125, indicating laminar flow exists in the tube.

The Nusselt number is constant for internal flow in a circular tube with fully developed laminar flow, assuming uniform surface heat flux. In this case, the Nusselt number is equal to 4.36 [77]. MEA and MEG make up the bulk of the standard solution and have similar thermal conductivities, k. Therefore $k_{solution}$ is approximated by k_{MEG} at 373 K and is equal 0.263 W/mK [77]. The convection heat transfer coefficient, from Eq 6.10, is then 121 W/m^{2}K.

The external fluid (air) convection heat transfer coefficient, h_o, is

$$h_o = \frac{\overline{Nu}_{Air} k_{Air}}{D_o} \tag{6.12}$$

k_{Air} is equal to 0.03 (W/mK) [77]. $\overline{Nu}_{Air}$ for an external gas flow over a cylinder is defined by the Hilpert Equation [77]

$$\overline{Nu}_{Air} = C\, Re_D\, m\, Pr_{Air}^{1/3} \tag{6.13}$$

Constants C and m depend on Reynolds number, Re_{Air}

$$Re_{Air} = \frac{V_{Air} D_o}{\nu_{Air}} \tag{6.14}$$

For the air stream, V_{Air} from the cooling fan was measured at 2.1 m/s, and ν_{Air} is 16 x 10^{-6} m^2/s [77]. Re_{Air} is equal to 1640, again indicating laminar flow. Constants in the Hilpert equation for 40 < Re < 4000 are C = 0.683 and m = 0.466 [77]. Pr_{Air} is equal to 0.7 [77], giving $\overline{Nu}_{Air}$ of 19.1, and finally h_o is equal to 45.8 W/m^{2}K. From Eq 6.9 U is then 33 W/m^{2}K.

Rearranging Eq 6.5 and Eq 6.6 for L, the length of tube required, yields

$$\begin{aligned} L &= \frac{q}{U \Delta T_{log\,mean} \pi D_o} \\ &= 2.77\,(\mathrm{m}) \end{aligned} \tag{6.15}$$

The helix fits around the base of the absorber for efficient use of space, with insulation between the column and helix. This gave the helix a diameter of 320 mm, and fabrication of four coils at this diameter was possible without deterring regenerator flow. The actual length of the heat exchanger was 4.1 m, as shown in Figure 6.2, producing a surface area for heat dissipation of 0.16 m^2.

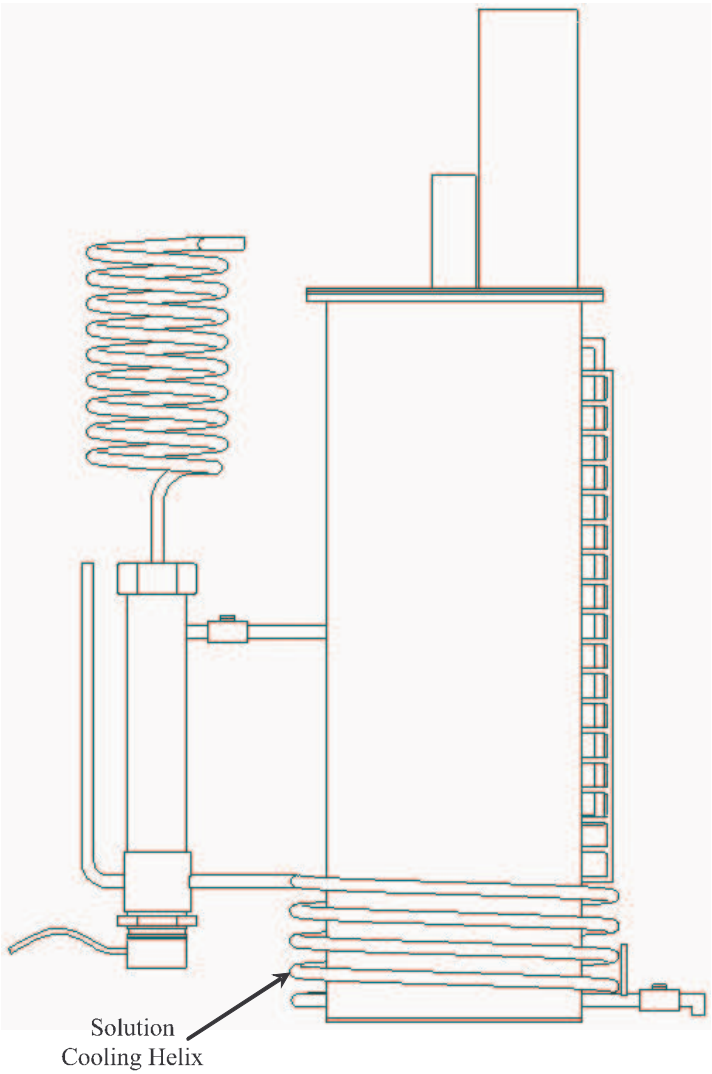

Figure 6.2 Absorber and regenerator apparatus with the solution cooling helix.

A horizontally mounted fan blew air over the helix, so little convective heat transfer occurred on the sections of helix in the shadow of the absorber. Furthermore, the previous analysis neglected the thermal resistance of the tube itself, and estimated

several liquid properties due to lack of data. The extra length over that calculated offsets these inaccuracies, and the absorber re-entry temperature was measured consistently at or near 40°C.

6.2 Provision for Regenerator Solution Flow

The gravity fed solution flow to the regenerator depends on the emulsion generated in the absorber. A hole in the side of the absorber, within the emulsion depth, is adequate to promote a flow of solution but can be sporadic, particularly if the hole is near the top of the emulsion (providing maximum head for the gravity feed). A fitting connected directly to the regenerator also introduces the risk of air lock in the flow, scrubbed air finding a low resistance path through the regenerator instead of the absorber exhaust, or conversely CO_2 rich flush gas flowing into the absorber.

A continuous liquid phase separating the absorber and regenerator reduces the likelihood of cross contamination. This was achieved by a placing a header within the emulsion, as in Figure 6.3, feeding a U tube which passed through the wall of the absorber.

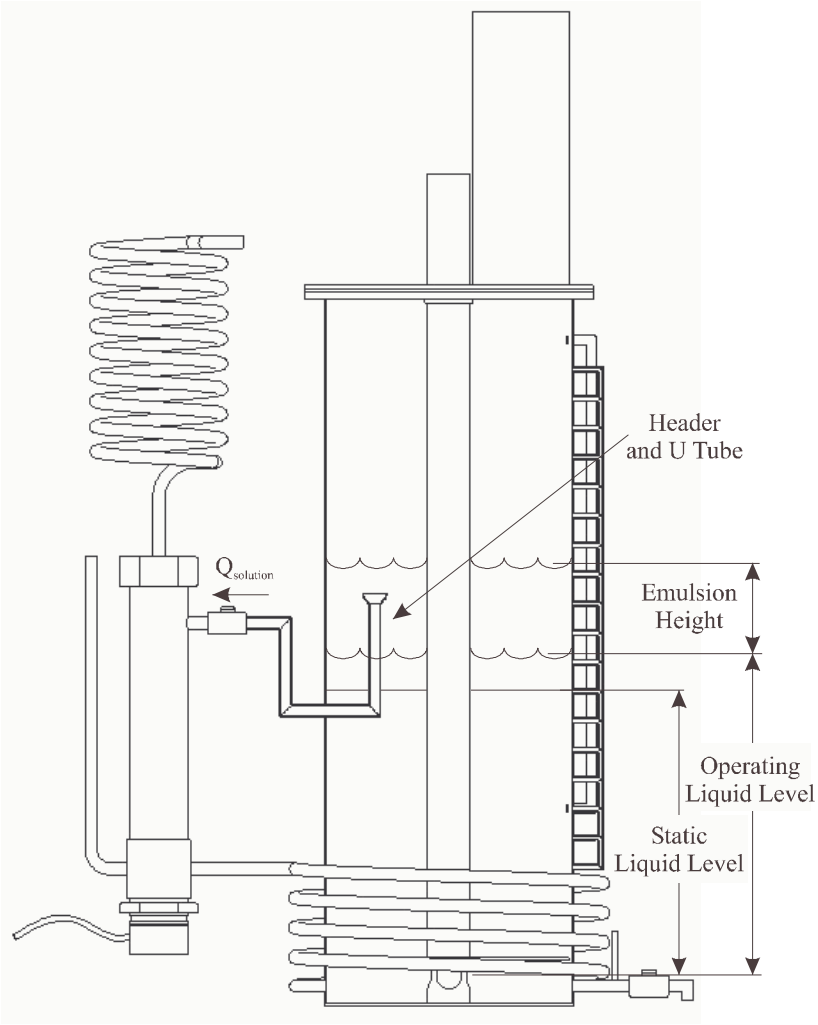

Figure 6.3 Integrated absorber and regenerator.

Absorber only sectioned to reveal header and U tube feeding solution to the regenerator. Packing and mist eliminator omitted.

The header enabled the capture of more solution from the emulsion and established a column of liquid in the U tube to separate the absorber and regenerator gas phases. The arrangement also provided an easy method of varying the height of the header, and so the pressure head available to the regenerator. A continuous column of liquid exists from the header, through the U-tube to the regenerator valve. The pressure head available to drive regeneration flow is therefore the difference in height between the header and valve.

The solution flow rate, Q, was found by measurement. The solution velocity, V, was determined by measuring the time taken for injected dye or small entrained bubbles to

travel a known length of clear plastic tube of known area A, which formed a leg of the U tube. The flow rate was approximated by

$$Q = VA \ (m^3/s) \tag{6.16}$$

A radial velocity profile existed in the tube, so both the dye and entrained bubble methods provided estimates of the flow. This was a non-intrusive measurement and did not affect the flow of solution.

6.3 Prototype System Component Integration

The absorber, regenerator and components developed for integration were assembled to form a prototype CDOCS scrubbing unit as in Figure 6.3. The CDOCS system operation was tested prior to experimental use. The first stage of testing the system involved running the scrubber and observing operation without regenerator flush gas.

Initially these conditions generated adequate emulsion depth, regenerator flow and heat exchange. However, as the experiment progressed, the coalescing material (a proprietary, heavy paper-like filter) in the Pall coalescer (Figure 6.4) became saturated with liquid, gradually increasing the pressure drop across it.

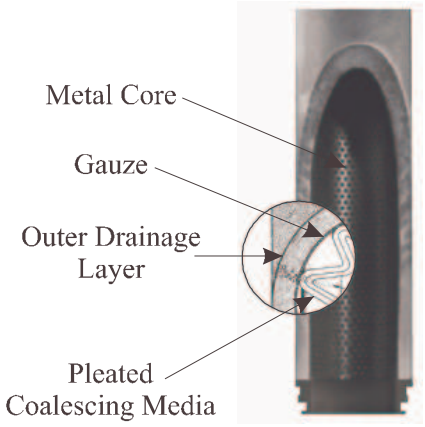

Figure 6.4 Detail of Pall coalescer from Figure 4.11.
The pleated filter absorbed liquid during experiments, increasing the pressure drop across it.

The increased pressure drop caused the static operating level in the regenerator to gradually rise, and the free surface in the header to fall, reducing and finally stopping regenerator flow. Eventually the pressure drop across the coalescer became so great that a lower resistance path existed through the U tube and regenerator than through the absorber exhaust.

The Pall coalescer is designed for high pressure systems, and is not considered blocked by the manufacturers until a pressure drop of 100 kPa exists across it. This is not acceptable for atmospheric operation of the CDOCS system. Washing the coalescer in water to remove MEA and baking in an oven at 70°C, the maximum safe temperature for construction materials, evaporated water absorbed into the fine filter structure. Over night baking at the end of each experiment reduced the pressure drop to the original level.

Stage two of prototype testing included the injection of regenerator flush air into the regenerator column. The flush gas caused the regenerator flow to stop and forced solution up the condensing helix. When this occurred, the regenerator exhaust was momentarily sealed by the liquid in the helix, forcing flush air through the U tube to the absorber. These effects were the result of pressure imbalance between the absorber and regenerator. Any backpressure, including that from an AFC system, causes the same effect.

Stable operation requires the pressure in the absorber and regenerator to be equal at all times. This calls for a pressure equalising valve capable of matching the regenerator to the absorber pressure, which may change with time due to short term fluctuations in fluid flow, and long term changes in liquid level and coalescer pressure. For simplicity and rapid response, continuous pressure matching requires a physical mechanism as opposed to a mechanical or electrical feedback device.

To ensure cross contamination does not occur, the valve must physically separate the CO_2 free absorber air and CO_2 rich flush gas. The valve must also drain fluid, including hot MEA, that may condense from the regenerator. Although a ready made

component is preferable, no such device exists. A pressure equalising device, shown in Figure 6.5, was designed to meet all of the aforementioned requirements.

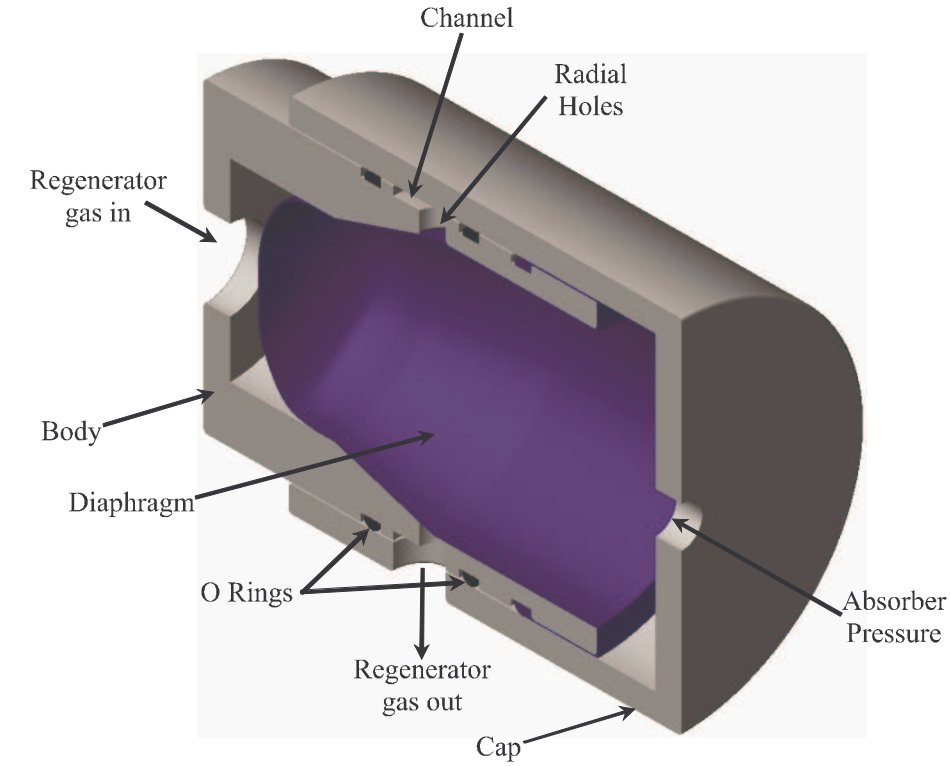

(a) Isometric Sectioned View

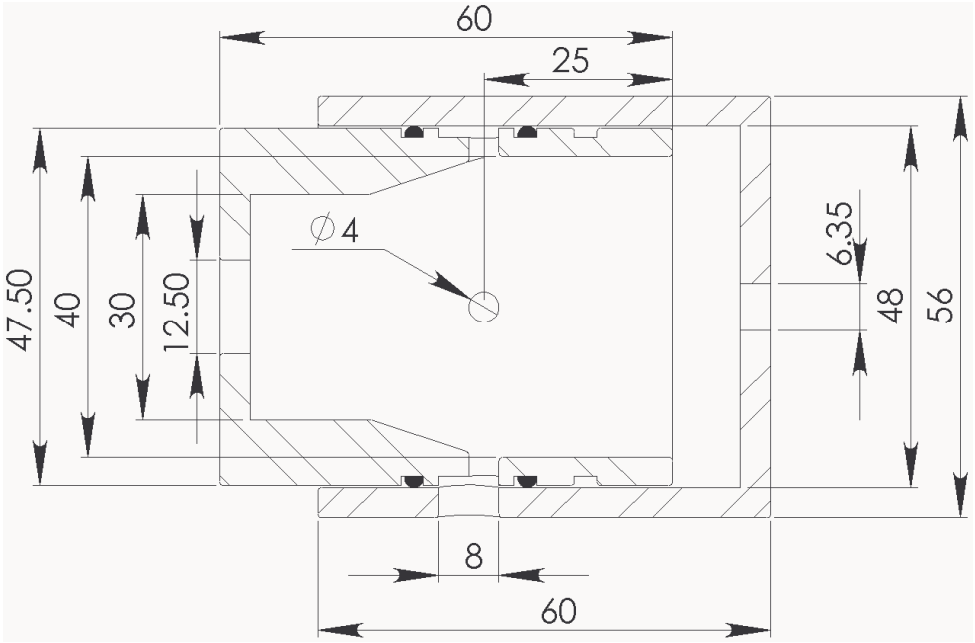

(b) Section Detail

Figure 6.5 Isometric and detail views of pressure equalising valve assembly.

A latex flexible diaphragm physically separates the regenerator and absorber gases. Via a fitting on the cap, air pressure in the absorber inflates the flexible membrane circumferentially against the valve body, sealing several radial holes. When pressure in the regenerator builds up to a fraction more than the absorber, CO_2 rich flush gas forces the membrane away from the radial holes, which feed a common channel on the outer surface of the body. Flush air escapes into the channel, which feeds an exhaust tube at atmospheric pressure.

The escape of a small amount of flush air lowers the pressure on the regenerator side to just below the pressure in the absorber, causing the membrane to reseal against the radial holes. This cycle occurs continuously and allows rapid equalisation of pressure at all times, regardless of the absolute pressure in the absorber. Orientation and mounting of the valve allows condensed liquid on the regenerator side to drain down the condensing helix to the regenerator. Pressure taps from the absorber and regenerator caps connect to the legs of a water manometer to monitor valve operation. The latex diaphragm performed well for the period of experiments, and was replaced for each new experiment.

6.4 Final Prototype CDOCS System

The full complement of components developed were combined to provide a fully operational prototype CDOCS unit, Figure 6.6. The regenerator was not insulated due to solution seeping from some of the BSP fittings that form the regenerator column.

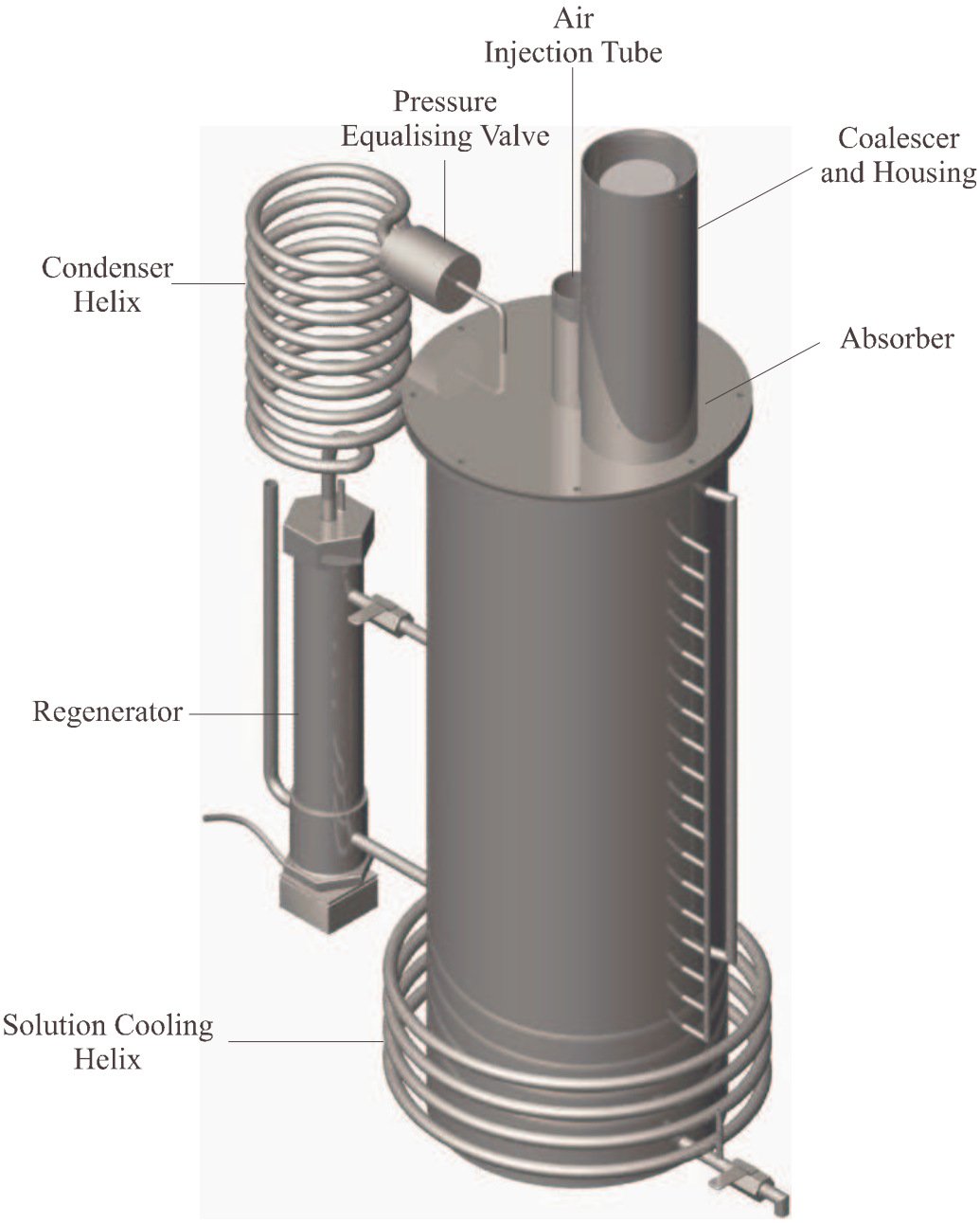

Figure 6.6 Model of integrated experimental CDOCS prototype.

Chapter 7

CDOCS EXPERIMENTAL CHARACTERISATION

A prototype CDOCS system (Figure 7.1) was constructed and tested under a range of operating conditions to determine long term performance characteristics. Operational parameters investigated include regeneration temperature, absorbent solution composition and the gradual addition of absorbent solution during long term experiments. Chapter 7 reports results from the testing including experimental verification of theory developed to determine the solution depth in the absorber.

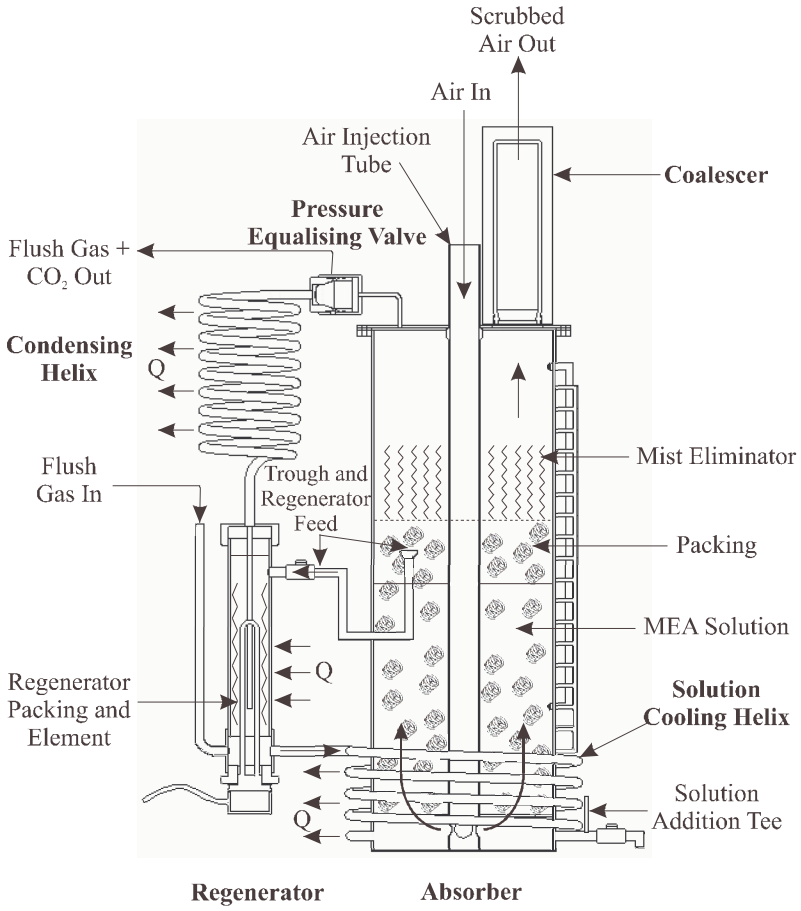

Figure 7.1 CDOCS prototype system, main components and functions labelled.

CDOCS performance was measured by regularly monitoring the CO_2 concentration in scrubbed air exiting the absorber with the GC-TCD. MEA concentration in the scrubber was monitored by titration of solution with hydrochloric acid.

7.1 100 Degree Regeneration

The prototype system was tested over a 22 day period with a regenerator temperature of 100ºC. The experiment employed 17 litres of standard solution, giving a liquid depth of 300 mm and a residence time of 3.5 seconds with 20 m^3/hr air flow rate. A peristaltic pump maintained the absorber solution level by the regular addition of water. A PID controller maintained regeneration temperature initially at 100°C then at 110°C, as determined by the shielded thermocouple in the regenerator. The regenerator flush gas was air at 1.8 litres/minute, and regenerator power was measured intermittently by the YEW power meter. The first full prototype experiment provided data for comparison to the absorption without regeneration experiment of section 5.1.2. Figure 7.2 shows results of scrubbed air CO_2 analysis by GC-TCD.

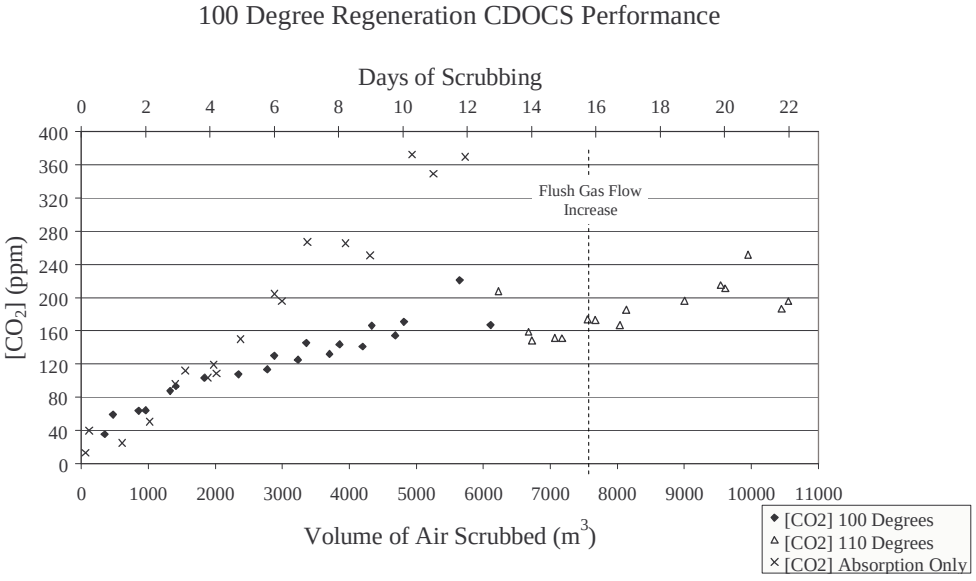

Figure 7.2 CDOCS performance at 100°C regeneration temperature.
Comparison to absorption without regeneration case. Error bars omitted for clarity.

A significant improvement in long term CO_2 absorption was gained over the absorption without regeneration case described in section 5.1.2 and overlaid in Figure 7.2. Initial performance mirrored that of the absorption without regeneration case, since both solutions had identical high absorption capacity. At approximately 2000 m^3 scrubbed air the 100°C regeneration experiment deviated, showing performance improvement. The CO_2 concentration in the scrubbed air decreased compared to the absorption without regeneration case, but the overall trend of linearly increasing CO_2 concentration in the exhaust gas remained, indicating inadequate regeneration.

For 100°C regeneration temperature, the uninsulated regenerator consumed between 300 and 400 W continuously. At 6000 m^3 scrubbed air, the target temperature was increased from 100 to 110°C to observe the effect on performance. The heating element was unable to heat the flow of solution to the new target temperature, necessitating a reduction in solution flow rate and offsetting the effect of increased temperature to some extent. Other variations in regenerator flow and therefore temperature, such as that caused by changing emulsion height due to evaporative losses, were minimised by water addition with the peristaltic pump.

The higher regeneration temperature resulted in rapid performance enhancement, as CO_2 evolved from solution to achieve equilibrium at the new operating point. Due to inadequate regeneration with time, the effect was temporary - the solution loading gradually increased and performance continued the original trend.

At 7600 m^3 scrubbed air the flush air flow rate was adjusted from 1.8 to 4 litres/minute. As expected from results in section 5.3.3, no change in performance, and therefore regenerator effectiveness, was apparent. At flush gas flows larger than 4 litres/minute the emulsion in the regenerator column approached the solution inlet and the gas exit to the condensing helix, interfering with operation.

The experimental results showed that the regenerator had a tangible effect on overall performance. At the regeneration temperature investigated, CO_2 evolved and performance enhancement was achieved, but continuous low ppm scrubbing was not accomplished.

7.2 120 Degree Regeneration

The regeneration temperature was increased to 120°C and flush air flow rate to 4 litres/minute, with conditions otherwise identical to the previous experiment. Scrubbed air CO_2 concentration is shown in Figure 7.3.

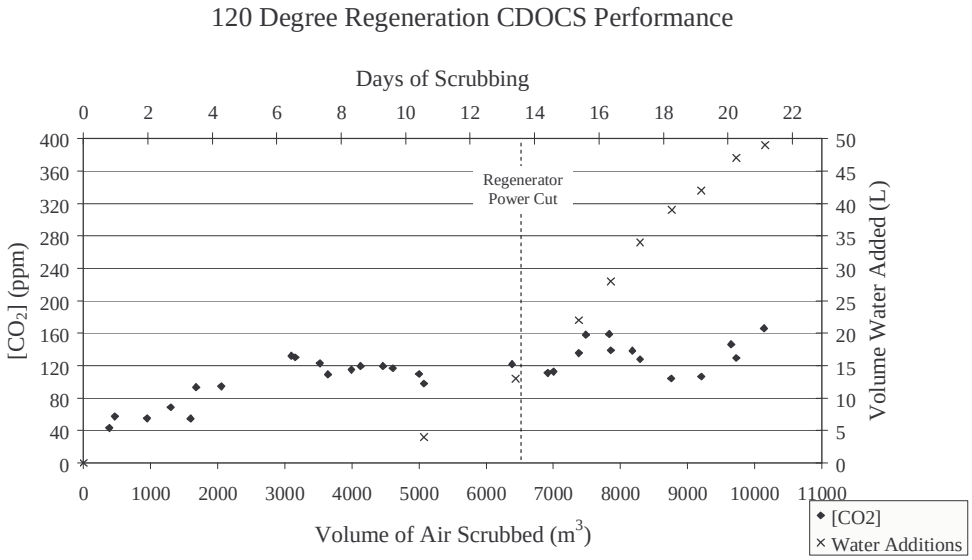

Figure 7.3 CDOCS performance at 120°C regeneration temperature.
Air flow rate 20 m^3/hr, air flush gas flow rate 4 litres/minute, solution depth 300 mm.

In the early stages of the experiment, up to approximately 2000 m^3, the CO_2 concentration in the scrubbed air followed a linear increase identical to that of the previous experiment and the absorption without regeneration case. At approximately 3500 m^3 scrubbed air the system developed a stable operating point, where regeneration was sufficient to maintain performance averaging 120 ppm for an extended period.

120 ppm represents the equilibrium achieved for the particular absorption rate, regeneration temperature and regenerator flow. A variation in any of these parameters alters the operating point, as demonstrated by the peak in CO_2 concentration between 7500 and 8500 m^3 scrubbed air. The increase was the result of a power cut to the heating element, occurring at 6500 m^3 scrubbed air and lasting for 12 hours, or 240

m^3 air. The system displayed a feedback style response, taking some time to react to the changing parameters.

Adjusting for the power loss, the apparatus maintained scrubbing to 120 ppm up to approximately 9000 m^3 air, at which point a linear increase, similar to that observed with previous experiments, occurred. The increase corresponded to a reduction in regeneration temperature at 6000 m^3 scrubbed air, from 120 to 95°C, for the remainder of the experiment.

The temperature drop was related to the flow rate of solution through the regenerator. Water addition to the absorber occurred regularly to maintain a constant liquid level. Averaged over the entire experiment, the addition of 2.2 litres per day maintained the correct level. However there was a disproportionately large water requirement towards the end of the experiment, hinging about 6000 m^3 scrubbed air. The absorber required 13 litres of water up to 6000 m^3 scrubbed air, or 2.16 litres/1000 m^3 air, whereas the remainder of the experiment required 9.25 litres/1000 m^3 scrubbed air.

It is not known why the change in water addition occurred so suddenly, but the volume of water added caused the viscosity of the solution to decrease, thereby allowing the regenerator flow rate to increase. This increased the load on the heating element to a point where the available power could not raise the temperature beyond 100°C. The rapid increase in water addition generated a cascade effect on losses since the vapour pressure of water is orders of magnitude larger than MEA or MEG. The excess water also caused the solution to become less alkaline with time, further reducing CO_2 absorption performance.

7.3 Solution Addition

The solution addition experiment investigated the effect of adding standard solution to maintain the correct liquid level in the absorber (Figure 7.4), as opposed to water. Aside from the unfortunate effect on performance, the volume of water added for the 120°C regeneration experiment was unacceptable for practical AFC applications, where water may be a valuable resource. Loss of liquid from the scrubber is

unavoidable, but replacement with water exacerbated the problem. All other aspects of the experiment were identical to the 120°C case above.

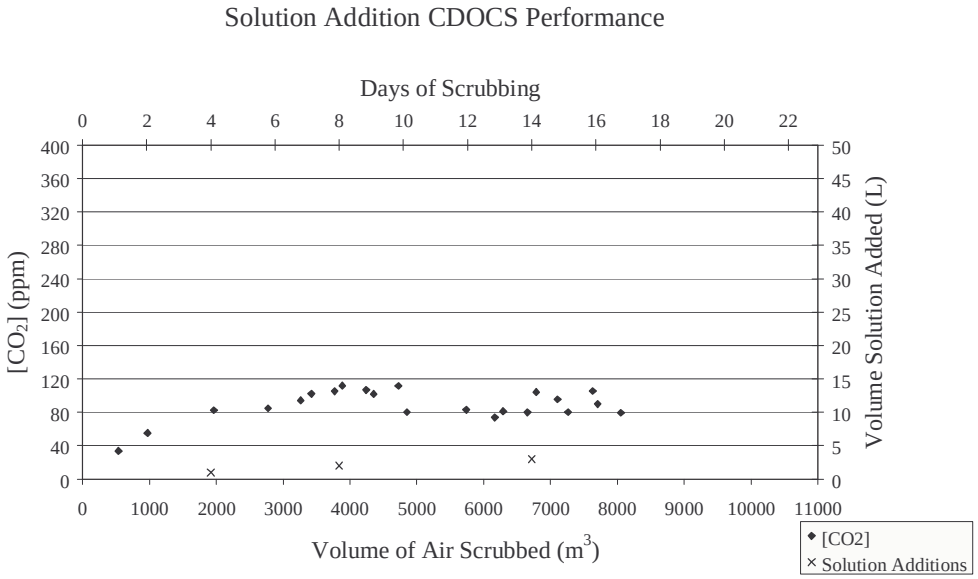

Figure 7.4 CDOCS performance at 120°C regeneration temperature with solution addition.

Standard solution, as opposed to water, added to maintain liquid level. Air flow 20 m^3/hr, solution depth 300 mm.

Addition of solution instead of water remedied the dilution problem. The performance of the system was identical to the 120°C regeneration experiment up to 5000 m^3, and showed slight improvement thereafter, scrubbing to approximately 80 ppm. Solution addition had the benefit of adding fresh MEA gradually, so helping to maintain performance as well as avoiding the adverse effect experienced with water addition.

Regeneration temperature remained constant throughout the experiment, indicating that regenerator flow was stable. The absorber required just 3 litres of solution (0.38 litres/1000 m^3 air) for the entire experiment, and liquid additions remained constant throughout. The improved performance after 5000 m^3 was attributable to the extra MEA added, maintained regeneration temperature and flow and less dilution of the MEA solution compared to the previous experiment. The experiment was considered successful at 8000 m^3 and stopped to enable further experimentation and performance enhancement.

7.4 Chemical Mixture

The effect of the chemical solution on long term scrubbing performance was investigated. The chemical composition of the scrubbing solution, while based on chemistry and reported information, was partially established on anecdotal evidence (section 4.4.2). It was therefore of interest to evaluate the effect of varying the concentration of components. Experiments were performed using MEG free solution (MEA and H_2O remaining), water free solution (MEA and MEG remaining) and increased MEA concentration, at the expense of, but not eliminating, MEG.

7.4.1 Monoethyleneglycol Free Solution

A scrubbing solution comprised of 50 wt% MEA and 50 wt% water was tested to confirm that the presence of MEG in previous experiments was not detrimental to performance. The boiling point of the solution was less than 120°C (section 4.4.2), therefore requiring a regeneration temperature of 110°C with all else being the same as the 120°C solution addition experiment. Solution was continuously added by the peristaltic pump to maintain the correct level in the absorber. Figure 7.5 presents results from the MEG free and solution addition experiments

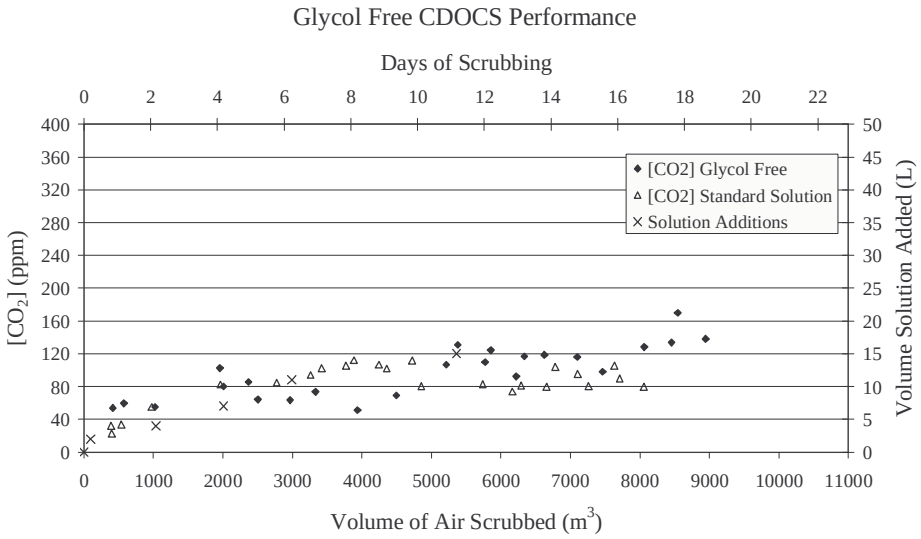

Figure 7.5 CDOCS performance with a 50 wt% MEA aqueous solution. Comparison to performance from standard solution.

Performance up to 2000 m^3 air, when the solution is strongest, was similar to previous experiments. Some improvement occurred between 2500 and 5000 m^3 of scrubbed air, after which the performance matched that of the standard solution. However, the current experiment required 15 litres of solution, or 1.5 litres/1000 m^3 air. This increase over the standard solution case corresponded to the higher initial percentage of water in solution, which increased evaporative losses. The large volume of supplementary solution also represented an 8 kilogram MEA addition, almost as much as present at the beginning of the experiment. Considering this, it is reasonable to conclude that for CDOCS operation the performance of the MEA-H_2O system was worse than the standard solution.

7.4.2 Water Free Solution

The effect of running the CDOCS apparatus with an 80 wt% MEA 20 wt% MEG solution was investigated. The MEA - CO_2 chemical system requires water to sustain absorption, eliminating the obvious possibility of using 100% MEA to increase performance. For direct comparison to other experiments, the solution depth was maintained at 300 mm, air flow at 20 m^3/hr and regeneration temperature 120°C with 4 litres/minute flush air. Results are presented in Figure 7.6.

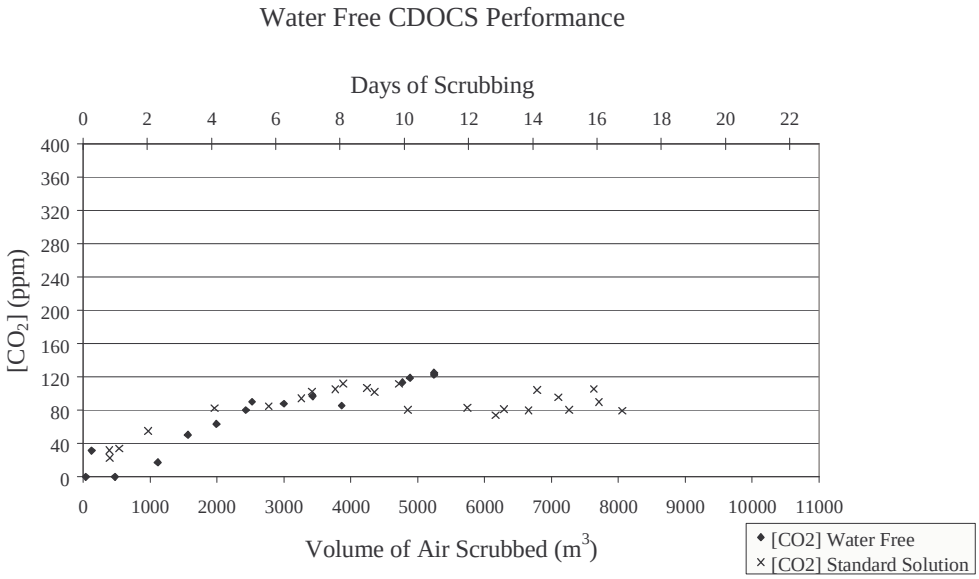

Figure 7.6 CDOCS performance with a water free solution.
80 wt% MEA, 20 wt% MEG, and comparison to standard solution.

The water free solution showed improvement in the early stages of the experiment where performance is solely dependant on MEA strength. By 2000 m^3 scrubbed air the performance deteriorated to match that of 50 wt% MEA standard solution, and after approximately 5000 m^3 became worse than the standard solution.

The water free solution gained approximately 3 litres in liquid volume in the first 1000 m^3 scrubbed air. The increase in volume was due to absorption of water from the scrubbed (atmospheric) air by MEA and glycol, which are hygroscopic. There was therefore a small quantity of water in solution to satisfy the chemical reactions in the MEA - CO_2 system to some extent. The long term performance of the water free solution was inferior to that of standard solution due to inadequate water availability for the chemical system.

7.4.3 Increased Monoethanolamine Concentration

The MEA concentration was increased from 50 to 60 wt% at the expense of 10 wt% MEG. Marginal improvement in performance was anticipated by the use of over 50 wt% MEA in solution, a fact considered in determining the standard solution makeup.

The MEA concentration was of particular interest to determine if a relatively small increase could reduce CO_2 in scrubbed air closer to the goal for AFC systems. Again, for comparative purposes the experiment used a solution depth of 300 mm, air flow of 20 m^3/hr, regenerator temperature of 120°C and a flush air flow rate of 4 litres/minute. Results are shown in Figure 7.7 with comparison to an identical experiment using standard (50 wt% MEA) solution.

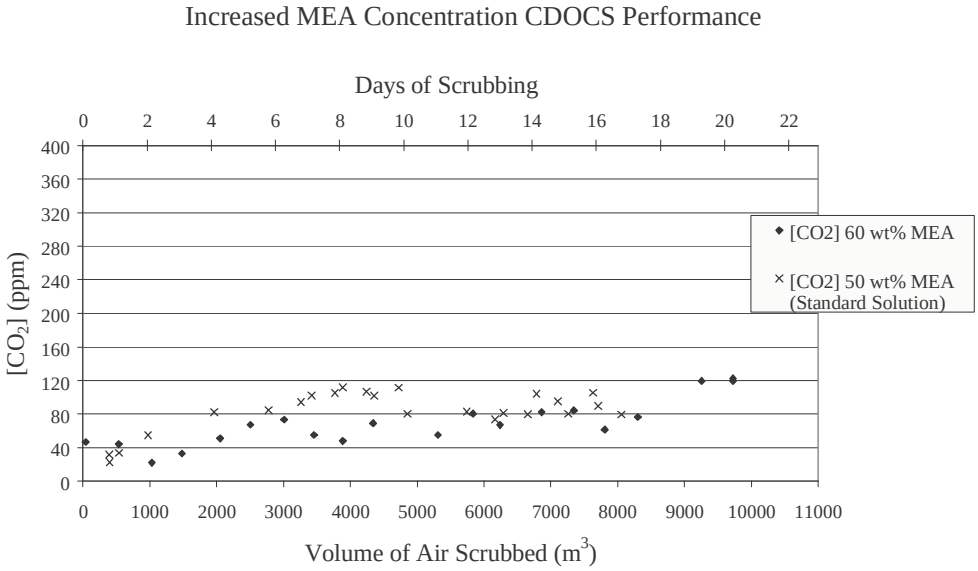

Figure 7.7 CDOCS performance with increased MEA content of 60 wt%. Comparison to standard solution.

The 60 wt% MEA concentration resulted in slight improvement for approximately 5000 m^3 air due to increased absorption capability, but the performance subsequently approached that of the 50 wt% solution. The experiment required 0.6 litres of solution per 1000 m^3 scrubbed air to maintain the correct liquid depth in the absorber, which was comparable to the 50 wt% MEA case. Overall, the 60 wt% solution achieved a very slight improvement in absorption capability for little cost difference, since the extra MEA displaced similarly priced MEG.

7.5 CDOCS Performance

Experimental results from the prototype CDOCS system were analysed to determine parameters for a long term experiment aimed at determining the best performance currently achievable. The experiment used standard 50/35/15 wt% MEA/MEG/H_2O solution to a depth of 300 mm with standard solution additions to maintain the liquid level. An air flow rate of 20 m^3/hr gave a residence time of 3.5 seconds. The regeneration temperature was 120°C with 4 litres/minute flush air. Results are presented in Figure 7.8.

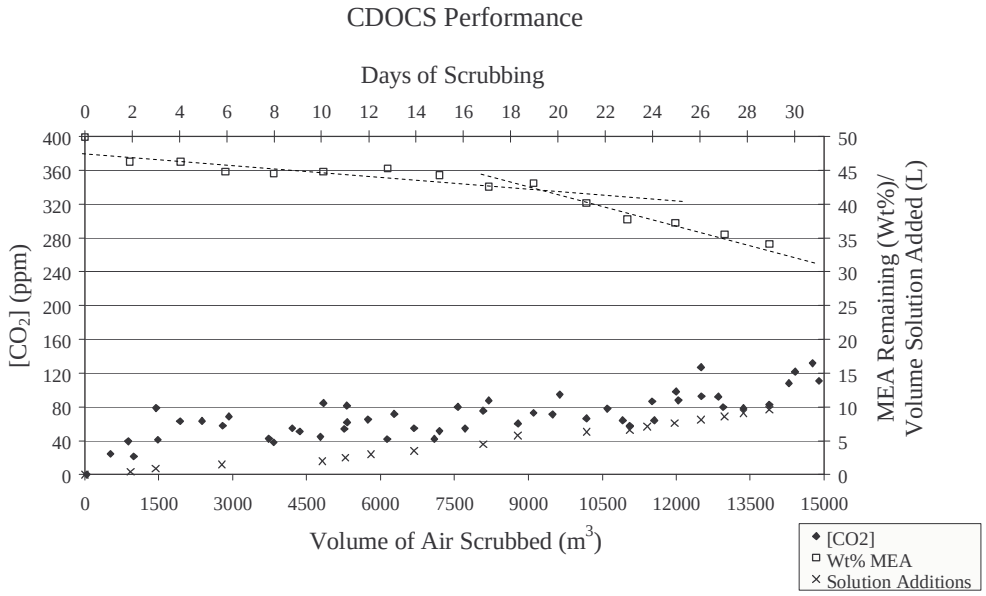

Figure 7.8 Optimum CDOCS performance.
Note change in x-axis limit from 22 to 31 days scrubbing.

The regenerator flow was regularly monitored and maintained at 4 litres/hour, the maximum flow at which the heating element could raise the solution temperature to 120°C. From Eq 4.30 this corresponded to a power consumption of 310 W (with an 85ºC temperature difference from 35ºC to 120ºC). The increased temperature and flow rate over that originally calculated may be due to overestimated regenerator efficiency or underestimated effects of degradation, vapour loss or the fraction of free MEA in solution derived from section 5.1.2. Maintaining the regenerator flow at 4

litres/hour resulted in improved performance compared to the solution addition experiment (Figure 7.4), in which the regenerator flow was allowed to fluctuate.

The CO_2 concentration in the absorber exhaust was reduced to approximately 60 ppm for a considerable period (0 - 11000 m^3 scrubbed air) and to 80 ppm for a further 3000 m^3 scrubbed air. A relatively sudden darkening of the solution at 11000 m^3 coincided with an increase in the rate of solution addition and a change in the rate of MEA wt% remaining. As previously observed, it appeared the solution had a sudden change in properties but no explanation is offered. Averaged over the whole experiment, the absorber required 10 litres of solution over a one month period, or 0.7 litres/1000 m^3 air scrubbed.

7.6 Residence Time Maximum

The final experiment investigated the prediction from section 5.1.1 that increasing residence time beyond a maximum, specific to each solution, will not improve performance. The experiment uses conditions identical to those described for Figure 7.4 excepting the liquid depth, which increased from 300 to 400 mm. The residence time for the solution addition experiment, Figure 7.4, was 3.5 seconds. Referring to Figure 5.3, the scrubbing ability of all solutions investigated approached the respective asymptote by approximately 3 seconds. Therefore, increasing the residence time in the solution addition experiment should not yield any change in performance.

The 400 mm liquid depth provided an emulsion height of 500 mm and a residence time of 4.5 seconds, almost a third increase over the 300 mm depth experiment. The corresponding increase in solution volume was 5 litres for a total of 22 litres. Results of the increased depth experiment are plotted with those from Figure 7.4 (3.5 s residence time) for comparison.

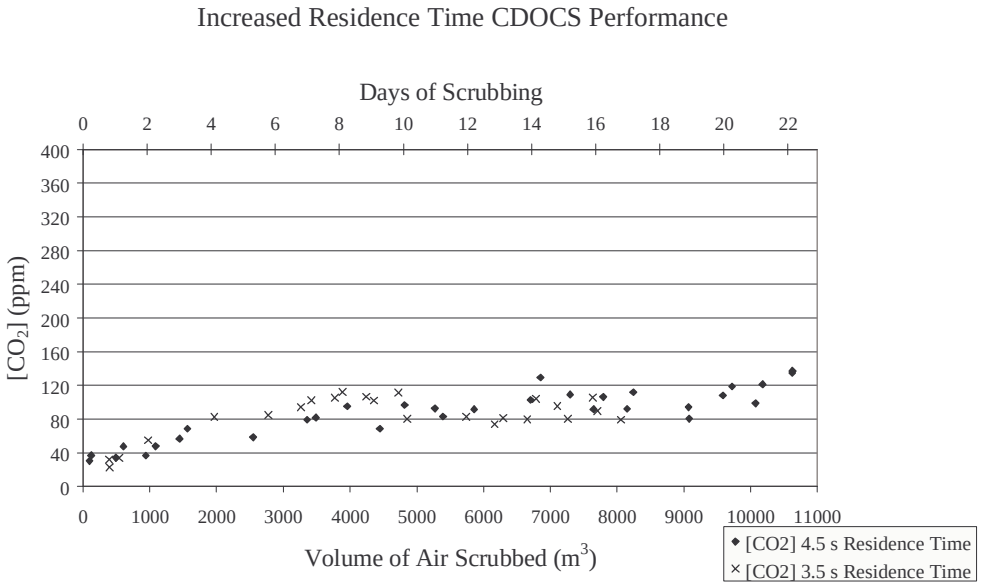

Figure 7.9 CDOCS performance with increased residence time. Comparison to solution addition case.

As predicted no improvement in performance was observed over the 300 mm depth case despite the considerable extra volume, residence time and pressure drop incurred. This confirmed the important finding that for a given solution, a maximum liquid depth and associated pressure drop exists for a given degree of scrubbing.

Chapter 8

PRODUCT CONCEPT

Chapter 8 defines the form and function of the CDOCS specifically for a 6 kW AFC system. Thermal integration of the systems is considered, to maximise energy efficiency. Operation, monitoring and control of the CDOCS system are discussed and maintenance and servicing detailed. Production and disposal of CDOCS chemicals and existing scrubbing media, soda lime, are compared and evaluated. Finally a capital and running cost comparison of the CDOCS and soda lime is provided.

8.1 Integration

8.1.1 CDOCS Form

From the literature review and subsequent experimental characterisation, the scrubber form, dimensions and operating parameters specifically for a 6 kW AFC system were established (Figure 8.1 and Table 8.1).

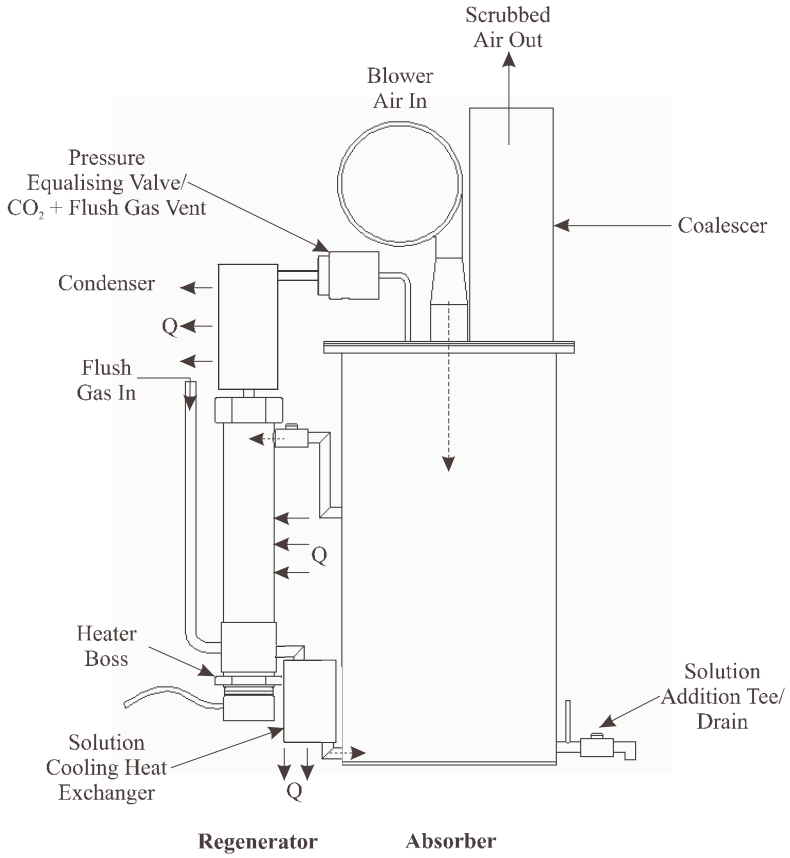

Figure 8.1 CDOCS function and form for 6kW AFC System.

Table 8.1 Key parameters for CDOCS unit suited to 6 kW AFC system.

Parameter	Value
Air Flow rate	40 m^3/hr
Absorber Diameter	260 mm
Absorber Height	500 mm
Regenerator Power	300 W
Pressure Drop	3.5 kPa
Liquid Depth	350 mm
Overall Dimensions	0.49 x 0.35 x 0.6m high
Overall Footprint	0.17 m^2
Overall Volume	0.1 m^3
Overall Weight	30 kg (empty)

8.1.2 Thermal System Integration

Ideally the CDOCS unit will make use of some AFC system resources including waste heat and exhaust air, but availability of those resources may differ for each system integrators product. Figure 8.2 shows basic thermal integration of the CDOCS with an AFC system.

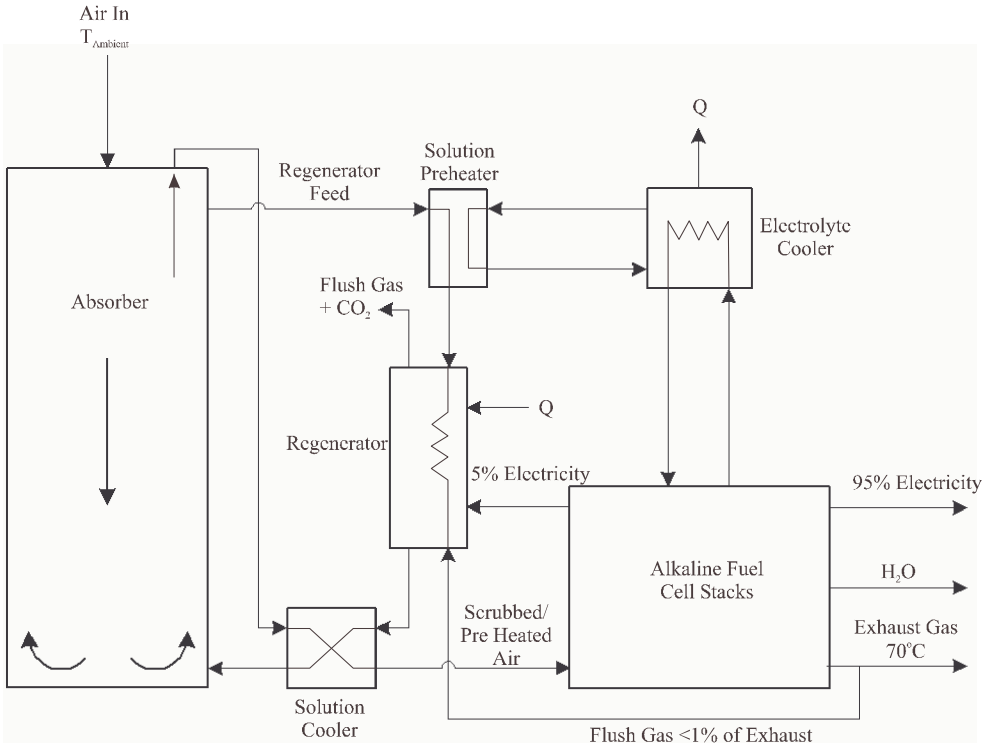

Figure 8.2 Diagram of thermal integration between CDOCS and AFC system.

Regenerator Flush Gas

The fuel cell exhaust is an ideal source of regenerator flush gas. This is likely to be suitable even for systems making use of the exhaust air (low quality heating, moisture recovery) since the flush gas is a small proportion, just over half a percent, of the overall air flow rate. Having already been scrubbed of CO_2 and depleted in oxygen somewhat, the exhaust gas is almost inert with respect to MEA. This reduces the degradation by oxygen in the regenerator environment and aids CO_2 evolution by the reduction in partial pressure of CO_2 compared to atmospheric air. The exhaust is also pre heated and humidified to fuel cell operating conditions at approximately 70°C.

The regenerator requires flush gas at approximately 2 kPa to bubble through the solution. Zetek, the manufacturer of the fuel cell stacks powering the IRL system, recommends an operating backpressure of approximately 4 kPa (section 4.6.3), allowing ample pressure for the regenerator flush gas. If the required pressure is not available from a system, a small pump will achieve flush gas flow from the exhaust air. Alternatively, the main blower can inject a small portion of bled atmospheric air into the regenerator.

Scrubbed Air Convection

Scrubbed air, prior to entry to the fuel cell, is a convenient fluid for convective heat transfer from the cooling helix. To accommodate an enclosure around the helix, it may be practical to separate the cooling helix horizontally from the absorber, while maintaining the appropriate elevation. This increases the volume of the overall system, but careful integration can make adequate use of the extra space developed. Though pre heated air would benefit fuel cell operation, the actual temperature increase is small, as indicated in section 6.1. The main function of the convection heat transfer is therefore to cool the regenerated solution.

Solution Pre Heat

If a system integrator does not employ waste heat from the exhaust or KOH cooling system, preheating the regenerator solution flow is an option. This situation could occur in applications removed from human activity, such as telecommunications posts, where low quality heat is not useful for space or water heating. In all cases system integrators exploit as much energy as possible to increase overall efficiency, so any waste heat is likely to be low quality. The benefit gained by using available energy must be weighed against the extra cost and complication.

8.1.3 Operation and Control

Air flow

Ametek blowers, as selected for the scrubber and AFC system, are electronically controlled. The dynamic pressure in the injection tube, which can be monitored with a pressure transducer, is related to the air velocity. Since the transducer can be located in a section of tube of known cross sectional area, the dynamic pressure can be correlated to the volumetric flow rate of air. A feedback loop between the blower controller and the pressure transducer would enable the air flow rate to be electronically managed (Figure 8.3).

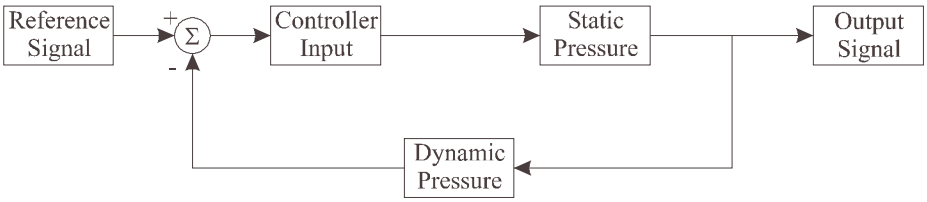

Figure 8.3 CDOCS blower control feedback loop.

A second transducer monitoring the static pressure in the absorber would enable the controller to correct for varying power output and operating parameters such as backpressure. Thus the blower is automatically able to maintain the proper volume flow rate of air to the fuel cell stacks for a wide range of conditions.

Regenerator Solution Flow

The most important aspect of the regenerator is achieving the target temperature, which is highly dependant on solution flow rate relative to heater power. The flow to the regenerator varied considerably with solution properties and liquid depth in the absorber, and it is not sufficient to set a specific pressure drop (for example valve opening) for long term running.

An electronically controlled proportional valve with feedback from a shielded thermocouple in the regenerator could continually adjust the regenerator flow. If the solution were below regeneration temperature, the valve would close slightly to decrease the flow, and open to increase flow when the target temperature is met. For

this operation, the maximum output of the heating element should to be limited, for example to 300 W, as the valve feedback loop would ensure the element is always running at full power.

The advantages of this system are maximum flow of solution through the regenerator at all times, within the capability of the heating element, and automatic compensation for changing emulsion depth and fluid properties. A Buerkert ½" stainless steel Type 6223 Flow Solenoid Control Valve (Appendix 6) is suitable but expensive at NZ$800. A more viable option could be to purchase a valve and actuator at a cost of approximately NZ$250 and produce an in house control mechanism at a relatively low cost.

Regenerator Heating Element

In normal operation the valve feedback loop would ensure the element is constantly at maximum allowed output. A PID controller would be required to manage the heater power input and avoid excessive element surface temperatures and solution burning. The controller could also set the maximum power to the element, and a maximum temperature cut out for safety.

Malfunction Insurance

A protection mechanism is sensible to guard the fuel cell stacks from a scrubber malfunction. The most simple and effective device to accomplish this is a soda lime cartridge at the exit of the scrubber. In normal CDOCS operation very little CO_2 would reach the cartridge, increasing soda lime longevity. If a CDOCS malfunction should occur, the soda lime is capable of removing CO_2 to low levels until exhaustion. The desired period for long term running, and protection in the case of malfunction (for example 1 month operating period and 12 hours cover in the case of malfunction) dictates the quantity of soda lime required. Replacement of the soda lime should be part of regular maintenance.

From section 5.2, soda lime capacity is approximately 25 kWh generation per kilogram. Twelve hours generating capacity after a scrubber malfunction, or 72 kWh,

requires 3 kilograms of soda lime. However the soda lime will absorb a residual amount of CO_2 even when the scrubber is working satisfactorily. Assuming this residual to be 20 ppm, the soda lime capacity becomes

$$\frac{380}{20}\text{ppm}\times 25\left(\frac{\text{kWh}}{\text{kg soda lime}}\right)=475\left(\frac{\text{kWh}}{\text{kg soda lime}}\right) \qquad (8.1)$$

One month's operation (750 hours) equates to 4500 kWh, or 9.5 kilograms of soda lime. Therefore, 13 kilograms of soda lime would provide insurance protection for one month.

Performance Monitoring

Continuous or regular in line measurement of absolute CO_2 concentration is not possible for low ppm levels. It is possible to acquire infra red analysers capable of triggering an alarm (or other desirable action) if the CO_2 concentration rises significantly, say by 100 to 200 ppm. The analyser may not give an accurate absolute reading, but it would be clear that the CO_2 concentration has risen significantly above normal operating concentration.

This may be reasonable for prototype and developmental systems, but a dedicated analyser contributes a significant cost and is not practical in the long term. This problem is not unique to the CDOCS system – any CO_2 removal unit, including soda lime, must be monitored and it is up to system integrators to weigh the risks, benefits and cost of a monitoring system or lack thereof.

For prototype and commercial systems, the use of electronic feedback and control provides the opportunity for data acquisition and monitoring. The control response of the blower, flow valve and heater provides information for analysis and use as an early warning system. Live or regular feedback to an operations centre or monitoring station would enable automatic analysis for malfunction criteria, such as the regenerator flow valve closing to a preset limit, indicating that the CO_2 content of scrubbed air is likely to rise.

8.1.4 Maintenance and Servicing

Air Redirection for CDOCS Maintenance

Currently AFC systems are shut down regularly for soda lime exchange. Using the CDOCS, interruptions become far less frequent, but ultimately the scrubber should be replenished without a shutdown. The simplest way to achieve this is to bypass the scrubber via a tee and valve below the blower, and allow atmospheric air into the fuel cells for the short time it takes to change the CDOCS solution.

Assuming the fuel cell output reduces to 1 kW for the maintenance period (the AFC requires 7 m^3/hr air per kW generated), a 5 minute bypass of the scrubber equates to 0.583 m^3 of atmospheric air entering the stacks. The quantity of CO_2 in this air is equal to that in 22 m^3 of air that has been scrubbed to 10 ppm, or half an hour generation at full power (40 m^3/hr air).

An alternative is to use the soda lime in the insurance cartridge to absorb CO_2 from air while bypassing the CDOCS. There is ample capacity in the cartridge to remove CO_2 from air for the maintenance period, after which replacement of the soda lime occurs as part of routine maintenance. Each method of bypass requires some extra plumbing but this is simple to provide with no exotic materials or parts required.

CDOCS Chemical Solution Replacement

Replacement of the CDOCS chemical solution is simple and quick. After turning off regenerator power and stopping or redirecting air flow, the solution can be drained into a suitable resealable container for transport and recycling. Ideally, a water rinse of the scrubber would remove residual solution but this is not essential. The absorber is recharged with fresh solution through either the air injection tube or a capped opening in the lid specifically for the purpose, depending on the air redirection method.

Coalescer Replacement

The prototype CDOCS system uses a Pall coalescer to remove droplets of solution from the scrubbed air stream. The coalescer absorbs moisture over time causing the

pressure drop across it to increase, so replacement should be part of routine maintenance. Replacement is a simple matter of removing a retaining rod and replacing the coalescer, ensuring the O-ring is lightly greased with MEA solution. A water wash and bake out of the used coalescer enables multiple reuse.

Pressure Equalising Valve Maintenance

The flexible diaphragm within the pressure equalising valve requires replacement at maintenance intervals. This is not difficult but if a significant volume of CDOCS systems were built it may become economical to manufacture disposable, plastic bodied valves to eliminate the possibility of improper installation.

Safety

The CDOCS is subject to standard safety precautions and does not introduce any new hazards to an AFC system. The regenerator position should eliminate the risk of contact with other components and reduce the likelihood of contact with maintenance personnel. Provisions to vent the fuel cell exhaust safely to atmosphere exist, due to the presence of unspent hydrogen. The same must apply to the regenerator flush gas, which is rich in CO_2 and contains residual MEA vapour. The usual precautions should be observed when handling chemicals and working near electrical hazards. For environmental safety, the used MEA solution should be recycled as far as possible and the remainder disposed of safely.

8.1.5 AFC System Architecture

AFC system engineering is still in developmental stages, so no ideal or preferred layout of components is defined. The exact layout and function of available AFC systems is commercially sensitive and appears to differ markedly between manufacturers. This includes the design and layout of existing soda lime CO_2 scrubbers, which are integrated into systems from early in the design phase.

At present, therefore, the CDOCS system must be tailored for each application. However, as the industry matures it is likely that some common parameters will

evolve, allowing after market CDOCS units to be designed and manufactured with minimal dependence on the parent AFC system. Conversely, future AFC systems may incorporate the CDOCS unit into the design from the earliest stage, as soda lime scrubbers currently are, allowing full integration.

For tailored units in the immediate future, there are some CDOCS components and parameters that retain flexibility to aid integration. Horizontal location of the regenerator and cooling helix, air stream plumbing, coalescer and pressure equalising valve location, for example, can be altered to meet special requirements. Figure 8.4 is a schematic representation of a possible layout for the AFC and CDOCS systems, showing the size of the CDOCS relative to fuel cell stacks and overall system size. As presented in Figure 1.3, the plumbing of the KOH, hydrogen and air streams to the fuel cell stacks and auxiliary components is highly interdependent.

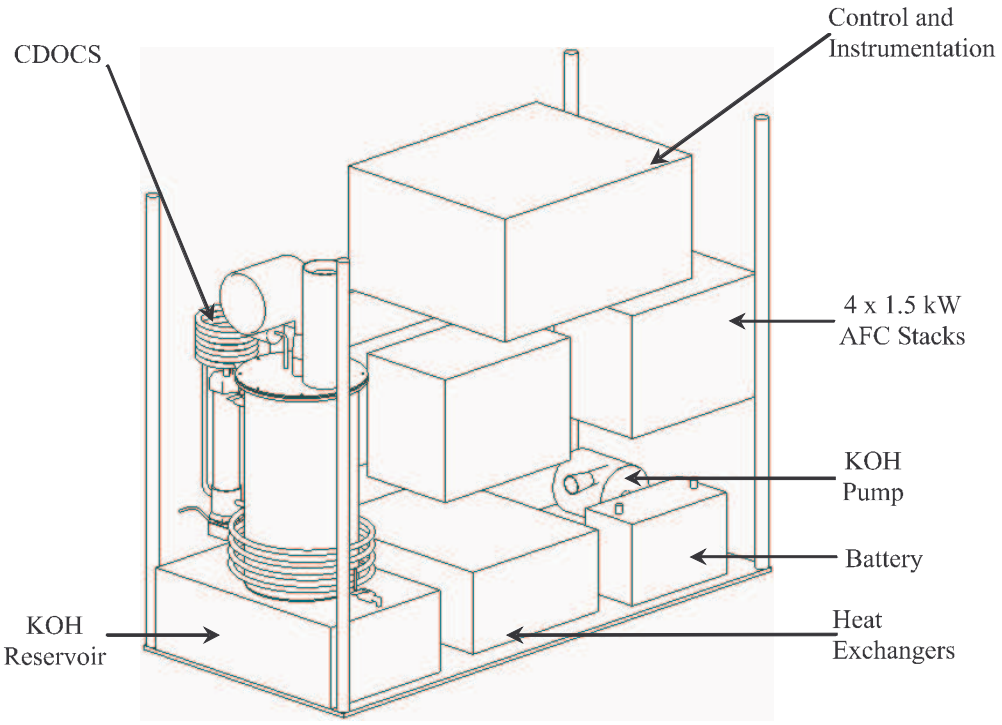

Figure 8.4 Basic architecture of main AFC and CDOCS components. Fluid reservoir and insurance devices omitted.

The heart of the IRL system, similar to that represented in Figure 8.4, measures approximately 2.5 metres long, 0.8 metres wide and 1.8 metres high, or just over 3.5

m^3, which appears to be representative of AFC systems in the 6 kW range. Approximately 0.07 m^3 (0.25 x 0.4 x 0.7 metres), or 2%, of the system volume is taken up by the two soda lime scrubbers currently used for CO_2 removal, which provide a recommended 24 hours generation capacity. The CDOCS scrubber volume is comparable to the current scrubbers, though in different proportions (0.49 x 0.35 x 0.6 metres, or 0.1 m^3). The CDOCS as shown in Figure 8.4 forms approximately 8% of the footprint of the system, similar to the 9% of existing soda lime scrubbers.

8.2 Chemical Production and Disposal

The long term sustainability of the scrubbing medium is of obvious importance if the AFC is widely adopted for power generation. Of equal importance is the disposal of chemicals in an environmentally and economically sound manner. The manufacture and disposal of CDOCS chemicals and soda lime were considered.

8.2.1 CDOCS Chemicals

The CDOCS uses MEA and MEG, both of which are common chemicals used in CO_2 absorption and many other industries. The manufacture of both chemicals from hydrocarbons is well established given their importance in such a wide range of applications.

Disposal of small and irregular quantities of CDOCS chemicals, such as that resulting from experimental work, is straightforward but no attempt is made to recycle either chemical. The disposal of large quantities in a satisfactory and sustainable manner requires research and costing analysis. The intention is for used solution, which still contains a significant amount of amine and glycol, to be separated from the irrecoverable compounds by fractionation. The amine and glycol (boiling points 171 and 198°C respectively) need not be separated from each other – once recovered the mixture can be analysed and appropriate additions made to match the original solution composition. The unrecoverable compounds are disposed of in a controlled manner for organic decomposition, as is common practice at present.

8.2.2 Soda Lime

The components of soda lime are relatively simple and find application in other areas. Manufacturers develop and guard the combination of chemicals and manufacturing processes used to form the final granular product to gain a competitive advantage.

Like the CDOCS chemicals, disposal of small quantities is effortless. However the large quantities arising from extensive AFC use would require the development of a safe and sustainable disposal method since soda lime is not practically regenerable. The used soda lime requires neutralisation prior to disposal, probably in a landfill. The sheer volume of product is challenging, and ground or water contamination that results from excessive disposal in a localised area warrants consideration. If the technology were adopted a disposal investigation would be required.

8.3 CDOCS and Soda Lime Cost Analysis

8.3.1 CDOCS Capital Cost

The parts and costs listed (Table 8.2, Table 8.3 and Table 8.4) are representative of one-off production of apparatus very similar to that in Figure 6.6. Some minor deviations from the experimental apparatus exist, where expensive or over complicated components were used to provide flexibility for experimentation. The cost of a CDOCS unit falls dramatically with increasing production volume, and alternatives such as an ABS absorption column and components become more economically attractive. The cost of chemicals varies with time so indicative (current at time of writing) costs are shown. The cost of control electronics was omitted as full integration with the AFC system is required.

Table 8.2 Absorber components and costing.

All material stainless steel (SS) unless otherwise specified.

Absorber					
Part	**Material**	**Cost / Unit**	**Quantity**	**Cost ($)**	**Comment**
Body	Dia 254x2mm spiral welded tube	$270/m	0.5 m	135	
Base, Cap, Distribution Plate	300x300x3mm plate	$131/$m^2$	0.27 m^2	35	
Flange	300x300x6mm plate	$250/$m^2$	0.09 m^2	25	
Injection Tube	10S 40NBx2.77mm tube	$20/m	0.7 m	14	
Pall Coalescer		$300 each	1 off	300	
Coalescer Housing	10S dia 100x3mm tube	$54/m	0.3 m	16	
Housing Fabrication	Labour	$40/hr	0.5 hours	20	Estimated
Wire Mesh	SS		0.06 m^2	10	Estimated
Cap Gasket	300x300x3mm Natural Rubber		0.09 m^2	5	Estimated
Packing	Dia ½”x0.9mm tube	$8/m	60 m	450	160 elements/litre, 4000 15mm elements
Packing Fabrication	Labour	$20	8 hours	160	Estimated
Woven Mist Eliminator	SS mesh			50	Estimated
Drain Valve	SS	$40	1 off	40	
Header, U Tube	Dia ½”x0.9mm Tube	$8	0.5 m	4	
Absorber Fabrication	Labour	$40/hr	5 hours	200	Estimated
Solution	MEA	$2/kg	9kg	18	
Solution	MEG	$2.50/kg	6.3kg	16	
Insurance Soda Lime Vessel	ABS Plastic		1 off	100	Estimated

Table 8.3 Regenerator components and costing.
All material stainless steel (SS) unless otherwise specified.

Regenerator					
Part	**Material**	**Cost / Unit**	**Quantity**	**Cost ($)**	**Comment**
Element		$210 each	1 off	210	
Body	40S 2”x4mm Pipe	$36/m	0.3m	10	
Reducer	1 ¼” to 2” BSP SS	$10	1 off	10	
Socket	2” BSP SS	$10	1 off	10	
Cap	2” BSP SS	$5	1 off	5	
Flow Valve	SS valve and actuator		1 off	500	Estimated
Cooling and Condenser Helix	Dia ½”x0.9mm Tube	$8	6 m	50	
Helix Fabrication	Labour	$40/hr	2 hours	80	Estimated

Table 8.4 Remaining system components and costing.
All material stainless steel (SS) unless otherwise specified.

System					
Part	**Material**	**Cost / Unit**	**Quantity**	**Cost ($)**	**Comment**
Pressure Equalising Valve	Bar or tube		0.2 m	10	Estimated
Valve Fabrication	labour	$40/hr	2 hours	80	Estimated
Miscellaneous Fittings/Parts	SS			200	Estimated
Assembly	Labour	$40/hr	2	80	Estimated
Total				**2850**	**Estimated**

8.4 CDOCS Performance Comparison with Soda Lime

The CDOCS and soda lime systems operate very differently, so the best comparison is of performance, capital costs and running costs for each system over a time period. Experimental data from the soda lime and CDOCS performance experiments were compiled for comparison. Capital costs for each system were then compared, with subsequent evaluation of aspects to which a dollar value is not readily attributable. Since a standard soda lime scrubber does not exist, comparison was drawn to the IRL AFC system scrubbers. However, the capacity of the soda lime was increased from 7.2 kWh/kilogram suggested by IRL to 25 kWh/kilogram, found experimentally. This better represents the actual CO_2 absorption capacity of soda lime.

8.4.1 Performance Comparison

Figure 8.5 provides a comparison of performance between CDOCS and soda lime systems over a one month period. Soda lime data were extrapolated from the scaled experiment, detailed in section 5.2, by multiplying the air flow rate by the scale factor 10, giving an equivalent of 20 m^3/hr, as per the CDOCS data. The equivalent volume of air scrubbed by the soda lime was then doubled to account for two scrubbing units as used by IRL. CDOCS data is reproduced from Figure 7.8, CDOCS Performance.

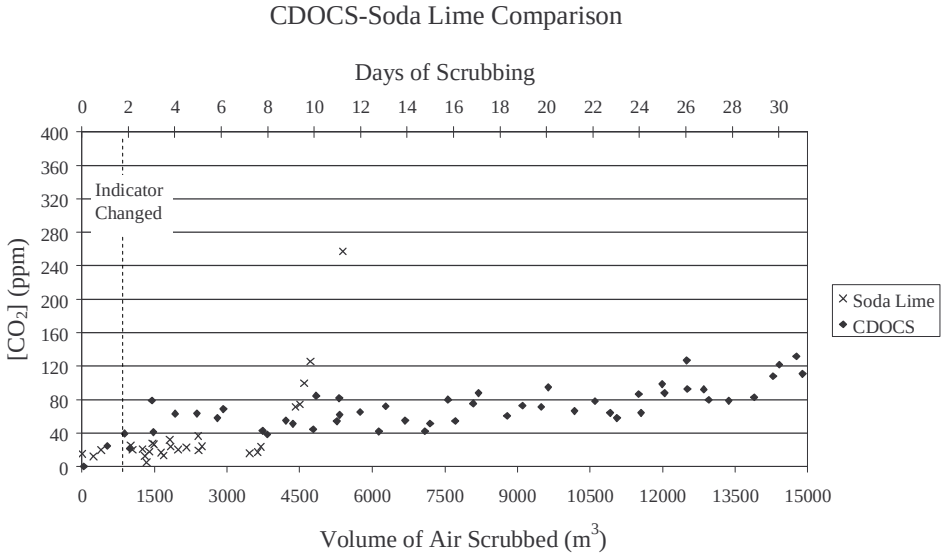

Figure 8.5 Comparison of performance between CDOCS and soda lime systems. Soda lime results extrapolated from Figure 5.9, CDOCS results from Figure 7.8.

Figure 8.5 shows that soda lime absorbs CO_2 to a lower concentration than the CDOCS apparatus for the first 3500 m^3 air scrubbed. Subsequently the CO_2 concentration in the soda lime experiment increases rapidly to atmospheric concentration, 380 ppm, as the soda lime becomes exhausted. The colour change of the soda lime indicator occurs prematurely at 800 m^3 air, leading to the low capacity specified by IRL. For operation with an AFC the soda lime would be replaced after scrubbing approximately 4000 m^3 air, assuming a monitoring method was in place to identify exhaustion. This equates to an 8 day maintenance period, compared to approximately 30 days for the CDOCS system.

8.4.2 Direct-Cost Comparison

For an illustrative operating period of one month (31 days) at maximum 6 kW output, the AFC generates 4500 kWh of energy. Over this period 30 000 m^3 of air is scrubbed to approximately 10 ppm. The costs, advantages and disadvantages of running each scrubbing system are evaluated in Table 8.5. The break even point of CDOCS versus soda lime scrubbers, based on direct costs only, is illustrated in Figure 8.6.

Table 8.5 31 day direct cost comparison between CDOCS and soda lime.

		CDOCS		Soda Lime	
Item	**Cost / Unit**	**Quantity**	**Cost**	**Quantity**	**Cost**
Initial Cost					
Apparatus			$2850		$500
MEA	$2/kg	9kg	$18		
MEG	$2.50/kg	6.3kg	$16		
Soda Lime	$10/kg*	13kg	$130	20kg	$200
Sub Total			**$3014**		**$700**
Running Cost (31 Days)					
Additional Solution	$2/kg	15kg	$30		
Additional Soda Lime				180kg	$1800
Solution Disposal	$2/kg	20kg	$40		
Soda Lime Disposal	$2/kg	13kg	$26	180kg	$360
Power Consumption		✓		×	
Maintenance		×		✓	
Sub Total		**$96+Power**		**$2160+Maintenance**	

*Indicative cost from IRL and American source.

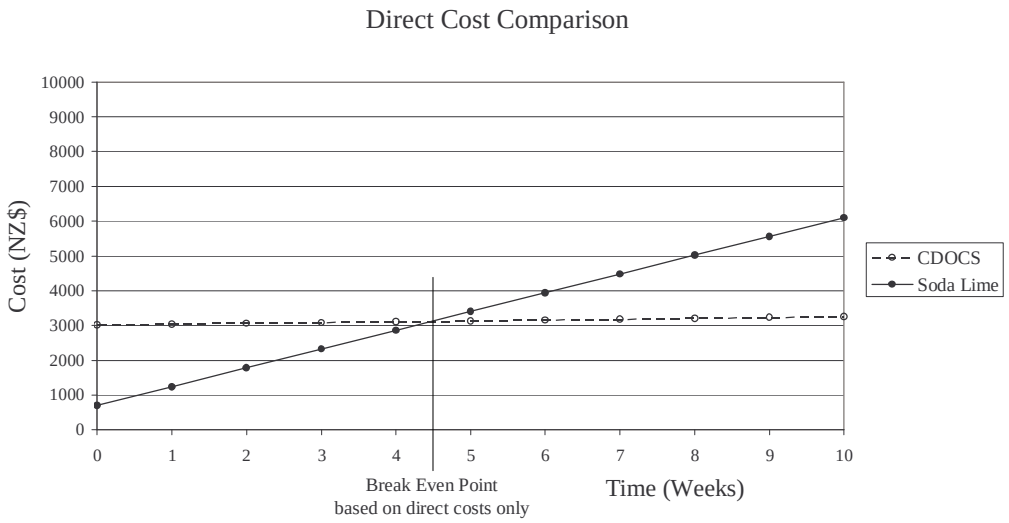

Figure 8.6 Direct-cost comparison of CDOCS and soda lime systems.
Based on costs from Table 8.5. Break even point between two technologies shown.

8.4.3 Indirect Cost Comparison

Parasitic Power Consumption

The soda lime scrubbers have the advantage of simple and independent operation, with no power consumption. The trade off for extended operation of the CDOCS unit is approximately 400 W parasitic power consumption. This is comprised of 300 W regenerator power and approximately 100 W extra power consumed by the blower to overcome CDOCS operating pressure. A total of 300 kWh, or 6.7% of total power generated, is consumed over the soda lime scrubbers.

The energy consumed by the regenerator has monetary value since it could otherwise have been supplied to the end user, increasing the overall efficiency of the AFC system. The exact value of the energy is subjective, and would depend on the location and importance of the application, and the alternative generating options available. For illustration, a generous value of NZ$0.50 per kWh is assumed in Figure 8.7. This reflects the potentially high value of electricity for applications warranting the cost of an AFC system, and illustrates a ‘worst case’ scenario for CDOCS economy. NZ$0.50 per kWh is very high compared to residential charges (approximately

NZ$0.15 per kWh) and considerably more than alternative remote generation equipment such as a diesel generator set (approximately NZ$0.25 per kWh).

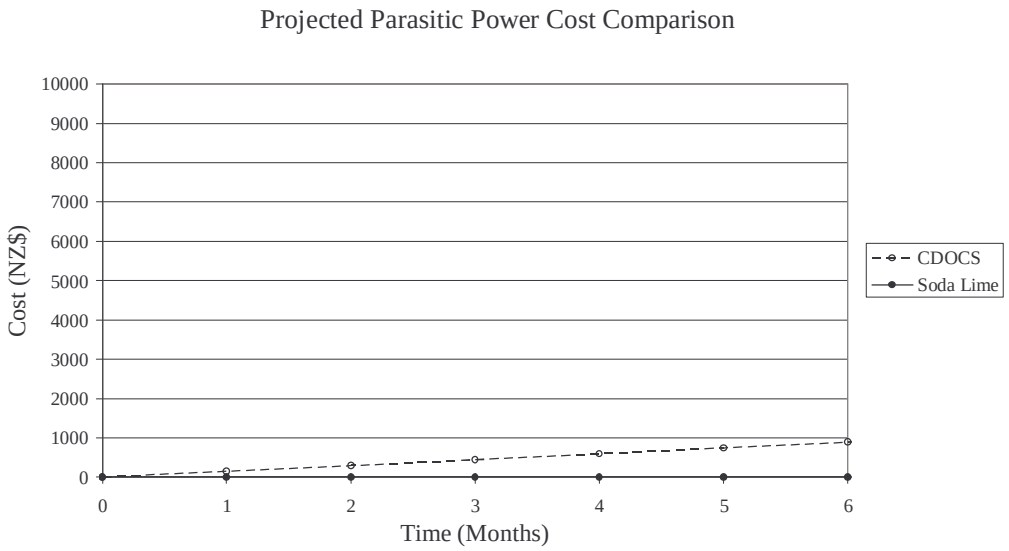

Figure 8.7 Projected power cost comparison of CDOCS and soda lime systems. Value of parasitic power estimated for illustration. Data are shown on the same y-axis scale as direct costs, Figure 8.6, for comparison of magnitudes.

Maintenance

The CDOCS system runs autonomously for the one month period, and requires approximately half an hour's labour to change the solution and expendable components. Maintenance does not require a shut down of the fuel cell and little disassembly is required. The coalescer removed from the CDOCS requires a water wash and bake out at 70°C overnight.

The soda lime scrubbers require a system shutdown and soda lime replacement approximately every eight days, though it may be possible to bypass one scrubber at a time. Recharging requires approximately half an hour's labour for disassembly and removal of the scrubbers, and to pour out and replace the soda lime. Manhandling of the apparatus and chemical sets a limit to the size of the scrubbers due to weight. Increasing the volume and/or number of scrubbers expands capacity, but physical size restrictions and flow dynamics, and weight restrictions for lifting, limit enlargement.

The actual cost of maintenance is very dependant on the relative location of the AFC system. For a stand alone power system situated in a town or city, (cases 1 and 3 in Figure 8.8, for example) regular replacement of soda lime may not equate to a prohibitive maintenance cost due to short travel times and the possibility of servicing multiple units in close proximity. Technician labour cost is estimated at NZ$60 per hour including overheads, travel and accommodation allowances if appropriate.

However the AFC system for which the CDOCS concept evolved is for remote applications such as an isolated telecommunications post in outback Australia. In this case a trained technician is likely to travel many hours (or travel at high cost such as by aeroplane), and the cost of maintenance is almost completely made up of travel costs. For remote servicing, the labour cost is estimated at NZ$200 per hour including overheads, travel and accommodation allowances. As illustrated by cases 2 and 4 in Figure 8.8, for remotely located AFC systems the maintenance period of the scrubber is of prime importance for economic application.

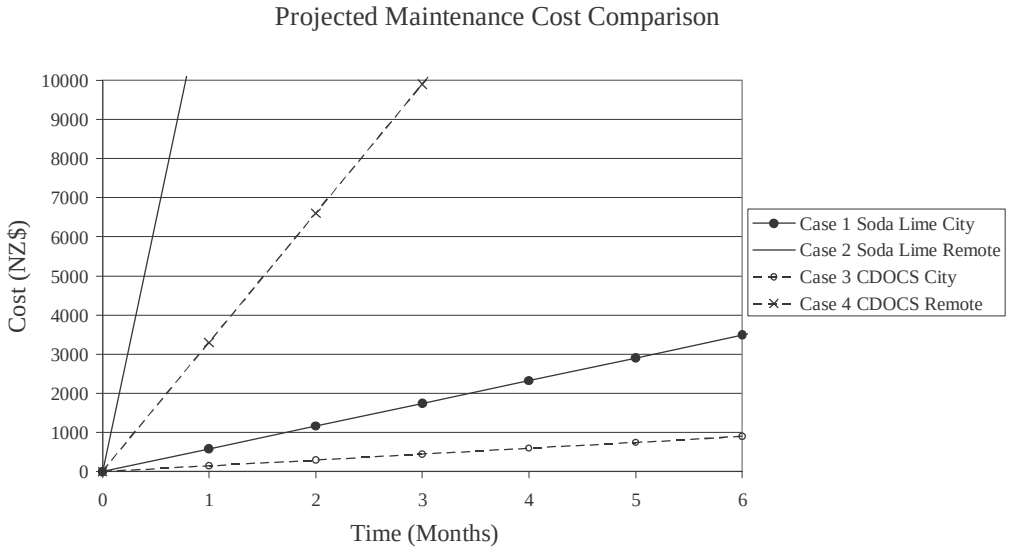

Figure 8.8 Projected maintenance cost comparison of CDOCS and soda lime systems. 'City' defined as one hour travel time each way, half an hour for maintenance; total two and a half hours for cases 1 and 3. 'Remote' defined as 8 hours travel each way, half an hour for maintenance; total sixteen and a half hours for cases 2 and 4.

8.4.4 Total Projected Cost Comparison

Figure 8.9 illustrates a projected cost comparison between CDOCS and soda lime scrubbers including direct, maintenance and parasitic power costs previously determined.

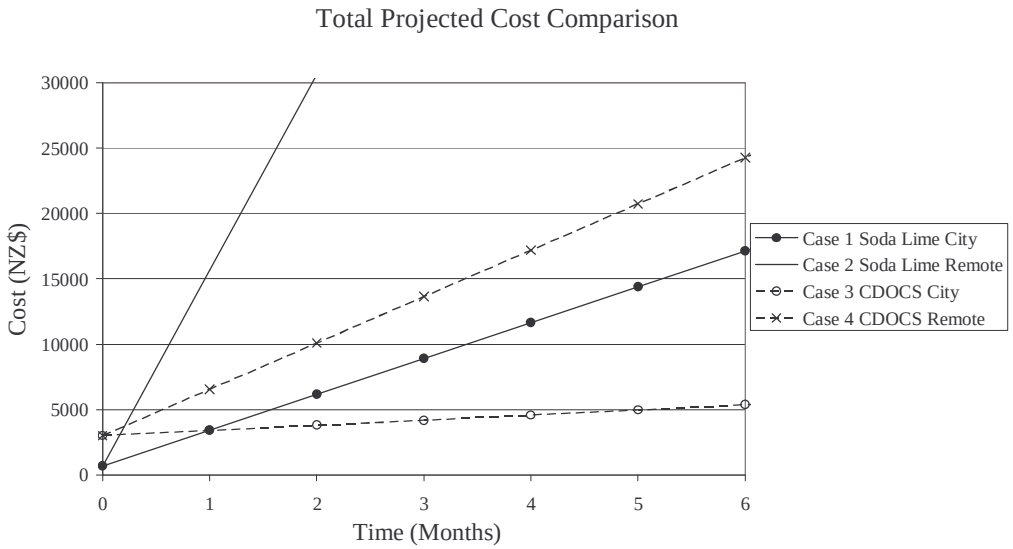

Figure 8.9 Total projected cost comparison of CDOCS and soda lime systems. Values other than direct costs are estimates to illustrate the dependence of cost on the maintenance period.

Values other than direct costs are purely speculative but Figure 8.9 indicates clearly the importance of long maintenance periods, which is the CDOCS prime advantage over soda lime. As discussed in Chapter 9, additional research of the CO_2 absorbing chemical solution is expected to lengthen the maintenance period of the CDOCS scrubber, further increasing the cost benefit of the CDOCS system over soda lime technology.

8.5 Scaling

AFC manufacturers and system integrators generally produce small units, in the 1-10 kW range, for applications previously specified. Some developers have longer term goals of several MW units as the technology is proven. An attractive feature of fuel

cell systems is scalability. Fuel cell stacks are modular - the IRL 6 kW system contains four 1.5 kW stacks as indicated in Figure 8.4.

It is therefore desirable to adopt a scrubbing technology which is similarly scaleable. Soda lime scrubbers meet this requirement in principle, but are only practical for small systems due to maintenance and the volume of soda lime required. The CDOCS system offers more flexibility in the 1-50 kW range, for which scrubbing needs may be met by scaling the system and/or using multiple systems in parallel.

AFC's require an air flow rate directly proportional to power generation, about 6-7 m^3/hr per kW. It was noted previously that the superficial gas velocity is a suitable criterion for scaling packed bubble columns, but other parameters are also important to ensure CDOCS performance. Analysis and experimental results indicate that the residence time of gas within the liquid and the degree of mixing are significant.

The CDOCS column diameter, liquid depth and air flow combination must generate turbulence within the scrubber and adequate emulsion depth for regenerator flow. The L/D ratio should be held close to 3 to avoid channelling or inadequate turbulence (L/D << 3), and excessive liquid depth or inadequate turbulence (L/D >> 3). Thus a mixture of parameters must be modified to meet requirements, rather than scaling based on one parameter.

There are practical limits to scaling the CDOCS system, other than adequate performance. For very small systems, for example 1 kW, the capital and running costs of the CDOCS system become disproportionately large. The material, fabrication and component costs do not scale down directly with physical size, and regenerator power consumption is likely to grow as a percentage of generated power. However, systems of this size are not very useful and are more likely to be used as research, development and learning tools. In this case, the CDOCS system may reduce the running cost and maintenance compared to soda lime by using mains power for regeneration.

Conversely, as the AFC system output increases, the capital and running costs of the CDOCS decrease as a proportion of the system cost and power output. The limiting

factor for large CDOCS systems may be the pressure drop resulting from increased air flow. As flow increases the performance requirement departs further from the abilities of common blowers, and approaches that of positive displacement pumps or compressed air. At this point the air source should be evaluated for economic operation. An alternative option is the use of multiple CDOCS units with reduced flow, which together contribute the required air flow rate. In this way the flow and pressure requirement from each blower is reduced.

Chapter 9

FUTURE WORK

Two key development and design obstacles to producing an autonomous and marketable CDOCS system are discussed in chapter 9. Several further refinement issues to improve or expand CDOCS performance and application are addressed.

9.1 Developmental

9.1.1 Vapour Carry Over to Fuel Cell

Blowing a gas through a volatile liquid, including water and MEA, causes evaporation of the liquid and entrainment of small droplets. Water vapour is welcome in scrubbed air to aid water management in the fuel cell. However the carry over of MEA vapour from the absorber, entrained in the scrubbed air, demands investigation before the CDOCS is tested on an AFC system. The Pall coalescer removes fine mist but incurs a significant pressure drop which changes with use, complicating the system with an extra component, cost and maintenance.

The effect, if any, of MEA on the fuel cell components and operation requires evaluation. KOH and MEA are both very alkaline chemicals and call for the same chemically resistant materials such as ABS plastic and stainless steel, therefore material compatibility is unlikely to cause a problem. Nor do the chemicals themselves react when mixed. More likely problems are the gradual dilution of KOH if a significant amount of MEA accumulates, and side reactions of MEA with oxygen in the fuel cell, possibly at the electrodes. Determination of MEA content in the scrubbed air would quantify the problem.

Industrially, a post scrubber water wash in a separate column is used to remove MEA vapour, but this greatly increases complication and size of the CDOCS system. Additionally, water must generally be treated as a scarce resource for AFC

applications. Alternative amines with lower vapour pressures (MEA has the highest vapour pressure of amines by an order of magnitude) warrant investigation to mitigate vapour carry over.

9.1.2 Fluid Addition to Absorber

Vapour loss in the exhaust air causes a gradual decrease of liquid depth in the absorber, which affects scrubbing performance and particularly regenerator flow. For experimental work, a peristaltic pump regularly added standard solution to maintain the correct level. Ultimately the liquid level must be kept constant automatically from a reservoir, preferably by gravity feed. Changes in liquid level would be mitigated significantly by solving the vapour loss problem previously described.

9.2 Integration with Fuel Cell System

The experimental CDOCS system is in a generic form - the exact layout and components depend wholly on the AFC system with which it must be integrated. AFC system developers are understandably reluctant to release detail design information to the public. To acquire information needed to tailor an integrated CDOCS system for testing, collaboration and confidentiality agreements have been arranged with two AFC system developers with the aim of sharing information beneficial to both parties.

9.3 Refinement of CDOCS System

9.3.1 Scaling

The range of AFC system requirements already in existence and the importance of scaling have been emphasised. Currently a mixture of experience, theoretical background and experimental data enable some scaling of the CDOCS apparatus. The development of rules or guidelines is necessary to meet the needs of various AFC systems.

In particular, for larger systems there may be a size of scrubber beyond which it is more practical, economical or effective to employ two smaller CDOCS units over one large one. This method is employed frequently by chemists to execute, for example, chemical reactions, where two smaller apparatus offer enhanced performance over one large apparatus.

9.3.2 Regenerator Feed Pump

The flow of solution to the regenerator was very sensitive to operating parameters, necessitating an electronic valve with feedback for autonomous operation. Effective regeneration depends very much on the solution flow rate through the regenerator; too high a flow results in inadequate temperature for regeneration and too low a flow causes the loading in the solution to increase over time and reduces scrubbing performance.

The economics of the valve controlled flow system should be compared to the use of a chemically resistant liquid pump with electronic control. A suitable pump could reliably deliver a preset volume flow rate to the regenerator, independent of other conditions in the CDOCS system. Power consumption of a small pump is unlikely to be more than 20 W; however the capital cost may be substantial for components made from materials resistant to MEA, and long term performance must be evaluated.

9.3.3 Chemical Solution

MEA is an effective CO_2 absorbent, demonstrably capable of removing CO_2 to low ppm concentration. However degradation, vapour loss and high regeneration energy are problematic for the CDOCS system using MEA. MEA is a member of the amine family of chemicals, many of which absorb CO_2 with varying absorption and physical characteristics. The CDOCS system is not alone in its problems, prompting researchers to develop and investigate new and mixed amines to overcome the disadvantages of MEA while retaining the advantages. The CDOCS warrants investigation of these alternatives with the aim of improving performance and extending the maintenance period.

The use of a surfactant also justifies investigation. As stated a surfactant can greatly increase the interfacial area, and therefore may increase the absorption of CO_2. However any chemical addition to the system requires examination to ensure the absorption reaction is not hindered, and that no significant side reactions take place with other chemical components or hardware.

9.3.4 Alternative Markets

Some types of fuel cell derive H_2 gas from on board reformers which separate hydrogen from hydrocarbons. This process also generates a significant amount of carbon monoxide, carbon dioxide and hydrogen sulphide, all of which are absorbed by MEA and some other amines. Scrubbing the fuel stream for a fuel cell is a very different problem to the air stream for an AFC, but the need exists and could well be met by the CDOCS apparatus. There is a large potential market for reformate scrubbing since many types of fuel cell may, at least initially, run on reformed hydrogen.

For research, development and teaching applications of AFC systems, the CDOCS represents a significant running cost saving over soda lime. For these applications, the CDOCS regenerator and blower can be powered by mains electricity, allowing the fuel cell to run for extended periods at low cost compared to soda lime scrubbers. This may be a significant market during further development of AFC's and AFC systems.

Chapter 10

CONCLUSIONS

Current technology for scrubbing CO_2 from air for alkaline fuel cells is not a practical or economical solution for commercial AFC systems. This research undertook to develop a novel CO_2 scrubbing device to provide low cost, continuous scrubbing at atmospheric pressure with low energy consumption.

A novel CO_2 scrubbing concept, dubbed CDOCS, was proposed by the author, his final undergraduate year project team and supervisor at the University of Canterbury in 2002. The concept used a chemical absorbent, monoethanolamine, to absorb CO_2 from air. Monoethanolamine is a widely used industrial chemical and was chosen because of the ability to absorb and evolve CO_2 in a temperature swing reaction. A packed bubble column provided intimate gas-liquid interaction to aid absorption, and provided an air flow induced dynamic pressure head to circulate the absorbent solution through a regeneration loop.

Proof of concept testing indicated that a monoethanolamine, monoethyleneglycol and water solution would absorb CO_2 and regenerate with lower energy input than used in industry, and a PCT patent for the process was granted. ASCO Carbon Dioxide Ltd became an industrial sponsor of the PhD project, in partnership with Canterprise, to develop the continuous CO_2 scrubber as a potential new product. Requirements of the CDOCS for application to stationary AFC power systems include scrubbing to less than 50 ppm, low capital and running cost, low power consumption and low maintenance.

The purpose of the research was to characterise and refine a CDOCS system to enable the design of a prototype unit for use with an AFC system. Objectives were to generate and refine concepts for the absorber and regenerator apparatus, conduct experimental investigations to characterise performance, modify and refine concepts,

and determine absorber and regenerator design relations. Results would then be used to construct a CDOCS system prototype, characterise the system performance, modify and refine the system and components, and determine system design relations.

The packed bubble column absorber is a cylinder filled with chemical solution and high surface area, low volume packing material designed to enhance gas-liquid interaction. A simple model of absorption from a rising gas bubble was developed to describe column behaviour. Parameters important to the absorption process include solution concentration, the degree of mixing and contact time between gas and liquid.

A theoretical derivation for the relationship between gas residence time and performance, an important design parameter, was proposed and empirically confirmed. This relationship enabled the absorber to be optimised for performance and pressure drop with minimal empirical information. Theoretical analysis and experimental characterisation resulted in a good understanding of operational parameters for absorption of CO_2 from air with MEA solution in a packed bubble column, an application not previously reported in literature.

Considerable effort was put into development of apparatus to measure CO_2 in air as low as 10 ppm. A gas chromatographic technique was developed specifically for this purpose. The GC was able to monitor CO_2 concentration in scrubbed air on demand, with good accuracy (84%).

Operational parameters for the regenerator apparatus were investigated experimentally since the process had not been reported in literature. A second, smaller packed bubble column provided the conditions necessary for regeneration of the MEA solution. The apparatus was heated and a flush gas passed through to facilitate regeneration. The regeneration of CO_2 saturated MEA solutions (high loading) at different temperatures and flush gas flow rates was investigated, as well as the regeneration of solutions with low CO_2 loading. It was confirmed that under specific conditions provided by a packed bubble column, MEA solutions with low CO_2 loading could be regenerated with low energy input.

Characterisation of the absorber and regenerator enabled prototype apparatus to be built and integrated to form an operational continuous CO_2 absorption system. Several components were designed to complete system integration, including heat exchangers and a pressure equalising valve. The stainless steel developmental prototype was used to further characterise the performance of the CDOCS system. The effects of varying regeneration temperature and solution composition on long term operation were investigated and the optimum MEA concentration found.

The developmental prototype scrubbed 20 m^3/hr air to an average of 80 ppm for 30 days with acceptable pressure drop and predicted power consumption. This was well above the ideal target of 10 ppm but approaching the acceptable level of 50 ppm. Continued development of the CDOCS system, in conjunction with AFC development, would result in improved performance as the technology matures.

A low production volume CDOCS unit was designed to match a 6kW AFC system. Consideration was given to integration with an AFC system, particularly efficient use of thermal energy. Methods of monitoring and control were proposed to enable autonomous operation and protection against scrubber malfunction. Maintenance requirements were also specified for the apparatus. The CDOCS unit is comparable in size to soda lime scrubbers, but has a significantly higher capital cost. A running cost comparison showed that the CDOCS apparatus provides low maintenance and extremely low running costs compared to current technology. The compromise for long term operation is the parasitic power consumed by the CDOCS regenerator. Initially it is proposed that a combination of existing and CDOCS technology be used to provide long term, economical and effective scrubbing for AFC development.

Scalability of the CDOCS apparatus was addressed and it was recognised that further work could elaborate on scaling the system to match a wide range of AFC systems. The main technical goal requiring further attention is the investigation and reduction or elimination of MEA vapour carry over to the fuel cell in the scrubbed air. This needs to be addressed prior to the ultimate goal of integration of the CDOCS with an AFC system. Considerable effort was spent establishing relationships with several AFC developers to achieve this goal. Once the system architecture is established the CDOCS can be designed for manufacture and unit costs reduced.

The project fulfilled the objective to further develop the novel CDOCS apparatus to remove CO_2 from air for a 6kW AFC system. Basic design relations were established and a developmental prototype embodied. This project lays a foundation for continued development of the CDOCS and integration with an AFC system. By solving the problem of CO_2 removal from air, the AFC will be relieved of its biggest disadvantage, allowing further development and commercialisation of the technology.

REFERENCES

[1] J. Larminie and A. Dicks, *Fuel cell systems explained*. Chichester [England] ; New York: Wiley, 2000.

[2] L. Carrette, K. A. Friedrich, and U. Stimming, "Fuel cells - fundamentals and applications," *Fuel Cells*, vol. 1, pp. 5-39, 2001.

[3] A. J. Appleby and F. R. Foulkes, *Fuel cell handbook*. New York: Van Nostrand Reinhold, 1989.

[4] L. J. M. J. Blomen and M. N. Mugerwa, *Fuel cell systems*. New York: Plenum Press, 1993.

[5] Fuel-Cell-Control-Ltd, "http://www.fuelcellcontrol.com/specs.html," 2005.

[6] H. A. Carlson and R. N. I. Sexauer, *A Submarine Advanced Integrated Life Support System*, vol. microfiche. Warrendale, Pa: Society of Automotive Engineers, 1991.

[7] R. J. Hook, "An investigation of some sterically hindered amines as potential carbon dioxide scrubbing compounds," *Industrial & Engineering Chemistry Research*, vol. 36, pp. 1779-1790, 1997.

[8] R. S. Lillo, A. Ruby, D. D. Gummin, W. R. Porter, and J. M. Caldwell, "Chemical safety of U.S. Navy Fleet soda lime," *Undersea & Hyperbaric Medicine*, vol. 23, pp. 43-53, 1996.

[9] J. A. Baum and H. J. Woehlck, "Interaction of inhalational anaesthetics with CO2 absorbents," *Best Practice & Research, Clinical Anaesthesiology*, vol. 17, pp. 63-76, 2003.

[10] S. Satyapal, T. Filburn, J. Trela, and J. Strange, "Performance and Properties of a Solid Amine Sorbent for Carbon Dioxide Removal in Space Life Support Applications," *Energy & Fuels*, vol. 15, pp. 250-255, 2001.

[11] M. Gutjahr, *From Electrocatalysis to Fuel Cells*. Seattle: University of Washington Press, 1972.

[12] S. Budavari, *The Merck index : an encyclopedia of chemicals, drugs, and biologicals*, 11th , centennial . ed. Rahway, N.J., U.S.A: Merck, 1989.

[13] V. Ahuja, *CO2 removal from air for alkaline fuel cells operating with liquid hydrogen : a thesis submitted for the degree of Doctor of Philosophy, Department of Mechanical Engineering, University of Canterbury, Christchurch, New Zealand*, 1996.

[14] E. D. Geeter, H. V. d. Broeck, P. Bout, M. G. Woortmann, J. P. Cornu, V. Peski, A. Dufour, and B. Marcenaro, "EUREKA Fuel Cell Bus Demonstration Project," *Hydrogen Energy Prog. X, Proc. World Hydrogen Energy Conf., 10th*, vol. 3, pp. 1457-60, 1994.

[15] H. Poiperopoulou and D. Bloomfield, "CO2 Management for Alkaline Fuel Cells," presented at Proceedings of Workshop on Renewable Fuels and Advanced Power Sources for Transportation, 1982.

[16] Eneco-Ltd, "http://www.eneco.co.uk/fuelCells.html," 2005.

[17] A. L. Kohl and R. Nielsen, *Gas purification*, 5th / ed. Houston, Tex.: Gulf Pub., 1997.

[18] R. Judkins and T. Burchell, "CO2 Removal From Gas Streams Using a Carbon Fiber Composite Molecular Sieve," presented at First National Conference on Carbon Sequestration, 2001.

[19] L. M. Handley and A. P. Meyer, "Electrolyte regeneration in alkaline fuel cells," *Proceedings of the Power Sources Symposium*, vol. 24, pp. 188-92, 1970.
[20] Independent-Power-Technologies, "http://www.independentpower.biz/," 2005.
[21] B. F. Dodge, "Removal of impurities from gases to be processed at low temperatures," *Advances in Cryogenic Engineering*, vol. 17, pp. 37-55, 1972.
[22] G. Astarita, *Gas treating with chemical solvents*. New York: Wiley, 1983.
[23] F. Y. Jou, A. E. Mather, and F. D. Otto, "The Solubility of Co2 in a 30-Mass-Percent Monoethanolamine Solution," *Canadian Journal of Chemical Engineering*, vol. 73, pp. 140-147, 1995.
[24] O. Falk-Pedersen and H. Dannstrom, "Separation of carbon dioxide from offshore gas turbine exhaust," *Energy Conversion and Management*, vol. 38, pp. S81-S86, 1997.
[25] M. L. Gray, Y. Soong, K. J. Champagne, H. W. Pennline, J. Baltrus, R. W. Stevens Jr., R. Khatri, and S. S. C. Chuang, "Capture of carbon dioxide by solid amine sorbents," *International Journal of Environmental Technology and Management*, vol. 4, pp. 82-88, 2004.
[26] A. L. Kohl and F. C. Riesenfeld, *Gas purification*. N.Y.: McGraw-Hill, 1960.
[27] C. Branan, *Rules of thumb for chemical engineers : a manual of quick, accurate solutions to everyday process engineering problems*, 3rd ed. Amsterdam ; New York: Gulf Professional Pub., 2002.
[28] P. Tontiwachwuthikul, A. Meisen, and C. J. Lim, "CO2 absorption by NaOH, monoethanolamine and 2-amino-2-methyl-1-propanol solutions in a packed column*1," *Chemical Engineering Science*, vol. 47, pp. 381-390, 1992.
[29] P. V. Danckwerts and M. M. Sharma, "Absorption of carbon dioxide into solutions of alkalies and amines. Hydrogen sulfide and carbonyl sulfide," *Chemical Engineer (1904-20)*, vol. No. 202, pp. CE244-CE280, 1966.
[30] P. Nasir and A. E. Mather, "MEASUREMENT AND PREDICTION OF THE SOLUBILITY OF ACID GASES IN MONOETHANOLAMINE SOLUTIONS AT LOW PARTIAL PRESSURES.," vol. 55, pp. 715-717, 1977.
[31] J. T. Yeh and H. W. Pennline, "Study of CO2 Absorption and Desorption in a Packed Column," *Energy & Fuels*, vol. 15, pp. 274-278, 2001.
[32] K. R. Westerterp, W. P. M. v. Swaaij, A. A. C. M. Beenackers, and H. Kramers, *Chemical reactor design and operation*, Student . ed. Chichester: Wiley, 1987.
[33] P. V. Danckwerts and K. M. McNeil, "The Absorption of Carbon Dioxide into Aqueous Amine Solutions and the Effects of Catalysis," *Transactions of the Institution of Chemical Engineers*, vol. 45, pp. T32-T49, 1967.
[34] S. H. Lin and C. T. Shyu, "Carbon dioxide absorption by amines: system performance predictions and regeneration of exhausted amine solution," *Environmental Technology*, vol. 21, pp. 1245-1254, 2000.
[35] A. Aboudheir, P. Tontiwachwuthikul, A. Chakma, and R. Idem, "Kinetics of the reactive absorption of carbon dioxide in high CO2-loaded, concentrated aqueous monoethanolamine solutions," *Chemical Engineering Science*, vol. 58, pp. 5195-5210, 2003.
[36] A. L. Kohl and F. C. Riesenfeld, *Gas purification*, 4th ed. Houston: Gulf Pub. Co. Book Division, 1985.
[37] A. Veawab, P. Tontiwachwuthikul, and S. D. Bhole, "Studies of corrosion and corrosion control in a CO₂-2-amino-2-methyl-1-propanol (AMP)

environment," *Industrial & Engineering Chemistry Research*, vol. 36, pp. 264-269, 1997.
[38] D. DeMontigny, P. Tontiwachwuthikul, and A. Chakma, "Parametric studies of carbon dioxide absorption into highly concentrated monoethanolamine solutions," *Canadian Journal of Chemical Engineering*, vol. 79, pp. 137-142, 2001.
[39] J.-C. Charpentier, "Pt 1 Gas Liquid Absorptions and Reactions," *Advances in chemical engineering*, vol. v. 11, pp. 2-133, 1981.
[40] R. Zarzycki and A. Chacuk, *Absorption : fundamentals & applications*, 1st . ed. Oxford ; New York: Pergamon Press, 1993.
[41] J. D. Seader and E. J. Henley, *Separation process principles*. New York: Wiley, 1998.
[42] D. L. Bennett, "Part II: Packed columns," *Chemical Engineering Progress*, vol. 96, pp. 27-34, 2000.
[43] M. K. Krumdieck S, Brill M, Cleland J, Green M, Wallace J, "APPARATUS FOR CONTINUOUS CARBON DIOXIDE ABSORPTION." NEW ZEALAND, 2001, pp. PCT/NZ02/00205.
[44] N. A. Spector and B. F. Dodge, "Removal of carbon dioxide from atmospheric air," *Transactions of American Institute of Chemical Engineers*, vol. 42, pp. 827-48, 1946.
[45] R. M. Smith, *Gas and liquid chromatography in analytical chemistry*. Chichester [West Sussex] ; New York: Wiley, 1988.
[46] G. Guiochon and C. L. Guillemin, *Quantitative gas chromatography : for laboratory analyses and on-line process control*. Amsterdam ; New York, U.S.A: Elsevier, 1988.
[47] A. Verdin, *Gas analysis instrumentation*. [London]: Macmillan, 1973.
[48] R. P. W. Scott, *Chromatographic detectors : design, function, and operation*. New York: Marcel Dekker, 1996.
[49] ShimadzuCorporation, *Practical Gas Chromatography Manual*, 2nd ed, 1983.
[50] H. M. B. McNair, E.J., *Basic Gas Chromatography*, 4th Printing ed. California: Varian Aerograph, 1968.
[51] ShimadzuCoporation, *Chromatopac C-R3A Instruction Manual*, 1983.
[52] R. S. Figliola and D. E. Beasley, *Theory and Design for Mechanical Measurements*, 3rd ed ed: John Wiley & Sons, Inc., 2000.
[53] L. Liaw, "Feasibility of Continuous Scrubbing of CO2 From Air at Atmospheric Pressure Using Amine Temperature Swing Chemistry." Christchurch, 2004.
[54] D. M. Austgen, G. T. Rochelle, X. Peng, and C.-C. Chen, "Model of vapor-liquid equilibria for aqueous acid gas-alkanolamine systems using the electrolyte-NRTL equation," *Industrial & Engineering Chemistry Research*, pp. 1060-1073, 1989.
[55] R. H. Weiland and O. Trass, "Titrimetric determination of acid gases in alkali hydroxides and amines," *Analytical Chemistry*, vol. 41, pp. 1709-10, 1969.
[56] R. A. Mashelkar, "Bubble columns," *British Chemical Engineering*, vol. 15, pp. 1297-304, 1970.
[57] W. D. Deckwer and A. Schumpe, "Improved tools for bubble column reactor design and scale-up," *Chemical Engineering Science*, vol. 48, pp. 889-911, 1993.

[58] Y. T. Shah, B. G. Kelkar, S. P. Godbole, and W. D. Deckwer, "Design parameters estimations for bubble column reactors," *AIChE Journal*, vol. 28, pp. 353-79, 1982.
[59] M. M. Sharma and R. A. Mashelkar, "Absorption With Reaction in Bubble Columns," *Institution of Chemical Engineers Symposium Series*, vol. No 28, pp. 10-21, 1968.
[60] P. Therning and A. Rasmuson, "Liquid dispersion and gas holdup in packed bubble columns at atmospheric pressure," *Chemical Engineering Journal*, vol. 81, pp. 69-81, 2001.
[61] M. C. Ruzicka, J. Zahradnik, J. Drahos, and N. H. Thomas, "Homogeneous-heterogeneous regime transition in bubble columns," *Chemical Engineering Science*, vol. 56, pp. 4609-4626, 2001.
[62] A. J. Carleton, R. J. Flain, J. Rennie, and F. H. H. Valentin, "Some properties of packed bubble column," *Chemical Engineering Science*, vol. 22, pp. 1839-1845, 1967.
[63] R. A. Mashelkar and M. M. Sharma, "Mass Transfer in Bubble and Packed Bubble Columns," *Transactions of the Institution of Chemical Engineers*, vol. 48, pp. T162-T172, 1970.
[64] P. H. Calderbank, "Gas absorption from bubbles," *Chemical Engineer*, vol. No. 212, pp. CE209-CE233, 1967.
[65] O. J. Curnow, S. P. Krumdieck, and E. M. Jenkins, "Regeneration of Carbon Dioxide Saturated Monoethanolamine-Glycol Aqueous Solutions at Atmospheric Pressure in a Packed Bubble Reactor," *Industrial & Engineering Chemistry Research*, vol. 44, pp. 1085-1089, 2005.
[66] B. R. Strazisar, R. R. Anderson, and C. M. White, "Degradation pathways for monoethanolamine in a CO2 capture facility," *Energy and Fuels*, vol. 17, pp. 1034-1039, 2003.
[67] R. E. Kirk, D. F. Othmer, J. I. Kroschwitz, and M. Howe-Grant, *Encyclopedia of chemical technology*, vol. 1, 4th ed. New York: Wiley, 1991.
[68] Dow-Chemicals, "Dow Ethanolamines Overview Brochure," 2005, pp. http://www.dow.com/amines/prod/ethano.htm.
[69] J.-H. Song, J.-H. Yoon, H. Lee, and K.-H. Lee, "Solubility of carbon dioxide in monoethanolamine+ethylene glycol+water and monoethanolamine+poly(ethylene glycol)+water," *Journal of Chemical and Engineering Data*, vol. 41, pp. 497-499, 1996.
[70] R. C. Ewing, "Evaluation Points Out Trouble Spots In Amine Plants," *The oil and gas journal*, pp. 125-129, 1967.
[71] R. H. Weiland, J. C. Dingman, D. B. Cronin, and G. J. Browning, "Density and viscosity of some partially carbonated aqueous alkanolamine solutions and their blends," *Journal of Chemical and Engineering Data*, vol. 43, pp. 378-382, 1998.
[72] Y. Fumitake and A. Kiyomi, "Performance of Gas Bubble Columns: Volumetric Liquid-Phase Mass Transfer Coefficient and Gas Holdup," *AIChE Journal*, vol. 11, pp. 9-13, 1965.
[73] Cole-Parmer, "http://www.coleparmer.com," in *Material compatibility*, 2005.
[74] R. H. Perry, D. W. Green, and J. O. Maloney, *Perry's chemical engineers' handbook*, 7th / ed. New York: McGraw-Hill, 1997.
[75] E. W. Flick, *Industrial solvents handbook*, 3rd ed. Park Ridge, N.J., U.S.A.: Noyes Publications, 1985.

[76] Y. A. Çengel and M. A. Boles, *Thermodynamics : an engineering approach*, 3rd ed. Boston: McGraw Hill, 1998.
[77] F. P. Incropera and D. P. DeWitt, *Fundamentals of heat and mass transfer*, 5th ed. New York: Wiley, 2001.
[78] CRC, *CRC handbook of chemistry and physics*, vol. 82nd ed. (2003-2004)-. Cleveland, Ohio: CRC Press, 2003.

Appendix 1

ENECO 9 KW ALKALINE FUEL CELL SYSTEM INFORMATION SHEET

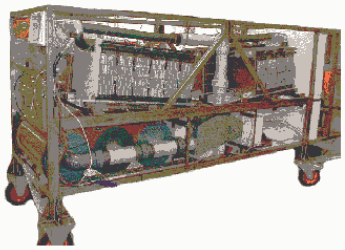

ENECO LTD

ALKALINE FUEL CELL DIVISION

The Eneco 9 kW Alkaline Fuel Cell Generator

A independent 9kW electrical Generator, runs on gaseous hydrogen, quite zero pollution operation.
Fully automatic microprocessor controlled. Prototype status product.

Fuel Supply

Industrial grade hydrogen at 99.999 %, Carbon dioxide less than 10ppm, mercury free
Supply pressure 2 bar, max consumption 7.2m^3 per hour / 120 litres/min at 9 kW

Utilities

Nitrogen for purging at 99.99 % industrial grade, Carbon dioxide less than 10ppm, mercury free,
Supply pressure 2 bar, intermittent flow 50 litres/min, consumption 100l/hour

Controls

Dedicated electronic control system for automatic start-up and shut down, full cell monitoring, automatic purging. Inbuilt safety monitoring and diagnostic warnings.
Alpha numeric operator display. System electrolyte operates at 70 °C.

Operation Environment

Covered area, max humidity 90%, minimum temperature 5°C (option for sub zero), maximum temperature 45 °C (option for higher temperatures)

Electrical Output

Open circuit 140 volts DC
Full Load 96 volts DC at 100 amp.

System Power

This is a self powered system combining internal start-up battery

Emissions

Water vapour from exhaust, low volume nitrogen at shutdown and intermittent purge.
Low volume hydrogen during purge cycles, vented via separate piped exhaust. Quiet operation.

Weight

300kg inc 40litre KOH electrolyte and CO_2 absorber material

Documentation and Training

System diagrams, operating instructions, installation instructions, service instructions.
Operation training at factory

Consumables

Sofnolime for $C0_2$ scrubber, exchange every 160 hours.

Options on request

Sub zero temperature operation, High ambient temperature operation, weather proof housing, electrical converters to match electrical output to suit customers requirements. Mains driven electrolyte heater for rapid start-up to full power

Price and Delivery and Terms

10 weeks from date or order, 50% deposit on order, balance on shipment, Cost one off at £65,000 plus taxes ex works. Price for multiples on application

Warranty

Full parts and labour at works for 12 months, excluding consumables.

Enquiries

Call Eneco Ltd

Alkaline Fuel Cell Division
Spring Copse Business Park
Slinfold West Sussex
RH13 OSZ
Tel 01403790114
Fax 01403 799512
www.automotive-consultants.fsnet.co.uk

Appendix 2

Independent Power Technologies Regenerative Scrubber

INDEPENDENT TECHNOLOGIES

REGENERATIVE CARBON DIOXIDE SCRUBBER FOR ALKALINE FUEL CELL ELECTROCHEMICAL GENERATOR (AFC ECG)

Future progress toward development of commercially viable Electro-Chemical Generators (ECGs) based on Alkaline Fuel Cell (AFC) technology largely depends on the effectiveness of technological solutions for the removal of carbon dioxide from air at the inlet of the generator. This removal is a necessary procedure in order to avoid carbonization of electrolyte, which drastically reduces operating time of AFCs.

Presently, conventional techniques employ sodalime and similar chemical reagents for the removal of carbon dioxide from incoming air. These techniques demonstrate satisfactory results and are relatively inexpensive. However, all of them require collection and recycling of used adsorbent, which becomes a significant drawback in case of large-scale operations.

Independent Power Technologies Ltd together with one of the leading Russian enterprises in the field of air regeneration systems for special applications developed and commissioned a regenerative carbon dioxide scrubber for AFC ECG. Comprehensive studies conducted at our company proved possibility to use this device for a deep scrubbing of ambient air with the residual concentration of carbon dioxide below 20 ppm (0.002%). The optimum modes of operation of the integrated system "scrubber — fuel cell stack" were determined and tested. The scrubber employs a unique sorbent, which is relatively inexpensive, commercially available and has demonstrated reliable long-term performance (5000 h+) in other applications.

Table 1. Technical specification for the carbon dioxide scrubber for 3 kW ECG

Incoming air flow, m^3/h	≤ 20
Concentration of CO_2 in scrubbed air, ppm	≤ 20
Pressure drop, mm H_2O	≤ 160
Power consumption, W	≤ 200
Volume of sorbent, liters	2

1

INDEPENDENT POWER TECHNOLOGIES LTD
Alexander Yuzefovsky, Ph.D.
managing director
t. +7 (095) 231 2109
f. +7 (095) 231 2078
m. +7 (812) 940 8440
e. ayuzefovsky@yahoo.com
www.independentpower.biz
3-d Mytishchinskaya 18
bldg 60
Moscow, 129626
Russian Federation

Table 2. Comparison between conventional (sodalime) and regenerative scrubbers (per 1 kW net power of ECG)

	Conventional	Regenerative
Air flow, m^3/h	6	6
Operating time, h	5000	5000
Amount of sorbent required, kg	233	1.5
Price of sorbent, USD	300	20
Estimated cost of the system (excluding sorbent) for mass production, USD	50	150
Estimated total cost, USD	**350**	**170**
Maintenance	Frequent change of sorbent is required	None
Recycling/utilization of sorbent	Difficult	Easy

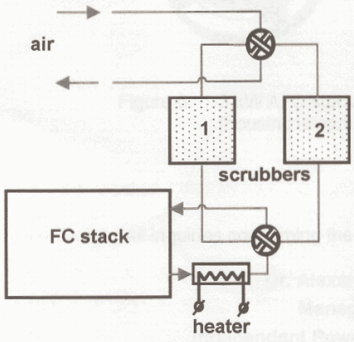

Figure 1. Flow chart diagram of the carbon dioxide scrubber

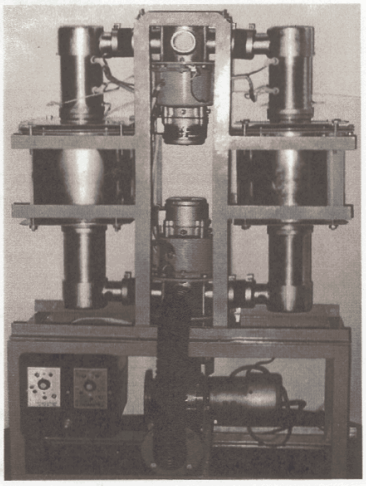

Figure 2. Main fragment of the carbon dioxide scrubber test bench

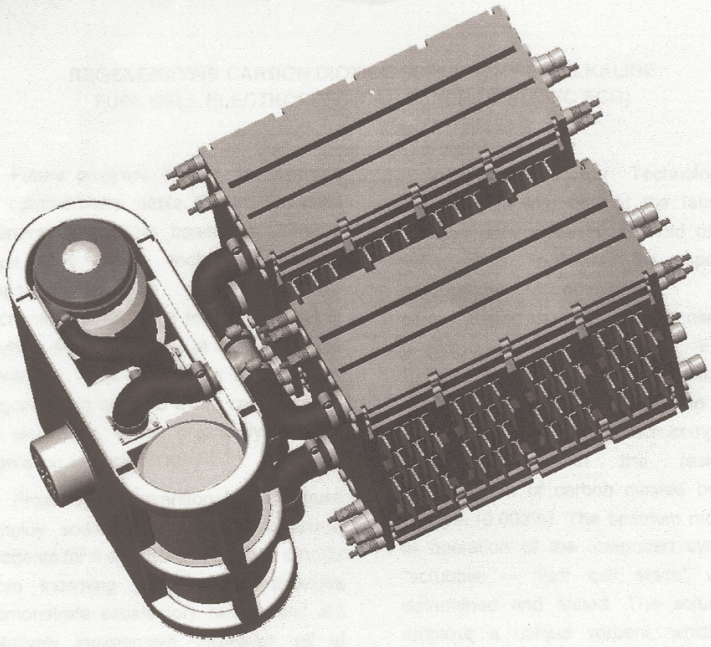

Figure 3. 3 kW AFC stack with integrated carbon dioxide scrubber (housing is partly removed)

All inquiries concerning the scrubber should be addressed to:

Dr. Alexander Yuzefovsky
Managing Director
Independent Power Technologies Limited
3rd Mytishchinskaya Street 16
Moscow 129626, Russia
T: +7 095 231 2109 • F: +7 095 231 2078
e-mail: info@independentpower.biz

Appendix 3

CHEMICAL PROPERTIES

Property	Temp (℃)	Source	Chemical				Units
			MEA	MEG	H_2O	Standard Solution^	
Molecular Formula			C_2H_7NO	$C_2H_6O_2$	H_2O		
Molecular Weight		1,2	61.08	62.07	18.02	44.96*	g/mole
pH			12.5		7		
Density, ρ		1	9079	1113.5	1000		kg/m^3
		2	1012	1114.5			
		3	1017				
		6				1040	
Boiling Point (P_{atm})		1	171	197.3	100		℃
		2	170.8	197.6			
		3	170.4				
		6				135	
Melting Point (P_{atm})		1		-13	0		℃
		2	10.3	-13	0		
		3	10.5				
Specific Heat, c_p	20	1	3200	2370	4182		J/kgK
		3	2721				
		5,6				3180	
	100	1			4216		
		3	3140				
Thermal Conductivity, k	20-25	1	0.299	0.256	0.598		W/mK
	100	1	0.261	0.256	0.679		
		4				0.263**	

Property	Temp (℃)	Source	Chemical				Units
			MEA	MEG	H_2O	Standard Solution*	
Absolute Viscosity, μ	20-25	1	0.021	0.016	0.001		Pas
		2	0.0189	0.02			
		3	0.0241				
		4				0.01**	
	100	1	0.002	0.002	0.00028		
		4				0.002**	
Surface Tension, γ	20	1	0.048	0.048	0.073		N/m
		2		0.0484			
		3	0.0483				
	75-100	1	0.043	0.041	0.059		
Vapour Pressure	20-25	1	0.05	0.01	2.3		kPa
	35	1	0.1				
	86	1		1			
	100	1			101.3		
	110	1	10				

^ 50/35/15 wt% MEA/MEG/H_2O

* 37/25/38 mole% MEA/MEG/H_2O

** Property of MEG

Source

1 CRC Handbook [78]
2 Merck Index [12]
3 Dow Chemicals [68]
4 Incropera [77]
5 Perry [74]
6 Calculated/Measured

Appendix 4

AIR FLOW METER CALIBRATION CURVE

Annubar Flowmeter Calibration

Dietrich Standard Corp 1.049" Annubar
Lambrecht KG Gottenger Inclined Manomater (Inclination 1:2)

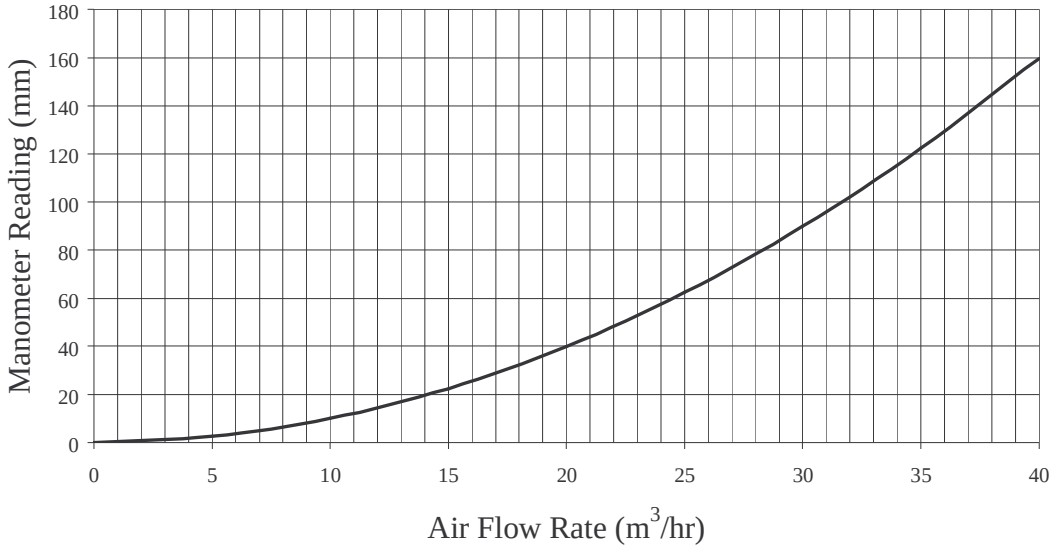

Appendix 5

AMETEK AIR BLOWER 116639

Tech Bulletin

5.7" (145mm) BLDC Bypass Blower **250 WATT, 120 VOLT**

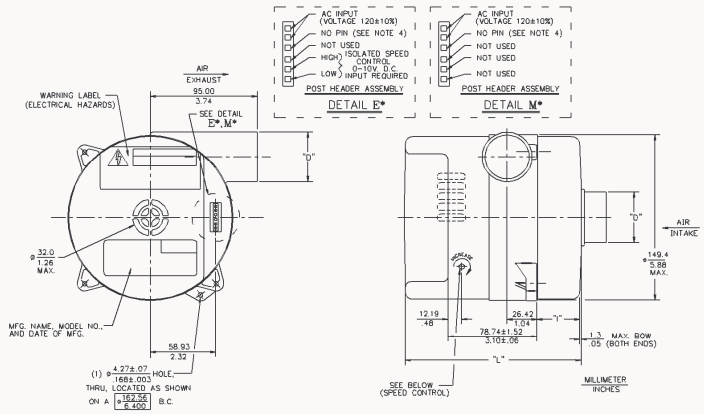

Blower Data	Unit of Measure	Part Number					
		Standard Flow			High Flow		
		116634 M*	116633 M	116632 M*	116637 M*	116636 M*	116635 M
		116640 E*	116639 E	116638 E*	116643 E*	116642 E*	116641 E
Stages		1	2	3	1	2	3
Vacuum, Max. (Sealed Vacuum)	in. H_2O	29	48	65	26	57.5	42
	mBar	72	119	161	64	143	104
Pressure, Max. (Sealed Pressure)	in. H_2O	32	56	76	27	68.0	46
	mBar	79	139	188	67	169	114
Flow Rate, Max. (Open Flow)	CFM	68	63	49	115	110	80
	L/sec	32	30	23	54	52	38
Inlet/Outlet Diameter	inches	1.25	1.25	1.25	1.75	1.75	1.75
	mm	31.75	31.75	31.75	44.45	44.45	44.45
Length (Dimension "I" above)	inches	0.33	1.25	2.14	0.47	1.53	2.53
	mm	8.38	31.75	54.36	11.94	38.86	64.26
Length (Dimension "L" above)	inches	5.08	6.35	6.89	5.22	6.27	7.28
	mm	129.03	161.29	175.01	132.59	159.26	184.91

Typical Performance Points

Air Flow	Pressure						
0 CFM	in. H_2O	31.8	56.1	76.2	27.1	48.1	46.0
10 CFM	in. H_2O	28.7	48.0	60.3	25.0	44.0	42.8
20 CFM	in. H_2O	27.7	44.3	44.1	24.4	41.6	39.2
30 CFM	in. H_2O	24.7	38.1	28.9	22.9	37.9	34.9
40 CFM	in. H_2O	20.1	28.9	16.1	21.2	32.2	30.0
50 CFM	in. H_2O	14.5	18.2		19.1	25.8	24.3
60 CFM	in. H_2O	7.3	4.2		17.2	20.5	16.2
70 CFM	in. H_2O				15.0	15.8	9.8
80 CFM	in. H_2O				12.2	7.1	
90 CFM	in. H_2O				8.0		
100 CFM	in. H_2O				5.5		

**These part numbers are available through AMETEK Rotron distributors. See page 54 for distributor information.*

NOTES:
Nominal input voltage: *120 Volts AC RMS +/- 10%, 60Hz*
Input current: *5 amps AC RMS maximum*
Temperature: *Working Air: 0°C to 50°C, Ambient Air: 0°C to 50°C, Storage Air: -40°C to 85°C*
Dielectric Testing: *1500 volts AC RMS 60Hz applied for one second between input pins and ground, 3mA leakage max.*
Speed Control: *E (Electrical): Pulse Width Modulation or Analog input voltage (User Supplied), 0 to 10 Volts DC Nominal, 10mA Maximum, 3 to 15 volts DC Maximum. Access to sensitivity adjustment for 0-10 VDC speed control. (Ref. pin connection)*
M (Mechanical): A potentiometer is available for speed control of the blower. The potentiometer can be preset for a specific speed. Access to speed adjustment.

AMETEK
ROTRON
TECHNICAL PRODUCTS

Windjammer

HIGH-VOLTAGE BLOWERS

5.7" (145mm) BLDC Bypass Blower — 250 WATT, 120 VOLT

Standard Flow

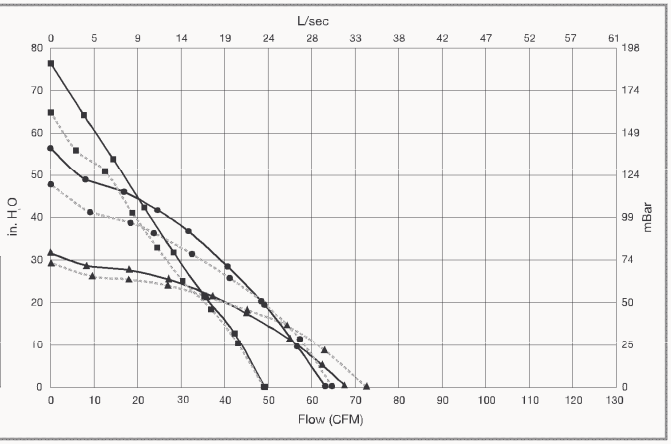

High Flow

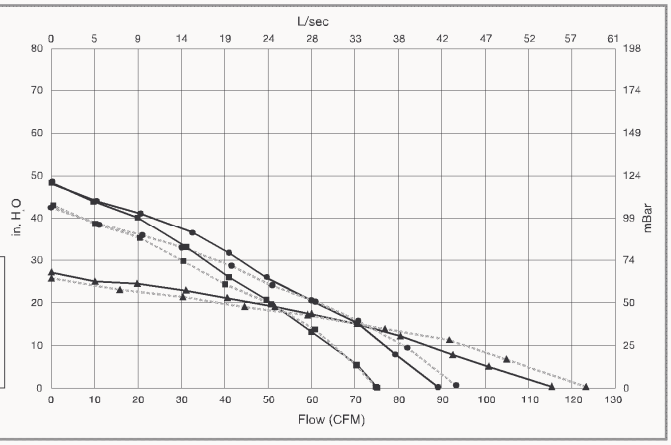

Regulatory Agency Certification: *Underwriters Laboratories, Inc. is qualified per UL507 under File E-94403; Canadian Standards Association is qualified per C22.2#113 under File LR 43448.*

Miscellaneous: *Intake & exhaust tubes, all cooling ducts and vents must not be obstructed. Intake and exhaust are free of grease, oil, or foreign particles. Amp housing #640250-6 (to be supplied by customer), mates with post header assembly.*

Appendix 6

BUERKERT FLOW SOLENOID CONTROL VALVE TYPE 6223

Easy Flow Solenoid Control Valve - General Purpose **Type 6223**

2/2-Way; servo-assisted; G 3/8"- G 1"; PN 0,5-10 bar

Advantages / Benefits

- **Optimization of process and product quality through continuous regulation**
- **Increase of efficiency**
- **Extremely high control accuracy:**
  - low hysteresis
  - high repeatability
  - high responsivity
- **Particularly good turn down ratio and thereby usage of an optimal control range**
- **Fail safe (self-closing in case of power failure)**
- **A complete control system "all from one" with Burkert sensors and controllers**
- **Brass or Stainless Steel body**

Design / Function

Type 6223 is a servo-assisted solenoid control valve for K_{Vs} flow rates from 1.4 to 5 m^3/h. The variable opening of the cross-section is continually changed proportional to the standard electrical input signal. The characteristic curve of the valve is practically linear; regulation deviations are extremely low.
With < 1%, the valve has a high sensitivity, due to a higher frequent pulse-width modulation.
The solenoid control valve consists of the basic components of armature, push-over coil and electronic control unit, and can be mounted in any position. The electronic control unit is integrated into the DIN 43650A cable plug, but can also be supplied as a standard DIN-rail mounting version.

- Adjustable ramp function from 0-10 s cushions set-point jumps
- Standard input signals 4-20 mA, 0-10V
- Monitor signal to assist set-up and indicaton of coil current
- Tight shut-off due to zero-point suppression
- Compensation of the coil heating
- Start of opening and max. opening adjustable
- Simple ordering procedure with one order number for valve and control electronics

Applications

Continuous control of larger flow rates of neutral and slightly aggressive media.

- General machine construction (in particular control for cooling circulations)
- Process technology in the chemical industry
- Paper and printing machines (e.g., damp control)
- Filling systems
- Machinery and plants for food and beverage industries
- Water treatment
- Medical technology (sterilization)
- Textile industry (dyeing, washing, drying)

bürkert *Easy* Fluid Control Systems

bürkert